Università
Ca'Foscari
Venezia

Scuola Dottorale di Ateneo
Graduate School

Dottorato di ricerca
in Scienze Ambientali
Ciclo XXX
Anno di discussione 2018

BIOMASS BURNING RECONSTRUCTION ANALYSING LACUSTRINE SEDIMENT CORES FROM THE TIBETAN PLATEAU

SETTORE SCIENTIFICO DISCIPLINARE DI AFFERENZA: CHIM/01
Tesi di Dottorato di Alice Callegaro, matricola 823218

Coordinatore del Dottorato	**Supervisore del Dottorando**
Prof. Bruno Pavoni	**Prof. Carlo Barbante**

BIOMASS BURNING RECONSTRUCTION ANALYSING LACUSTRINE SEDIMENT CORES FROM THE TIBETAN PLATEAU

December 12, 2017

PhD candidate
Alice Callegaro

PhD supervisor
Prof. Carlo Barbante

"You make observations, write theories to fit them, try experiments to disprove the theories and, if you can't, you've got something."

— Kary Mullis —

Alla memoria del Maestro Unico, nonché Direttore, Giovanni Pasqualetto.
Nonno.
1926 – 2009

Abstract

The present PhD thesis gives information about Holocene (begun 11700 years ago) fire events and vegetation changes occurred on the Tibetan Plateau and the surrounding areas and may help to determine the interactions between Holocene climate and fire activity. The work aims to report the first published study regarding levoglucosan analysed in Tibetan lacustrine sediment samples and a multi-proxy paleoclimate reconstruction using different biomarkers.
How land-use changes have been influencing Holocene's climate is a controversially debated topic. Increasing awareness of "The Early Anthropocene Hypothesis" led to chemical and physical investigations of natural archives such as sediments, peat bogs and ice cores. Lacustrine sedimentary cores provide continuous records of large-scale and local environmental modifications, intelligible due to specific organic molecular markers and pollens that accumulated in these archives during past millennia.
The Asiatic region is one of the centres of the advent of agriculture and pastoralism, and it is a strategic area to explore biomarker distributions. In order to improve the scientific knowledge on ecosystem changes due to biomass burning events and eventual human presence during the Holocene in this area, a small moraine lake called Paru Co, located in the South-Eastern Tibetan Plateau, and a bigger lake called Hala Hu, settled in the North-Eastern Tibetan Plateau, were selected.
The detection of organic compounds contained in sediment samples from these two lakes was performed with an effective analytical method, developed improving and integrating previous methods. Accelerated Solvent Extraction (ASE) technique was used, followed by purification and analysis with gas and liquid chromatography coupled with mass spectrometers (GC-MS, IC-MS). The investigated biomarkers were n-alkanes, indicators of vegetation, polycyclic aromatic hydrocarbons (PAHs) as combustion proxies, faecal sterols and stanols (FeSts), indicators of past human and grazing animals presence and monosaccharide anhydrides (MAs), specific markers of vegetation burning processes.
Paru Co MAs and PAHs results showed intensive biomass burning activity in the samples from the early Holocene, which corresponds to a drier climate as a result of the deglaciation. This period was followed by a decreasing trend of biomass burning towards the Early Holocene. The local vegetation

modifications registered by n-alkanes and MAs ratios, are in agreement with pollen records from the surrounding areas and with intensity's changes in the monsoonal precipitations rainfall. FeSts, instead, were not found probably due to the impervious location of the small lake. Hala Hu MAs results, instead, show higher fire intensity in the period between 7000 and 4500 years ago, started simultaneously to the abrupt climatic transition of the mid-Holocene. The information obtained from these organic geochemical data were compared with charcoal data, dust layers, meteorological information and also archaeological findings. In this way, a contextualization of the biomass burning events in a regional setting was possible. The more probable explanation of fire activity recorded in both lakes seems to be the climatic influence as a sum of dry/humid cool/dry alternate periods and enhanced windy events; however, the possible human influence cannot be totally excluded from Hala Hu, due to no sufficient evidences.

Acknowledgements

I would firstly like to thank my PhD supervisor, Prof. Carlo Barbante, who gave me the chance to become part of its international research group and let me free to perform the work in my own ways and to participate at summer schools, congresses and workshops. This brought me in contact with people from all over the world, giving me not only a scientific growth but mostly a personal enrichment.

I am also very grateful to Prof. Dario Battistel, who acted as a guide and always gave its friendliness with new ideas, methods and ways to fix the problems both inside and outside the lab.

I would really like to thank Dr. Dirk Sachse for kindly hosting me in his labs at GFZ Potsdam, where I found a fresh work environment with positive people. Dr. Elisabeth Dietze and Dr. Bernhard Aichner for their help, scientific suggestions and collaborating will.

Thanks to Dr. Natalie Kehrwald, for always replying to my emails from overseas. I am grateful to all my Delta Building colleagues (ex Santa Marta), especially Torben, for having believed in my capacities, becoming a real friend. Thank you Federico D. for always supporting me from the back desk and teaching me the secrets of LaTeX, together with Giovanni. Elena A., for her help with GC and patience in organizing bureaucratic stuff in EHI final workshop and SISC2017.

Thanks to all my old-time friends and to the new ones, especially Mari, who has become more than a sister over these 3 years, Alba and Angie, who are always from my side.

A special thank to Andrea for his food-plenty support and for being the first person reading the thesis.

Finally, I want to thank my parents and my sister for their love and patience and for always holding me during the difficult moments.

Contents

Abstract **i**

Acknowledgements **iii**

Acronyms **vii**

List of Tables **ix**

List of Figures **xi**

1 Introduction **1**
1.1 Background and Objectives 1
1.2 Biomass burning processes and markers 3
1.2.1 Monosaccharide Anhydrides 6
1.2.2 Polycyclic aromatic hydrocarbons 7
1.2.3 Charcoal 11
1.3 Past vegetation changes and human presence 13
1.3.1 N-alkanes 13
1.3.2 Faecal Sterols 15

2 Study Area **17**
2.1 Tibetan Plateau as paleoresearch area 17
2.2 Holocene climate 19
2.3 Paru Co and Hala Hu lakes 22

3 Materials and Methods **27**
3.1 The investigation of lacustrine sediment cores 27
3.2 Materials and Methods 28
3.2.1 Standards, reagents and solvents 29
3.2.2 Paru Co's method 31
3.2.3 Hala Hu's method 36
3.2.4 Composite analysis of charcoal data 39

4 Results and discussion **41**
4.1 Study of the Lake Paru Co 41
4.1.1 Paleoclimatic framework and lake's dynamics 41
4.1.2 Preliminary Results 42
4.1.3 Paleofire reconstruction 44
4.1.4 Inferences on past vegetation 52
4.1.5 Statistical Analysis 60
4.2 Study of the Lake Hala Hu 64
4.2.1 Paleoclimatic framework and lake's dynamics 64
4.2.2 Paleofire reconstruction 67
4.2.3 Statistical Analysis 71
4.3 Composite analysis of charcoal data 77
4.4 Relationship with other climatic records 82

5 Conclusions **89**

References **93**

Acronyms

Ace	Acetone
ACL	average chain length
AM	Asian Monsoon
asl	above sea level
A/T	aquatic/terrestrial
BC	Black carbon
BP	Before Present (1950 AD)
BSi	biogenic silica
BSTFA	N,O-bis(trimethylsilyl)trifluoroacetamide
CPI	carbon preference index
DAIS	Department of Environmental Sciences, Informatics and Statistics
DCM	dichloromethane
EASM	East Asian Summer Monsoon
ENSO	El Niño Southern Oscillation
FeSts	Faecal Sterols and Stanols
GC	Gas Chromatography
GFZ	Helmholtz Centre Potsdam, German Research Centre for Geosciences
GHGs	Greenhouse Gases
GR	grass
Hex	hexane

HW	hardwood
IC	Ion Chromatography
ISM	Indian Summer Monsoon
ITCZ	Inter Tropical Convergence Zone
ky	thousands years
MAs	anhydrosugars or monosaccharide anhydrides
MeOH	methanol
MS	Mass Spectrometry
NETP	North-Eastern Tibetan Plateau
NWTP	North-Western Tibetan Plateau
OM	organic matter
PAHs	polycyclic aromatic hydrocarbons
P_{aq}	submerged vs. emerged plants ratio
PCA	principal component analysis
PTFE	Polytetrafluoroethylene
SST	sea-surface temperature
SETP	South-Eastern Tibetan Plateau
SST	sea surface temperature
SW	softwood
T/(G+S)	trees/(grass+shrubs)
TOM	total organic matter
TP	Tibetan Plateau

List of Tables

1.1 Summary of the biomass exposed to fires, the total carbon released, the percentage of N to C in the fuel, and the total mass of N compounds released to the atmosphere by fires in the tropics 5
1.2 PAHs of interest and their abbreviations used in the text. . . 8
1.3 FeSts of interests and their abbreviations used in the text. . . 15

3.1 Mass to charge ratios, LOD and LOQ for PAHs and FeSts expressed in ng. 34
3.2 N-alkanes LOD and LOQ, expressed in ng. 35

4.1 MAs ratios values for Paru Co B11 test samples. 42
4.2 PCA loadings for Paru Co variables. 61
4.3 PCA loadings for Hala Hu variables. 72

List of Figures

1.1 Illustration of environmental processes affecting lakes and their sediments . . . 2
1.2 MAs: Levoglucosan (a), mannosan (b) and galactosan (c). . . 6
1.3 PAHs considered in this study: the priority 16 plus Benzo[e]pyrene and Retene. . . . 10
1.4 Relationship between fire and charcoal and approaches for reconstruction . . . 11
1.5 Location of paleofire sites and sampling density in the GCDv3 12
1.6 Products of Δ5-sterols reduction in the mammals' intestine and in soils . . . 16

2.1 Particular from the South-eastern TP . . . 18
2.2 Late Quaternary human migration in China along the course of the Yellow River . . . 19
2.3 Major climatic systems acting on the Tibetan Plateau . . . 20
2.4 Vegetation distribution on the Tibetan Plateau with the locations of the lakes Paru Co and Hala Hu . . . 22
2.5 A: Map of southern Asia; B: Expanded view of the study area showing the location of Paru Co and other nearby lakes; C: Satellite image of Paru Co and its immediate watershed . . . 24
2.6 A: Overview map of the area between Qinghai Lake and Hala Lake; B: Study site within China; C: Lake shape of Hala Lake; D: Oxygen and temperature graphs . . . 25

3.1 Instruments for mechanic grinding treatment. . . . 28
3.2 Chromatographers and spectrometers used for the analysis of biomarkers. . . . 29
3.3 Age Model obtained for Lake Paru Co. . . . 31
3.4 Standard mixture of MAs . . . 36
3.5 Age Model obtained for Lake Hala Hu. . . . 37
3.6 Clean-up of Hala Hu DCM-TLE with Pasteur pipettes filled with silica gel. . . . 38

4.1 Galactosan, mannosan and levoglucosan results from Paru Co test samples . . . 43
4.2 Levoglucosan results from Paru Co . . . 44
4.3 Mannosan results from Paru Co . . . 45
4.4 Galactosan results from Paru Co . . . 45
4.5 MAs results from Paru Co . . . 46
4.6 Sum of PAHs analysed in Paru Co . . . 47
4.7 PAHs results from Paru Co in fluxes. . . . 48
4.8 Results from Paru Co showing (A) ΣPAHs; (B) %BSi; (C) ΣMAs; (D) %TOM . . . 49
4.9 Results from Paru Co showing L/M and L/(M+G) ratios. . . 52
4.10 Results from Paru Co showing trend of L/M ratio and vegetation changes inferred from Hidden Lake pollen data . . . 53
4.11 Comparison between ACL and P_{aq} data . . . 54
4.12 Confrontation between CPI, T/(G+S) and Aquatic/Terrestrial ratios . . . 56
4.13 Confrontation between different ratios expressing the "grass to wood" quotient . . . 57
4.14 Sitostanol and sitosterol log fluxes detected in Paru Co compared with n-alkanes Norm31 ratio. . . . 59
4.15 Pearson correlation matrix for Paru Co dataset. . . . 60
4.16 Scree plot of PCA analysis for Paru Co dataset. . . . 62
4.17 Scores plot of PCA analysis for Paru Co dataset. . . . 63
4.18 Biplot of PC1 and PC2 of PCA for Paru Co dataset. . . . 63
4.19 H11 results for Si (detrital input), OM%, Ca ($CaCO_3$), Sr/Ca (salinity) . . . 66
4.20 MAs results from Hala Hu . . . 67
4.21 MAs isomers ratios results from Hala Hu lake, distinguished in 3 periods. . . . 68
4.22 Charcoal record from Gonghe Basin in the NETP . . . 70
4.23 Pearson correlation matrix for Hala Hu dataset. . . . 71
4.24 Scree plot of PCA analysis for Hala Hu dataset. . . . 73
4.25 Scores plot of PCA analysis for Hala Hu dataset. . . . 73
4.26 3D scores plot of PCA analysis for Hala Hu dataset. . . . 74
4.27 Biplots of PC1 vs PC2 and PC1 vs PC3 of PCA for Hala Hu dataset. . . . 75
4.28 Results from Hala Hu showing ΣMAs and XRF data for Al, K, Si . . . 76
4.29 Map with selected sites from the GCD, Chinese area . . . 77
4.30 Charcoal Index . . . 78
4.31 Charcoal data transformation, background estimation and homogenisation from multiple series to a unique one from the North-Eastern area outside the Tibetan Plateau. . . . 79

4.32 Charcoal data transformation, background estimation and homogenisation from multiple series to a unique one from the South-Eastern area outside the Tibetan Plateau. 79
4.33 Charcoal data transformation, background estimation and homogenisation from multiple series to a unique one from the North-Western area outside the Tibetan Plateau. 80
4.34 Charcoal data composite record from the Chinese region, compared to Hala Hu and Paru Co MAs record. 81
4.35 Holocene Bond events 0 to 7 (yellow bars) within fire and silica proxies in Paru Co and Hala Hu 84
4.36 Comparison of KE section climate evolution with other selected proxy records from the neighboring area during the last 10 ky 86

Chapter 1

Introduction

1.1 Background and Objectives

Well before the appearance of humans on Earth and of their use of fire, wildfires played a pivotal role in the emergence of plant adaptations as well as in the distribution and developments of ecosystems. By the beginning of the Paleozoic Era, 540 million years ago (mya) the atmospheric oxygen started to be sufficient for supporting fire, but the lack of terrestrial plant fuels limited the possibility of fire [1]. Then, with the origins of terrestrial plants in the earliest Silurian (geologic period started 444 mya, the third one in the Paleozoic Era) a first evidence of fire is documented [2].
When humans started using fire as a multifunctional tool the system became more complex. Between 1.5 and 1 mya *Homo erectus* started controlling fire and it is thought beginning of voluntary use of proper fires dates back to 200-400 ky BP [3, 4]. Biomass burning has been changing drastically the land surface since the Neolithic, when fires started to be used by men for slash and burn land clearance: first farmers and ranchers needed to grow cereals and to graze cattle, and fire was the fastest way to obtain free lands for these purposes. It was assumed that these anthropogenic activities have impacted natural fire regimes for millennia and that the majority (perhaps three-fourths) of total forest clearance occurred prior to the start of the industrial era [5]. The *Early Anthropocene Hypothesis* claims that anthropogenic emissions of green house gases (GHGs), specially CO_2 and CH_4, first altered atmospheric concentrations thousands of years ago. Ruddiman [6] supports this hypothesis with the cyclic natural variations in GHGs, that show anomalous increases of CO_2 and of CH_4 8000 and 5000 years ago respectively. Ruddiman suggested that these anomalies cannot be explained by natural forcing only, but also considering the beginning of deforestation 8000 years ago and of pastoralism and rice irrigation 5000 years ago, linked to the spread of Neolithic civilizations. During the Holocene, fire activity showed a long-term increasing trend at a global scale, and focusing on Asian

continent, records show that the early Holocene fire activity was relatively high, followed by a lower rate in mid-Holocene, and then a new increase close to late-Holocene [7, 8, 9].
Nowadays, fire still remains the most used and cheapest instrument to get new lands ready for plantations. The influence of these practices on climate, both in the past and in the present days, are certain but their quantification is difficult and still under discussion [7, 10]. Considering or not human influence on biomass burning, paleofire history is a valuable topic in highlighting fire sensitiveness to climate changes and its impact on global biogeochemical cycles and ecosystems [4, 11]. Searching for methods to reconstruct past fire events and vegetation changes, and their interactions with paleoclimate, researchers started taking advantage of the long-term accumulation of diverse substances and remains in natural archives. The reconstructed past variations of these preserved compounds (proxies) are used to indirectly infer information about past climatic modifications.

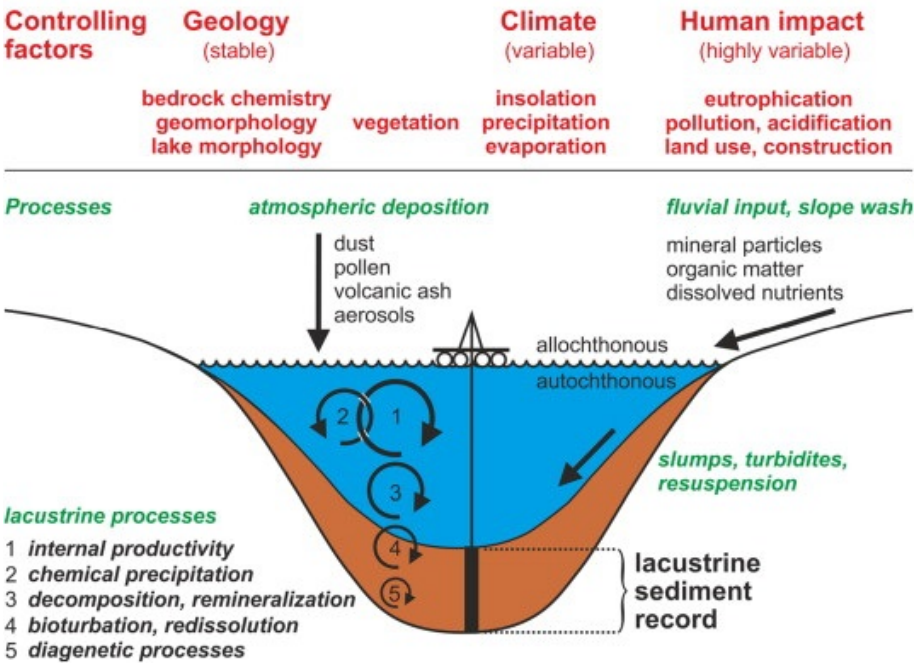

Figure 1.1: Illustration of environmental processes affecting lakes and their sediments. Image source: [12].

Lakes are the end member of interlinked sedimentary processes on a catchment scale, furnish implicative signals for high-resolution reconstruction of present and past sediment fluxes, hydrological and ecological modifications, as long as the lakes persist and the stored sediments are not eroded [13]. Sediment cores can be considered as polyglottal books, rich of information

you need to decipher with the right languages, which are in this case the natural science's branches of *analytical chemistry, sedimentology, climatology, paleoecology, paleolimnology.*
This thesis was part of Early Human Impact project ("Ideas" Specific Programme - European Research Council - Advanced Grant 2010 - Grant Agreement n^o 267696) with these specific objectives:

1. reconstructing the biomass burning history on the Tibetan Plateau during the Holocene;

2. improve the method using a multi molecular proxy approach, with biomarkers that are indicative not only of fire but also of ecosystem changes;

3. understanding the eventual early anthropogenic impacts on land surface, vegetation changes and terrestrial climate;

4. confirming the suitability of lake sediments as key storage materials that can contain specific molecular markers and therefore as archives that can be used for paleofire reconstructions using a multi-proxy approach.

The proposed markers are molecules produced in specific environmental conditions and then transported and accumulated in the lacustrine sediments: monosaccharide anhydrides (MAs - subsection 1.2.1), faecal sterols (FeSts - subsection 1.3.2), polycyclic aromatic hydrocarbons (PAHs - subsection 1.2.2), n-alkanes (subsection 1.3.1). The stability of the studied compounds in sediments after burial is supported by studies where significant amount of the used biomarkers is detectable in soil and sedimentary archives with ages older than 10 ky BP [14, 15, 16], thus suggesting that degradation, if it happens, is a low-kinetic process [17].
The analysis of these diverse biomarkers, stored into sediment cores coming from two different lakes, Paru Co and Hala Hu, and their comparison with other existing records allowed the discrimination between climate-induced and human-induced fire signals; the attempt of interpreting the interaction between climate and fire in the investigated Chinese area is the main goal of this thesis.

1.2 Biomass burning processes and markers

Fire must be considered as an ecosystem process, influenced by ignition source, fuel structure, seasonality and primary productivity [1]. Biomass burning is a complex process and it often comprises a sequence of stages, including ignition, flaming plus glowing plus pyrolysis, glowing plus pyrolysis (smouldering), glowing and extinction [18]. The chemical mechanism that

recurs during a forest fire event produces high quantity of particulate matter, greenhouse gases and a lot of other compounds which affect atmospheric dynamics, biogeochemical cycles of the elements and create persistent haze of unbreathable air.
Biomass combustion begins with a first drying phase with water release and volatile compounds production. Then, as temperature increases, the fuel pyrolysis take place, with the thermal breakdown of the molecules, that gives rise to by-products with effects not only on atmospheric and biogeochemical dynamics but also on human health [19]. During the combustion process, nitrogen contained in biomass is released as molecular nitrogen and, similarly to carbon and phosphorus, can be transported with atmospheric particulate matter. Hence, these nutrients decrease in ecosystems with the effect of variations in their biogeochemical cycles [3]. The vegetation fires also produce black carbon (BC) that can be transported to polar and alpine regions, and its subsequent deposition on icy and snowy surfaces [19] lead to a decrease in albedo, enhancing the capacity of these sensitive areas to absorb the heat of the sun and therefore to heat up and melt faster, in a positive feedback loop [20].
Forest clearance related fires contribute to the global burden of GHGs and cause associated global warming [21], again in a positive feedback mechanism, as the associated heating can amplify extreme fire events. The impacts of global climate change on the frequency, intensity, duration, and location of biomass burning are not well known and the estimates of fire contribution to emissions in past and future atmospheric composition are not clear [22]. FAO estimates made within the decade 2001–2010, regarding forestry and other land use (FOLU), report that total GHGs FOLU emissions were 3200 Tg of CO_2 eq per year, including deforestation (3800 Tg CO_2 eq y^{-1}), forest degradation and forest management (–1800 Tg CO_2 eq y^{-1}), biomass fires including peatland fires (300 Tg CO_2 eq y^{-1}) and drained peatlands (900 Tg CO_2 eq y^{-1}) [23]. Therefore, biomass burning and its emissions need to be observed and accurately mapped to comprehend variations in weather and climate over diverse temporal and spatial scales. Significant gaps remain in our understanding of the deforestation contribution to atmospheric emissions, but is known that nowadays fires in the tropical regions, most susceptible to these phenomena, are responsible for GHGs emissions quantifiable between 2000 and 5000 Tg CO_2 eq y^{-1} [3, 4] (Table 1.1) and that different fire fuels (savannah, forest, agricultural waste, and peat) lead to diverse gases and particulate matter emissions. In a global context where total anthropogenic GHGs emissions have continued to increase over 1970 to 2010 despite a growing number of climate change mitigation policies, anthropogenic GHGs emissions in 2010 have reached 49 $\pm$ 4500 Tg CO_2 eq y^{-1} [22]. Emissions of CO_2 from fossil fuel combustion and industrial processes contributed about 78% of the total GHGs emissions increase from 1970 to 2010, with a similar percentage contribution for the increase from 2000 to 2010 [22].

Table 1.1: Summary of the biomass exposed to fires, the total carbon released, the percentage of N to C in the fuel, and the total mass of N compounds released to the atmosphere by fires in the tropics [4].

Fire source or activity	**Carbon exposed** (Tg C year^{-1})	**Carbon released** (Tg C year^{-1})	**N/C ratio** (% by weight)	**Nitrogen released** (Tg N year^{-1})
Shifting agriculture	1000-2000	500-1000	1	5-10
Permanent deforestation	500-1400	200-700	1	2-7
Savannah fires	400-2000	300-1600	0.6	2-10
Firewood	300-600	300-600	0.5	1,5-3
Agricultural wastes	500-800	550-800	1-2	5-16
Total	2700-6800	1800-4700		15-46

1.2.1 Monosaccharide Anhydrides

Globally, terrestrial vegetation is the major biomass being burned, and cellulose, hemicellulose, and lignin are the three main polymeric constituents of plant biomass, nearly representing 30-60, 10-40 and 5-30 wt.% of dry biomass materials, respectively [24, 25]. Hemicellulose is a complex carbohydrate polymer whose thermal degradation occurs mainly between 220-315 ^{o}C; cellulose degradation mainly happens between 315 and 400 ^{o}C, owing to its high thermal depolymerisation resistance; lignin is a considerably hydrophobic, unstructured and highly branched polymer that decomposes between 280-500 ^{o}C (until 900 ^{o}C) and it is converted to more char than cellulose and hemicellulose [26, 27].
Cellulose pyrolysis creates the specific molecular marker levoglucosan (1,6-anhydro-β-D-glucopyranose) [28], while from hemicellulose combustion mannosan (1,6-anhydro-β-D-mannopyranose) and galactosan (1,6-anhydro-β-D-galactopyranose) are produced. These three isomers are called anhydrosugars or monosaccharide anhydrides (MAs; Figure 1.2) and, because of their accumulation and assumed persistence in natural archives, are in the focus as a tool for paleoenvironmental reconstructions [29]. Several studies about levoglucosan (L), mannosan (M) and galactosan (G) in aerosols and ice cores [30, 31, 32, 33, 34], but also in sediment cores [16, 17, 29], demonstrate the suitability of MAs as paleofire proxies.

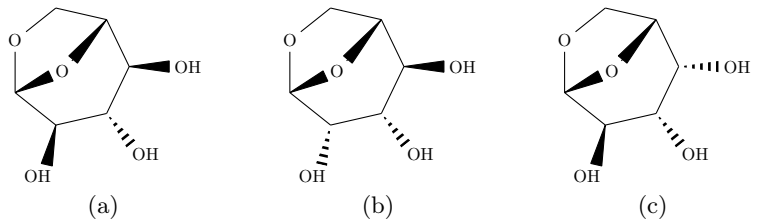

Figure 1.2: MAs: Levoglucosan (a), mannosan (b) and galactosan (c).

The level of levoglucosan increases with increasing combustion temperature [28], reaching maxima at 250 ^{o}C, and diminishing at higher temperatures [35], since cellulose pyrolysis over 390 ^{o}C has a low-rate degradation [25]. The eventually observed concentration peaks of levoglucosan could have been determined by some specific great fire events that could be correlated with changes in regional climate or with parameters such as dust transported by wind, precipitation, organic matter deposition in the lake, etc. The comparison of MAs with pollen and charcoal data is also fundamental in trying to disentangle fire's provenance and intensity and vegetation changes occurred in the area of interest.
Assuming that all three isomers are equally stable in the atmosphere and

in lake sediments and that MAs have a similar transport and deposition behaviour [29], the calculation of the ratios L/M and L/(M+G) is possible. These are promising tools in defining changes in vegetation at the source regions of the aerosols accumulated in sediments [36]. The notice of some abrupt changes in the trend of the two considered ratios may correlate with changes in vegetation recorded by pollen and n-alkanes data. Differences in their values are probably generated by different combustion conditions [35]. However, the major problem in assessing them is that the broad ranges of MAs ratio values from different studies overlap, limiting the conclusions about the burned biomass [16, 37, 38]. According to Kuo et al. [35], after 5 h of prolonged combustion at constant temperature (250 ^{o}C), mannosan and galactosan levels continuously decreased, compared to the results obtained after 0.5 h combustion, while levoglucosan presented no significant change. Higher combustion temperature (300 ^{o}C) and longer combustion duration result in higher ratios, regardless of plant species. This happens because mannosan and galactosan derive from the combustion of hemicellulose, which have a higher thermal lability, i.e. they can be changed or destroyed at higher temperatures, compared to that of levoglucosan, a cellulose combustion by-product, which may explain such overlapping data [27, 30]. Therefore, under such circumstances, the power of MAs ratios for source discrimination is seriously weakened and more complex parameters should be taken into consideration in order to better interpret the results. Therefore, PAHs, n-alkanes and FeSts were included in this study.

1.2.2 Polycyclic aromatic hydrocarbons

Polycyclic aromatic hydrocarbons (PAHs) are a wide group of organic compounds made up of two or more benzene rings combined together in a linear, angular, or clustered arrangement [39]. Their fused aromatic rings make them resistant to nucleophilic attack and to biodegradation, also because they possess physical properties, such as low aqueous solubility and high lipophilicity, which stand against their ready microbial utilization and promote their accumulation in the particulates of the terrestrial environment [15].

This class of molecules is produced by incomplete combustion in conditions of oxygen depletion of a large range of source processes, both natural and anthropogenic, such as volcanic eruptions, vegetation burning, fossil fuels and garbage combustion, car emissions, cigarette smoke [40, 41, 42]. PAHs are semi-volatile, persistent and ubiquitous in the environment, therefore are commonly detected in soil, air, and water [15, 42].

Few studies consider PAHs as tracers of biomass burning in past climate archives such as sediments [43] and ice [44], probably because of their multi-source origin. PAHs are often used in archives to reconstruct the most recent

(100-200 years) industrialisation and they have been rarely used for biomass burning reconstruction in Holocene or longer time scales, due to their low concentrations and, in ice cores, due to the need of large samples volumes. Thus, the correct interpretation of PAHs as biomass burning proxies must deal with a comparison to other fire tracers. PAHs deposited onto water bodies tend to precipitate and be stored in sediments, where particles they are adsorbed on prevent them from biodegradation [40, 45]. In addition to this, it is necessary to consider that some particles created from forest fires are quite coarse, thus, it is difficult for them to travel over large distances and PAHs attached to these particles provide a good preservation of the geochemical fingerprint of past fires [45]. Moreover, the lack of oxygen and the robust interplay with the sediments guarantee the stability of PAHs at high depth [46] and secondary deposition is not observed [47], making PAHs complementary to charcoal [48] and MAs [28].
The compounds of interest in this thesis are summarized in Figure 1.3 and Table 1.2.

Table 1.2: PAHs of interest and their abbreviations used in the text.

Compound	**Abbreviation**
Naphthalene	Naph
Acenaphthylene	Acy
Acenaphthene	Ace
Fluorene	Flu
Phenanthrene	Phe
Anthracene	Ant
Fluoranthene	Fl
Pyrene	Pyr
Benzo[a]anthracene	BaAnt
Chrysene	Chr
Retene	Ret
Benzo[b]fluoranthene	BbFl
Benzo[k]fluoranthene	BkFl
Benzo[a]pyrene	BaPyr
Benzo[e]pyrene	BePyr
Benzo[g,h,i]perylene	BghiPer
Indeno[1,2,3-c,d]pyrene	IPyr
Dibenz[a,h]anthracene	DBahAnt

PAHs are divided in four major categories on the basis of their sources: biogenic, diagenetic, petrogenic and pyrogenic. Biogenic PAHs are produced by plants, algae/phytoplankton, micro-organisms with post-depositional transformation of biogenic precursors, whereas diagenetic PAHs are produced

during the slow transformation of organic materials in lake sediments [39, 49]. Diagenetic PAHs refer to biogenic precursors, like plant terpenes, leading to the formation of compounds such as derivatives of phenanthrene. Other PAHs such as BbFl, Phe and Naph can be originated from vascular land plants or termite activity. Petrogenic PAHs are originated from petroleum, during crude oil maturation and similar processes and fossil fuels derivative substances [50] and are introduced into the aquatic environment through accidental oil spills, discharge from routine tanker operations, municipal and urban runoff [51].

Most pyrogenic PAHs follow a similar pattern along sediment cores, and the most abundant congeners tend to be the same in all records: Phe, Fle, Pyr, Ant, Fla, BaP, Chr. BghiPer (5-ring) generally has its origins in combustion and have been reported from high intensity paleovegetation fires [41, 47]. When fuel sources are uniform, hotter fires commonly produce elevated concentrations of 5- and 6-ring PAHs. In addition, highly condensed compounds, such as BePyr, are minimally susceptible to alteration and biodegradation [39] and well characterizes ancient records, being the most stable and often detected 5-ring PAH [43, 52].

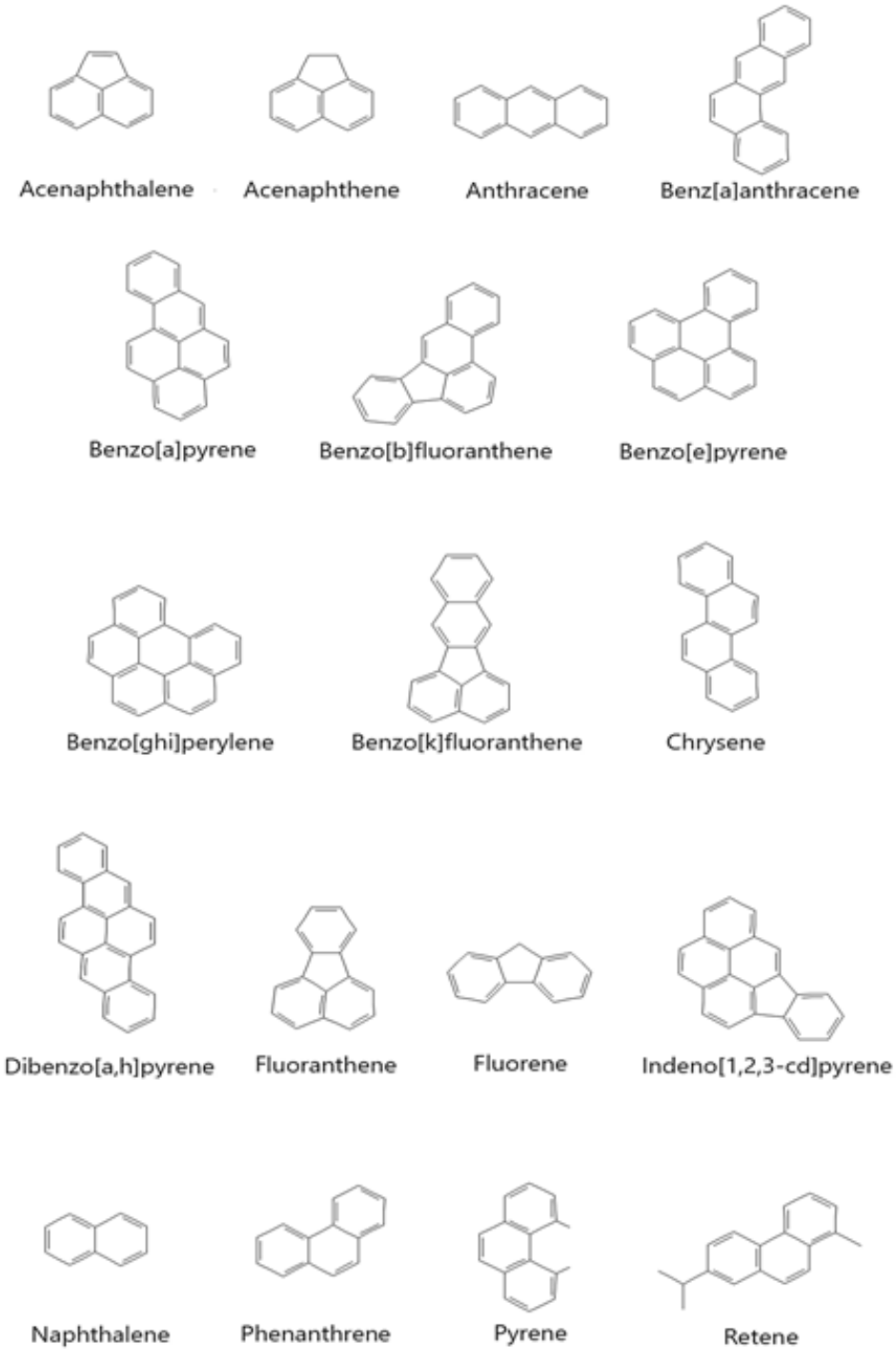

Figure 1.3: PAHs considered in this study: the priority 16 plus Benzo[e]pyrene and Retene.

1.2.3 Charcoal

In an archaeological and paleoenvironmental context, charcoal generally refers to micro and macroscopic residues resulting from the incomplete combustion of woody plant tissues [53] and, due to its easy sample pretreatment and to increasing interesting in fire regime reconstructions, it is the most used and reliable fire proxy [7, 53]. It is estimated that global biomass burning generates 40 million to 250 million tons of charcoal every year, part of which is preserved for millennia in soils and sediments [54]. It is an heterogeneous carbon-rich solid material formed during the pyrolysis of wood and coal, between 250 and 550 ^{o}C and it is also often used in radiocarbon dating processes. In most cases, pollen and charcoal data from the same cores are used to examine the linkages among climate, vegetation, fire, and sometimes anthropogenic activities in the past [55].

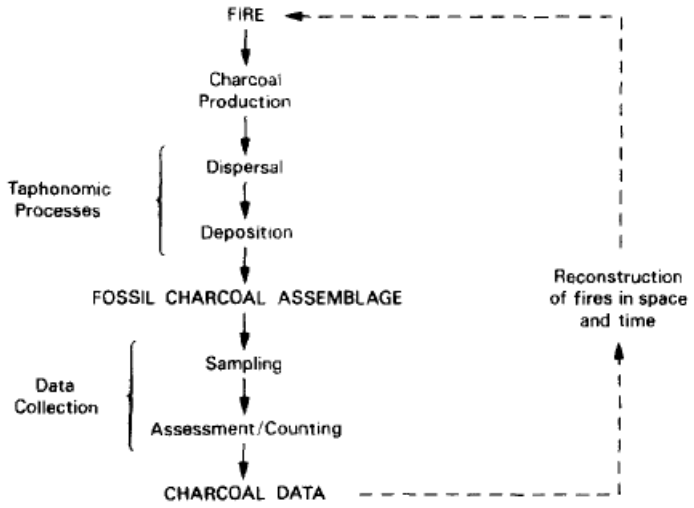

Figure 1.4: Relationship between fire and charcoal and approaches for reconstruction. Image source: [56].

Charcoal preserves well, but it may be subject to breakage, especially when transported by water [56]. Despite the stability and recalcitrance of charcoal, it does experience some environmental alteration and biodegradation in soil and may develop various surface functional groups over time [57]. Charcoal analysis quantifies the accumulation of charred particles in sediments during and following a fire event (Figure 1.4) and stratigraphic levels with abundant charcoal (called "charcoal peaks") are inferred to be evidence of past fires [55]. Charcoal particles vary in size from sub-microscopic to macroscopic, with small particles presumably being transported by wind and water further than large particles, differentiating local and regional/continental biomass burning

origin [56, 58, 59]. Larger charcoal particles (typically >100 μm in length) are predominantly isolated using wet sieving, and also referred as 'sieved' or 'macroscopic' charcoal [59]. Microscope is used to identify microscopic charcoal particles up to 10 μm, together on pollen slides [60]. In order to determine charcoal particles even smaller (indicative of large-scale biomass burning), a method with automated counting of the dark particles <0.2 μm^2, isolated by the image analysis of microscopic slides, is applied [61].
An open issue related to charcoal is that it may reflect residues derived from various processes and not solely from biomass burning [62], e.g. after the primary deposition it can also pass through secondary deposition effect [55]. A conjunct analysis of charcoal with other biomass burning proxies such as levoglucosan and BC [63] is therefore suggested.

The great advantage of charcoal is the high numbers of available records which can be collected and uploaded in the Global Charcoal Database (GCD). GCD is a public platform where fire datasets, acquired through a network of regional coordinators and working group members, are made free and available for anybody who needs them for scientific purposes. It provides easy access to an extensive network of fire history reconstructions [64] allowing global inferences about past biomass burning events and global synthesis [65] that revealed important variations in biomass burning during the last glacial period [66], the last 21 ky [67], and the last 2 ky [68].
Version 3 (GCDv3, n=736) of this database [69] (Figure 1.5) improves the previous ones, GCDv1 [67] and GCDv2 [65], by adding 57 records.

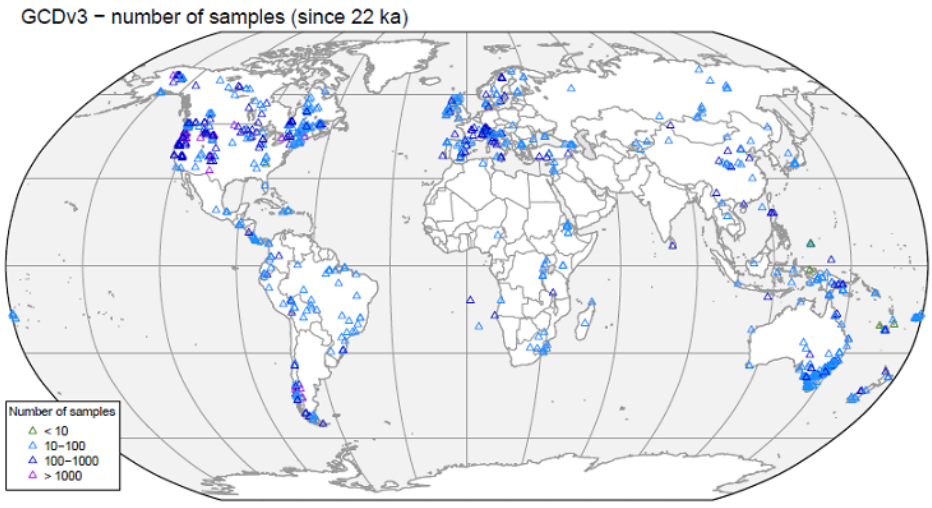

Figure 1.5: Location of paleofire sites and sampling density in the GCDv3. Image source: [69].

1.3 Past vegetation changes and human presence

1.3.1 N-alkanes

As the first interface between the plant and its environment, the cuticular wax layer, which consists predominantly of long-chain hydrocarbons, plays a key role in maintaining the plant's integrity within an inherently hostile environment, acting as a protective barrier [70]. In this work long-chain n-alkanes from C_{10} to C_{35} in sediment samples were investigated in order to infer paleoecology information of the studied area. Chain-length distributions of n-alkanes and their degradation products, n-alkanoic acids, help to distinguish different vegetation composition and watershed plant cover [71]. N-alkanes isotopic ratios are often calculated and studied to identify past climatic variations, especially regarding humidity, because organic molecules are usually depleted in δD compared with the water source, and subsequent correlations can be made. From a global point of view, site-averaged δDC_{29} and mean annual precipitation δD (δD_{MAP}) values are positively correlated, indicating that δD_{MAP} is the fundamental control on plant-wax δD values [72].
The leaf wax of higher plants is assumed to be stable, and difficult to be degraded during transportation, deposition and burial processes [73]. Different types of plants have in general diverse composition in chain-length of n-alkanes. That is the reason why the ratios among n-alkanes detected quantities are considered and used as paleo-proxies, instead of n-alkanes absolute concentrations.
Angiosperms generally produce more n-alkanes than gymnosperms and chain-length distributions are highly variable within plant groups, except for *Sphagnum* mosses, marked by their predominance of C_{23} and C_{25} [74]. Long chain n-alkanes (C_{27}–C_{33}) with a strong odd/even predominance are usually interpreted to be of terrestrial origin. Mid-chain n-alkanes (C_{20}–C_{25}) have been assigned mainly to aquatic macrophytes. Bacteria, algae and fungi are supposed to produce mainly short chain n-alkanes in the range C_{14}–C_{22}, while n-C_{17} in particular is considered to be a biomarker indicator for algae and photosynthetic bacteria [75, 76, 77, 78].
The average chain length (ACL) describes the average number of carbon atoms per molecule based on the abundance of the odd-carbon-numbered n-alkanes [79]:

$$ACL_{25-33} = \frac{\sum(n_{25-33})(C_{25-33})}{\sum(C_{25-33})}$$

It has been demonstrated that the modal carbon number of a higher plant n-alkane distribution is broadly related to latitude, with CPI (carbon preference index) and ACL values of n-alkanes in plants from low latitudes higher than those from high latitudes [79, 80]. Furthermore, the distribution of ACL has

been linked to the geographical distribution of fluvial and aeolian inputs and source regions [79].
In organic geochemistry CPI is used to indicate the degree of diagenesis of straight-chain geolipids, and it is a numerical representation of how much of the original biological chain length specificity is preserved in geological lipids [81]. It expresses odd/even predominance, with the formula according to Bray and Evans, 1961 [82]:

$$CPI_{23-33} = \frac{1}{2} \quad \frac{\sum C_{odd(23-33)} / \sum C_{even(22-32)}}{\sum C_{odd(23-35)} / \sum C_{even(24-34)}}$$

Terrigenous to aquatic (TAR) and aquatic to terrigenous (ATR) ratios can also be calculated [83, 84]:

$$TAR = (C_{27} + C_{29} + C_{31})/(C_{15} + C_{17} + C_{19})$$
$$ATR = (C_{15} + C_{17} + C_{19})/(C_{15} + C_{17} + C_{19} + C_{27} + C_{29} + C_{31})$$

Likewise, aquatic to terrestrial vegetation ratio can be calculated as:

$$(C_{23} + C_{25})/(C_{27} + C_{29} + C_{31})$$

Furthermore, Ficken et al. [85] proposed a ratio, P_{aq}, to identify submerged versus emergent aquatic plants, due to their different abundances in mid and long chain-length:

$$P_{aq} = (C_{23} + C_{25})/(C_{23} + C_{25} + C_{29} + C_{31})$$
$$or(C_{23} + C_{25})/(C_{27} + C_{29} + C_{31})$$

Proxies that reflect the relative proportion of waxy hydrocarbons derived from herbaceous plants to the ones coming from woody plants are these ratios [80, 86]:

$$C_{31}/C_{29}$$
$$Norm31 = C_{31}/(C_{29} + C_{31})$$
$$C_{31}/(C_{27} + C_{29} + C_{31})$$

D'Anjou et al. [14] used the ratio

$$(C_{25} + C_{27} + C_{29})/(C_{29} + C_{31})$$

as a proxy of changes in the relative composition of the terrestrial vegetation surrounding the lake, revealing transitions between birch woodland and a grassland-dominated system.
Finally, Bush et al. [74] put emphasis on the use of C_{23} as *Sphagnum* gender specific markers, especially using the ratio

$$C_{23}/(C_{23} + C_{29})$$

to readily distinguish modern *Sphagnum* mosses from woody angiosperms.
The ratios that can be applied to n-alkanes datasets are copious, but it is necessary to remember that these operations must be performed considering that the sedimentary post depositional processes can influence the results.

1.3.2 Faecal Sterols

Faecal sterols and stanols (FeSts) belong to the steroid faecal biomarkers that are mainly produced by humans and grazing animals. Table 1.3 lists the molecules analysed in the present study.

Table 1.3: FeSts of interests and their abbreviations used in the text.

Compound	**Abbreviation**
Coprostanol	CoP
Epicoprostanol	e-CoP
Cholesterol	Chl
Cholestanol	5α-Ch
Sitostanol	5α-Sit
Sitosterol	Sit

FeSts such as stanols and bile acids have been used as biomarker indicators in lake sediments for the detection of grazing in a lacustrine catchment [14]. 5β-stanols are organic compounds produced by the microbially mediated alteration of cholesterol in the intestinal tracts of most mammals, making them ideal faecal biomarkers [87]. Coprostanol and stigmastanol derive from hydrogenation of cholesterol and stigmasterol by indigenous bacteria present in the gut of humans or animals (Figure 1.6) and can indicate human presence and husbandry, respectively [88, 89]. Nowadays these molecules are also used as a chemical indicator of faecal pollution of lakes, rivers, drinking water [88, 89, 90]. Other metabolites of cholesterol are epicoprostanol, epicholestanol and cholestanol, which are stereoisomers. The sterols composition provides the potential for discriminating between sources due to the fact that human faeces differs from those of other animals [90].

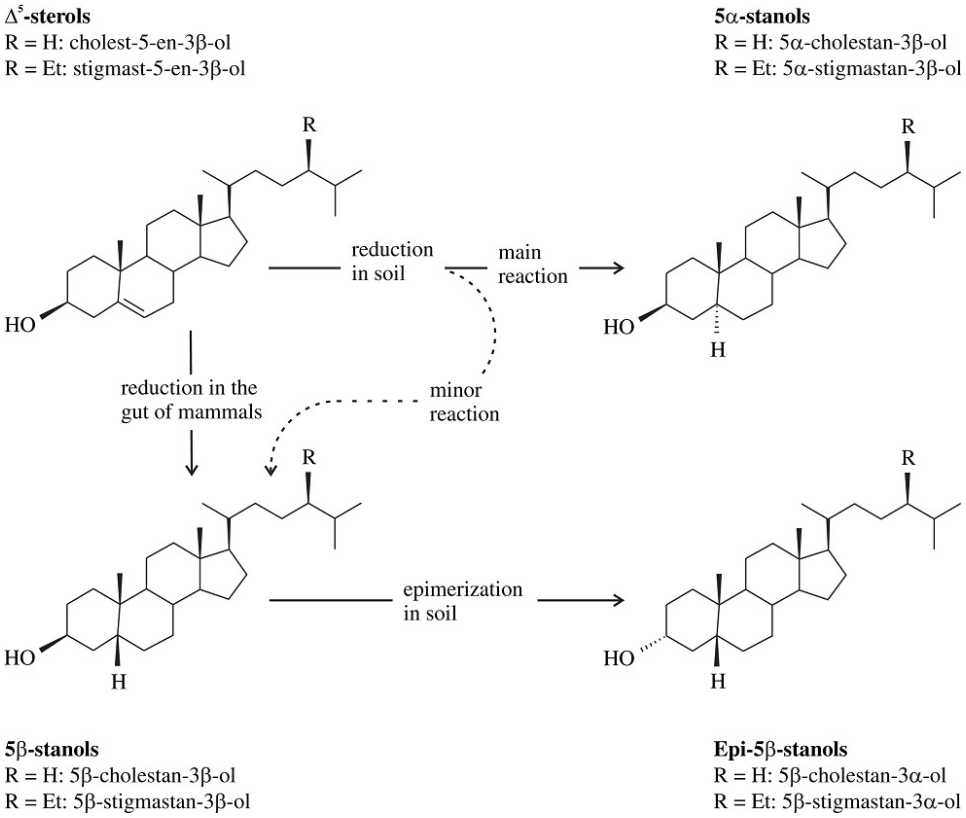

Figure 1.6: Products of $\Delta 5$-sterols reduction in the mammals' intestine and in soils. Image source: [91].

The following ratio was suggested by Bull et al. [92] to distinguish between omnivore (pig/human) and ruminant species:

$$\frac{coprostanol + epicoprostanol}{5\beta - stigmastanol + epi - 5\beta - stigmastanol}$$

where coprostanol (5β-cholestan-3β-ol) is mainly produced by humans and 5β-stigmastanol serves as the biomarker of herbivore faecal matter. Furthermore, FeSts can not only originating from animal sources but also from vegetation, e.g. β-sitosterol is synthesised by higher plants [93] and his derivative β-sitostanol is generated from its reduction in sediments.

Chapter 2

Study Area

2.1 Tibetan Plateau as paleoresearch area

The Tibetan Plateau (TP), or Qinghai-Tibetan Plateau, is a vast plateau in central Asia with an average elevation of about 4500 m above sea level (asl). It expands nearly 1000 km North to South and 2500 km East to West, covering an area of 2 x 10^6 km^2 [94]. The plateau encompasses an enormous range of altitude and latitude, both of which contribute to maintain a broad diversity of landscape (Figure 2.1) with a wide range of species distribution. It is considered a very important research area, due to its sensitiveness to century-scale or short-term climatic changes [95]. However, because of the rough conditions, the scarce investigations on the Tibet Plateau result in the sparse knowledge of its species diversity and plant communities [96] and distribution of biodiversity patterns along altitudes and latitudes in this area are still under investigation. The domination of meadow, steppe and shrubs and a weak monotonically increasing trend in species richness with increasing altitude were observed by Shimono et al. [97] between 3200 and 5200 m asl, looking at 23 sites from the Qinghai-Tibetan Plateau. Wang et al. [96] documented 242 different species of herbs, shrubs and trees in a transect of 600 km in the north-eastern Tibetan Plateau, with a decreasing trend in biodiversity in the altitude range from 3255 to 4460 m asl. In addition, Zhang and Mi [98] reported an increasing trend in plant richness in northern China with increasing elevation from 2100 to 3050 m asl, explaining that this phenomenon could be due to different grazing intensity, more severe at lower latitudes.

Focusing on human occupation of the Asiatic continent, initial steps towards settled agricultural villages started around 11 ky BP [99], concurrently with the starting of the Holocene, the present geological epoch that began 11.7 ky BP right after the Pleistocene. Evidences for the cultivation of millet, rice and other plants as well as animal husbandry are documented in different

Figure 2.1: Particular from the South-eastern TP, Lhasa River. Image source: CC0.

regions of China; ancient cultivations (mostly wheat, millet and barley) are reported also in the Tibetan Plateau [100, 101]. Human presence in this area during the Neolithic period is well known, due to recorded information about the human migrations during the Holocene in this country. Zhang et al. [101] report that people started moving at the beginning of the Last Deglacial Period starting from the North-eastern part of China and getting back on top of the course of the Yellow River (Figure 2.2). In the Early Holocene they spread into the north-eastern Tibetan Plateau and started colonizing it, moving southwards to the interior plateau, possibly with millet cultivation. In the mid Holocene the Neolithic agriculture was settled into low elevation river valleys in the north-eastern and south-eastern plateau areas. In the late Holocene (4–2.3 ky BP), Bronze Age's barley and wheat farmers further settled on the high elevation regions of the Tibetan Plateau, especially after 3.6 ky BP [101]. It appears that rice agriculture and domestication of animals was diffused to South China by about 3 ky B.C. [99, 102]. However, human impact in this zone could have started before, because Early Holocene's stone tools such as hafted axes for forest clearance were found [102].

Up to now, the current human impact generated an overall increasing trend in deposition fluxes of black and organic carbons since 1980, that is consistent with the emissions from Southern Asia, the major contributor due to coal, oil and biomass consumption in the area [20, 104].

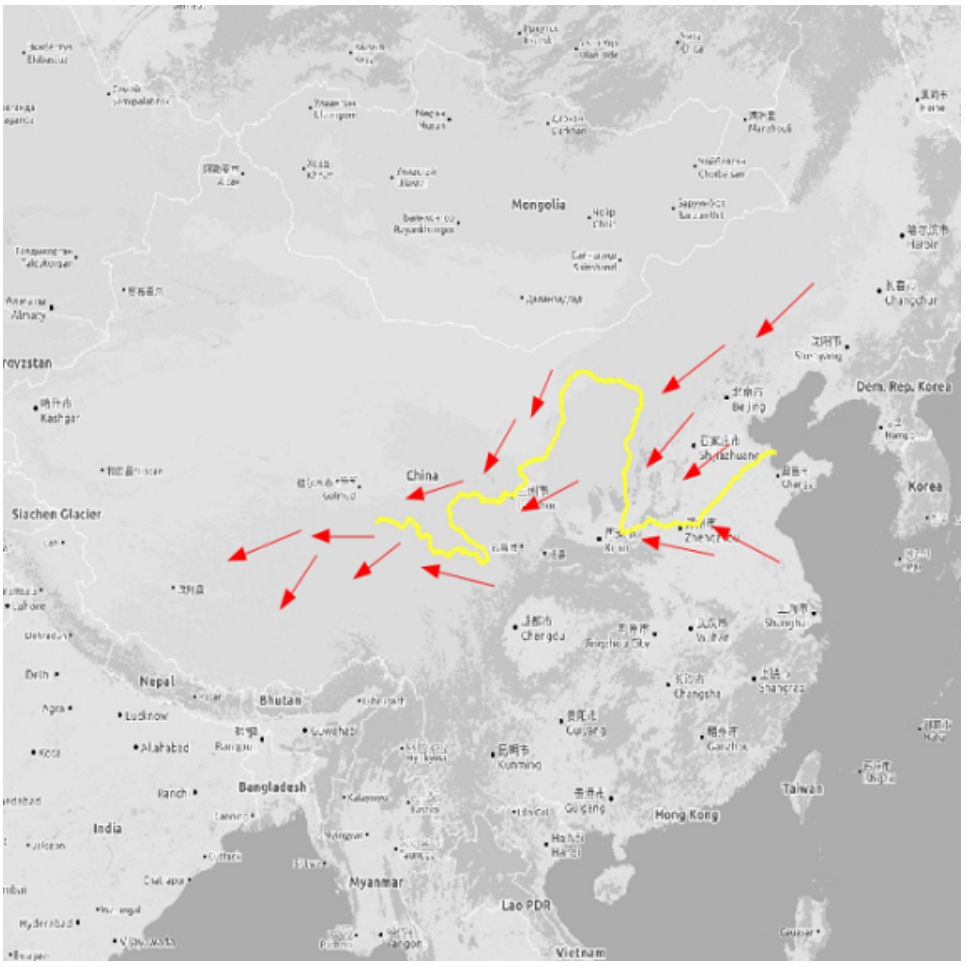

Figure 2.2: Late Quaternary human migration in China along the course of the Yellow River. Image source: [103].

2.2 Holocene climate

Numerous recent studies demonstrated climatic variations throughout China and its surrounding areas during the Holocene [105, 106, 107, 108]. Paleoclimate proxies such as carbonate, mineralogy, grain-size, elemental geochemistry, stable isotope composition, leaf wax long-chain n-alkanes, aquatic diatoms and terrestrial pollens recorded changes in lake levels, land cover, temperature and precipitation. However, few studies examined past biomass burning using charcoal in sediments [58, 9] or black carbon and ammonia in ice cores solving only the last century [109, 110, 111, 112, 113].
Tibetan Plateau's climate is regulated by the critical and sensitive junction of four climatic systems: the Westerlies, the East Asian Monsoon, the Siberian cold polar airflow (or Winter Monsoon), and the Indian monsoon [94]. West-

erly winds and the Southern monsoon are considered the major sources of atmospheric particulate matter derived from biomass burning in the plateau [33]. Moreover, TP induces and enhances the Asian monsoon that influences the plateau itself, East China and even the whole of Asia [114].

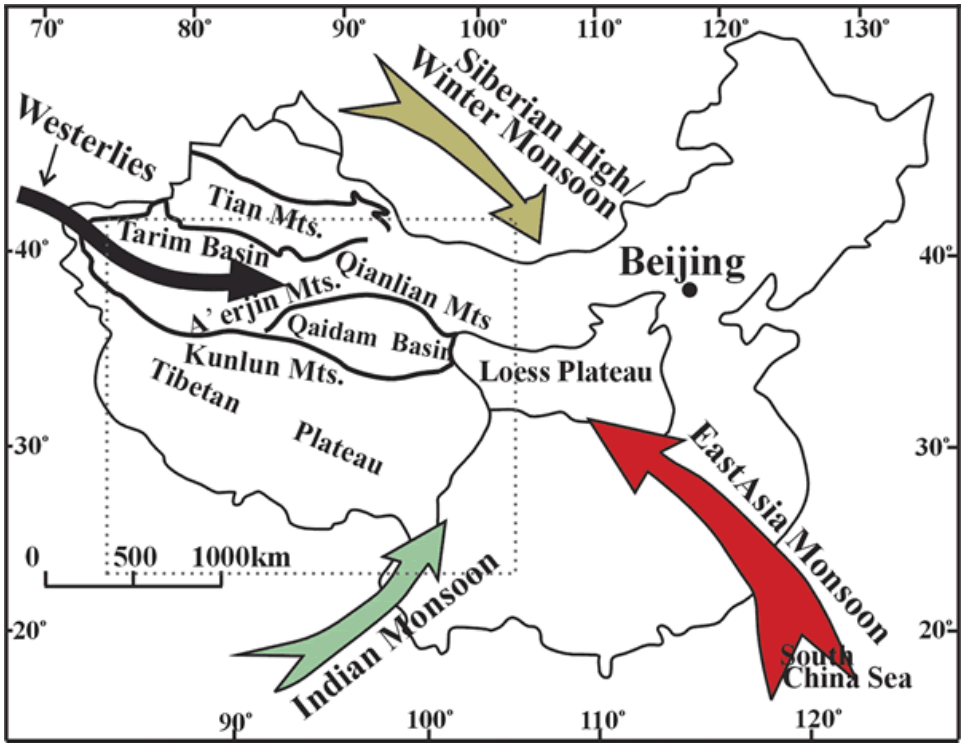

Figure 2.3: Major climatic systems acting on the Tibetan Plateau. Image source: [94].

At 16 ky BP, desert-steppe dominated the area owing to cold and dry climates [115] specific of the late Pleistocene. Paleoclimate studies globally indicate that this last glacial period concluded with a sudden warming event at 15 ky BP [116].
The subsequent transition to the Holocene was characterized by increasing temperature and precipitation that enhanced the permafrost and snow melting and facilitated trees to grow in the Tibetan Plateau after 12 ky BP [115, 117]. This period was delineated by frequent oscillations between warm and cold phases, in Tibet as well as in other parts of the world [114, 118, 106]. As an example, Tang et al. [115] suggest that the evolution of South Asian Monsoon has considerably fluctuated throughout the Holocene. The warm and humid climate in the early to mid-Holocene is registered in sediments and dust deposits worldwide [118]. The higher temperatures during this period accelerated evaporation and caused many Tibetan lakes to evolve from open freshwater systems to saline lakes [94] and between 9.2 to 6.3 ky BP forest and

forest-meadow increased in number [115]. A cooling trend was observed at Lake Donggi Cona (North-eastern TP) by Saini et al. [117] between 9.2 and 3.0 cal ky BP and it was accompanied by higher moisture availability caused by reduced evaporative conditions due to a drop in temperature and recovering Westerlies. Furthermore, Prokopenko et al. [119] found that warmer summers between 6 and 3.5 ka BP resulted in the decline, not expansion, of forest vegetation around Lake Hovsgol (Mongolia), apparently as a result of higher soil temperatures and lower available humidity. In spite of this, some cold events were identified studying Lake Ximencuo (Eastern Tibet) [120]; such events occurred between 10.3–10.0, 7.9–7.4, 5.9–5.5, 4.2–2.8, 1.7–1.3 and 0.6–0.1 cal ky BP, with the one at 4.2 cal ky BP considered as the most impacting and are confirmed also by Miao et al. [121].
During the late mid-Holocene to late Holocene, the warm-wet shifted towards a cooler and drier climate, due to a weakened solar insolation, and after 5 ky BP, temperature and precipitation decreased linearly [94, 115, 122]. More recently, human activities and related regional climate change have significantly altered the regional hydrology and ecosystem functions of the plateau, with degeneration of vegetation and grassland that led to desertification and frequently induced dust storms [123].

2.3 Paru Co and Hala Hu lakes

This PhD thesis is focused on a multi-proxy study applied to lakes Paru Co and Hala Hu, located in the South-Eastern Tibetan Plateau (SETP) and North-Eastern Tibetan Plateau (NETP) respectively. Paru Co (Figure 2.5) is

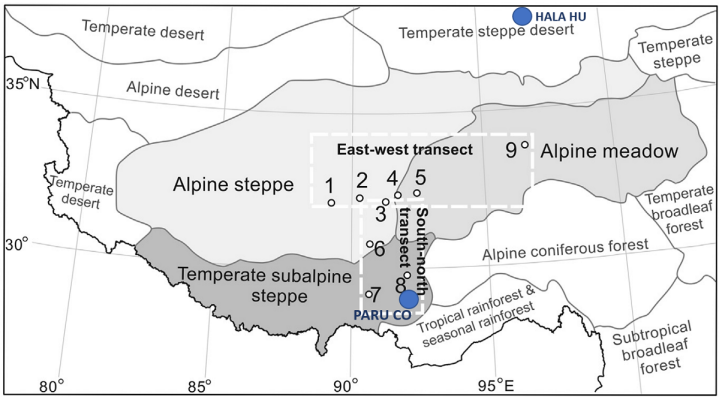

Figure 2.4: Vegetation distribution on the Tibetan Plateau with the locations of the lakes Paru Co and Hala Hu, indicated with blue circles. Numbers 1 to 9 indicate sites of lacustrine pollen records in central TP. In the east-west transect: 1. Selin Co, 2. Xuguo Co, 4. Co Ngion, 5. Ahung Co, 9. Koucha Lake. In the south-north transect: 3. Lake Zigetang, 6. Nam Co, 7. Chen Co, 8. Hidden Lake. Image source: [124], Editorial Committee of Vegetation Map of China (2007).

a small moraine dammed lake (0.1 km^2) in the Nyainqentanglha Mountains, at 4845 m a.s.l. (29^{o}47'45.6"N, 92^{o}21'07.2"E), located within the biome of the temperate subalpine steppe, near the border with alpine coniferous forest and tropical and seasonal rainforests (Figure 2.4). The lake's watershed (2.97 km^2) consists of a broad, shallowly sloping glacial valley measuring 0.5 by 2.0 km with lateral mountain ridges of 5170 to 5140 m a.s.l. and a central ephemeral stream channel. The local bedrock is geologically homogeneous, consisting of Pleistocene age andesite [125].
Circa 1000 km far from Paru Co is located Hala Hu (Figure 2.6), a 590 km^2 Tibetan lake located in the Qilian Mountains at 4078 m asl, $\sim$ 100 km Northwest of China's large inland Lake Qinghai. It has a catchment area of 4690 km^2 and it is surrounded by high mountain ridges, some exceeding 4700-5000 m asl, by large alluvial fans and by fluvial deposits related to runoff from glaciers. Nearly all perennial rivers around the lake contribute with melt water and sediments to the lake. A small, mobile barkhan dune developed at the eastern margin of the lake, indicating major wind from the west [126]. The north-western and eastern sub-catchments of Hala Hu are mainly comprised of siliciclastic sedimentary and low-grade metamorphic rocks (siltstone, sandstone, slate, quartz-schist, conglomerates, and breccia),

as well as carbonate rocks (limestone, marlstone, subordinately dolostone) in unknown proportions and of varying age, but mainly Permian and Triassic, with some from the Neogene. The southern sub-catchments include a huge body of Silurian sandstone, marlstone and intercalated andesite, as well as the aforementioned rocks from the Permian and Triassic successions. The northern sub-catchments mainly show sedimentary rocks of Neogene age, comprising sandstone, marlstone and conglomerates. The lower parts of all sub-catchments comprise Quaternary siliciclastic sediments of varying grain size, from clay to gravel [126].

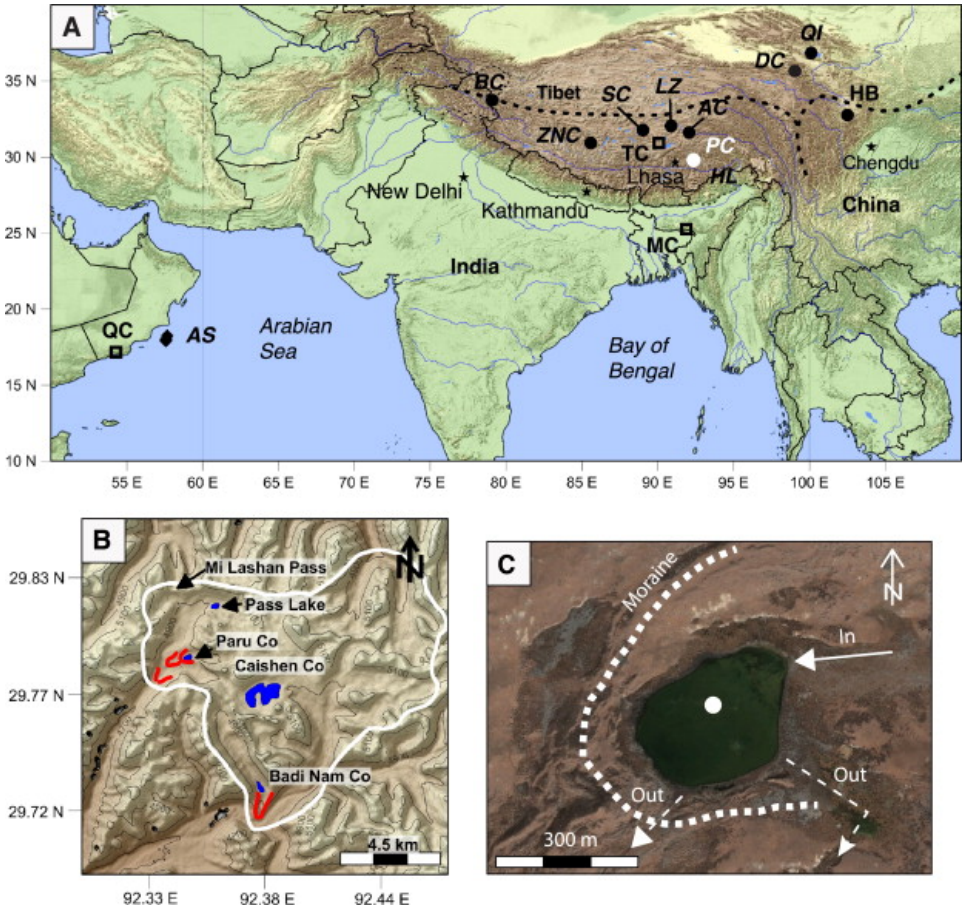

Figure 2.5: A: Map of southern Asia. Black dashed lines indicate the maximum extents of the Indian and Asian summer monsoons. Paru Co (PC), Hidden Lake (HL), Ahung Co (AC), Lake Zigetang (LZ), Tianmen Cave (TC), Seling Co (SC), Zhari Namco (ZNC), Bangong Co (BC), Qinghai (QI), Hongyuan Bog (HB), Mawmluh Cave (MC), Qunf Cave (QC) and the Arabian Sea sediment cores (AS). B: Expanded view of the study area showing the location of Paru Co and other nearby lakes. Moraines are identified with red lines. The white line marks the approximate extent of the hypothesized ice cap that at one time may have covered the study area. C: Satellite image of Paru Co and its immediate watershed, including the moraine dam (thick white dashed line), the core location (white circle), and the main location of seasonal inflow (solid white arrow) and the overflow point (dashed white arrow). Image source: [125].

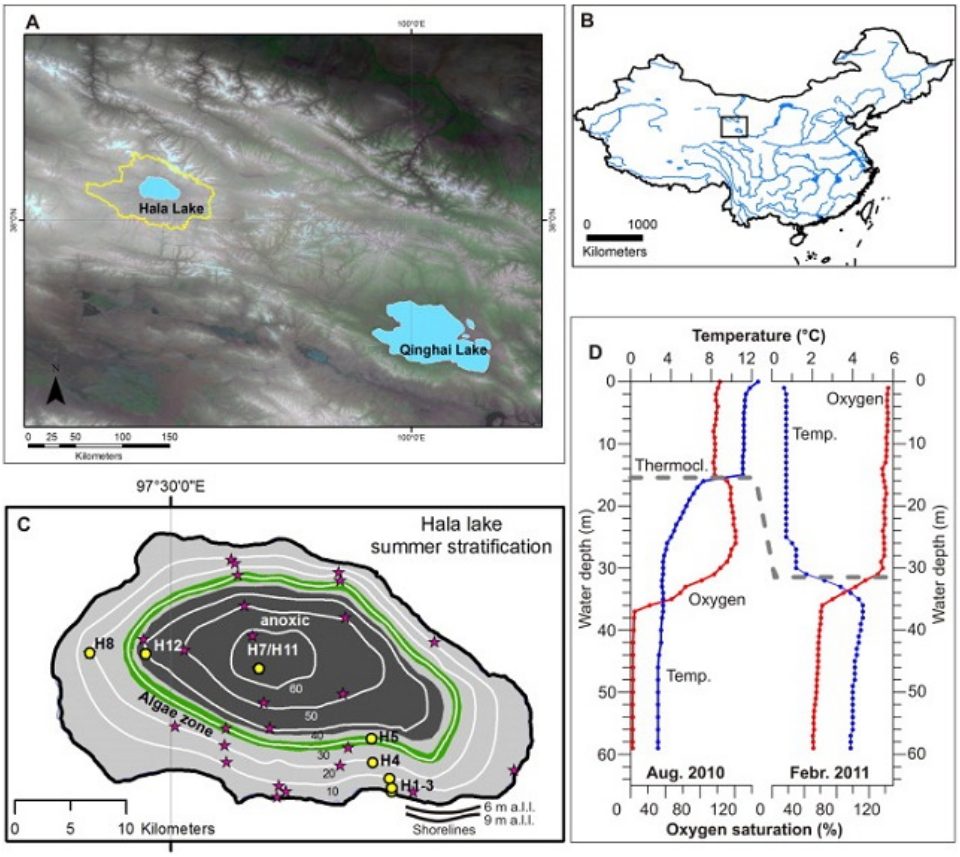

Figure 2.6: A: Overview map of the area between Qinghai Lake and Hala Lake. Catchment is marked with a yellow line. B: Study site within China. C: Lake shape of Hala Lake with bathymetry and the distribution of green algae and anoxic zones. Location of drill sites in yellow. D: Oxygen and temperature graphs, measured in summer and winter 2010, according to Wünnemann et al (2012) [126]. Image source: [13], Landsat TM, SRTM image.

Chapter 3

Materials and Methods

3.1 The investigation of lacustrine sediment cores

Based on a literature research, lacustrine sediments in the area of interest were investigated in order to find available samples already with geochemical description and core chronology covering the entire Holocene. A useful tool in these types of investigations is *LacCore*, the National Lacustrine Core Facility provided by the University of Minnesota. This institution collects cores and samples from continental coring and drilling expeditions around the world and supports projects from scientists dealing with core samples from any location.
Initially the research was focused on cores located in Eastern China due to the first advent of pastoralism and human migrations, but no samples were available and/or suitable to the aim of the research. This is the reason why other areas in the Asiatic continent started to be investigated, allowing to come into contact with different researchers from different countries, with expertise in studying sediments and drilling campaigns in China and Mongolia. As a result, some explorative lacustrine samples to be tested for MAs presence with the analytical methods developed by our research group were provided by the scientists listed below:

- Broxton Bird from Indiana University-Purdue University, USA: Lake Paru Co (PC), SETP;
- Alexander Prokopenko from University of Cologne, Germany: Lake Hovsgol, Mongolia;
- Bernhard Aichner from University of Potsdam, Germany: Lake Ozera Karakul, Tajikistan.

11 samples from Paru Co core were used for testing our analytical methods. Since interesting preliminary results were acquired from Paru Co (subsection 4.1.2), 72 samples from the whole length of Paru Co B-11 core were

requested and analysed.
Preliminary results obtained from Ozera Karakul did not show significant MAs concentrations, and Hovsgol samples were not suitable for our purposes (insufficient amount of material, not well conserved). Thus, these two lakes were excluded from this study.
Then, the collaboration with Dirk Sachse and Bernhard Aichner at the Helmholtz Centre Potsdam GFZ German Research Centre for Geosciences allowed to prepare 115 samples from core H-11 of lake Hala Hu (HH) located in NETP, with the aim of both assessing fire activity as well as investigating them for other proxies.

3.2 Materials and Methods

Sediments sub-sampled from the core of interest were weighted, freeze-dried, ground and re-weighted in order to get the water content and to assure that the quantity of the sample was enough to be extracted with organic solvents; in general 1 g of dry material is considered sufficient. The mechanic grinding treatment was performed using the ball miller (Mixer Mill MM 400, Retsch GmbH) for lake Paru Co and using mortar and pestle for lake Hala Hu (Figure 3.1).

Figure 3.1: Instruments for mechanic grinding treatment.

The subsequent steps were extraction, purification and analysis. The extraction was carried out with organic solvents at elevated temperature and pressure, in order to retrieve the organic compounds included in the total lipid content of the sediments. A mixture of DMC:MeOH 9:1 v/v was used for Paru Co, while firstly DCM and then MeOH were used for Hala Hu extractions. These different methods are due to diverse labs management

approaches regarding the use of the ^{13}C labelled internal standard, added before the extraction in Venice, and after the extraction in Potsdam, because it was not permitted in the ASE's lab due to isotopic analysis ongoing. The main problems generated by the use of two different methods are the dissimilar quantification of the fluxes and the not absolute comparability of the results of the two lakes.
The purification, or clean-up, was performed eluting silica gel columns with different solvent in order of polarity, with the aim to separate diverse compounds from the total lipid extract and also to remove dirty particles that can interfere with the analysis. The final step of the analysis was achieved with two analytical techniques (Figure 3.2): Ion Chromatography (IC Dionex ICS 5000, Thermo Scientific, Waltham, USA) coupled with a single quadrupole Mass Spectrometer (MSQ Plus^{TM}, Thermo Scientific) and Gas Chromatography (6890-N GC system) coupled to a single quadrupole Mass Spectrometer (MS 5975, Agilent Technologies, Santa Clara, CA, USA).

(a) *IC-MS.* (b) *GC-MS.*

Figure 3.2: Chromatographers and spectrometers used for the analysis of biomarkers.

Chromatographic peaks identification and calculation were performed with Chromeleon^{TM} 6.8 Chromatography Data System (CDS) Software (Thermo Scientific, Waltham, USA) and Agilent G1701DA GC/MSD ChemStation (Agilent Technologies, Santa Clara, CA, USA). Data elaboration and statistics were performed with Microsoft Excel, R, OriginPro 8 and MetaboAnalyst 3.0 [127].

3.2.1 Standards, reagents and solvents

All isotope-labelled standards of levoglucosan and PAHs were acquired from CIL (Cambridge Isotope Laboratories Inc., USA). 1,6-anhydro-β-D-

mannopyranose (mannosan) and 1,6-anhydro-β-D-galactopyranose (galactosan) were purchased from Molekula (Molekula Limited, UK). 1,6-anhydro-β-D-glucopyranose (levoglucosan), hexatriacontane, 5β-cholestan-3β-ol (CoP), 5β-cholestan-3α-ol (e-CoP), cholest-5-en-3β-ol (Chl), 5α-cholestan-3β-ol (5α-Ch), 24-ethyl-5α-cholestan-3β-ol (5α-Sit), 24-ethyl-cholest-5-en-3β-ol (Sit), ^{13}C-labelled cholesterol-25,26,27-$^{13}C_3$ ($^{13}C_3$-Chl) and cholesterol-3,4-$^{13}C_2$ ($^{13}C_2$-Chl) were purchased from Sigma-Aldrich (Sigma-Aldrich Co. LLC.) and used as internal standards and/or standards for the preparation of response factors. According to a correct conservation procedure, all the standard solutions were stored at -20 ^{o}C.
N-alkanes standards C_{10}-C_{35} and PAHs native standard solutions (PAHMix 9) were furnished by Dr. Ehrenstorfer GmbH (Augsburg, Germany). N-alkanes, PAHs and FeSts response factors were prepared in DCM.
As derivatizing agent BSTFA + 1% TMCS (N,O-bis(trimethylsilyl)trifluoroacetamide with 1 % trimethylchlorosilane, Sigma-Aldrich) was used.
At the laboratories of the Department of Environmental Sciences, Informatics and Statistics in Ca' Foscari University of Venice, lab's tools and glassware were washed with an aqueous 5% (v/v) Contrad® solution (Decon Laboratories Limited, UK), dried and rinsed with solvents. Ultra-grade acetone (Ace), dichloromethane (DCM), *n*-hexane (Hex), and methanol (MeOH) (Romil Ltd., Cambridge, UK) were used firstly to decontaminate glassware and lab's tools and secondly to extract, purify and analyse the samples. Anhydrous Na_2SO_4 (Carlo Erba Reagenti S.p.A., Milan, Italy) was dried in oven at 150 ^{o}C for 24 h, washed with both DCM and Hex, stored with Hex and then used as drying agent for the extractions. Metallic copper (Carlo Erba Reagenti S.p.A., Milan, Italy) was activated by rinsing it three times with hydrochloric acid and solvents (water, Ace and DCM), stored in de-aerated Hex and used as interference removal agent to prevent that molecular sulphur interferes with PAHs analysis. Diatomaceous earth and Ottawa sand (Applied Separations Inc., Allentown, PA, USA) were used as inert materials and inserted in the steel vessels for the extractions.
A spoon of aluminium oxide (Sigma-Aldrich) was added in the purification cartridges in order to remove particulates that could obtrude the analytical instruments' columns.
At the laboratories of the section 5.1 of Geomorphology at GFZ, Potsdam, glassware was cleaned in a dishwasher and dried in the oven a 500 ^{o}C to prevent the contamination from organic residues. Ultra-grade Ace, DCM, Hex and MeOH (Carl Roth GmbH + Co. KG, Karlsruhe, Germany) were used both for cleaning lab's tools and for extracting and purifying the samples.

3.2.2 Paru Co's method

The Paru Co B11 core is 435 cm depth and was collected by Prof. Broxton Bird in 2011. The material was radiodated in order to obtain its age model (Figure 3.3). Radiocarbon age determination by accelerator mass spectrometry (AMS ^{14}C) was conducted on seven samples of carbonized grass fragments and one sample of oogonia, after separation from sediment intervals, and it is already published [125]. The sedimentation rate is approximately 0.35 mm y^{-1} over the entire core length, except for the last section, between 10.9 to 10.7 ky BP, where it is ten times higher (3.3 mm y^{-1}). The final age model was constructed using linear regression between 434.9 and 364.1 cm and by fitting a 3^{rd} order polynomial to the AMS ^{14}C, ^{137}Cs (-0.013 ky) and sediment-water interface (-0.061 ky) ages between 364.1 and 0.0 cm and the associated error is between 15 and 90 years (see Bird et al. [125] for more details).

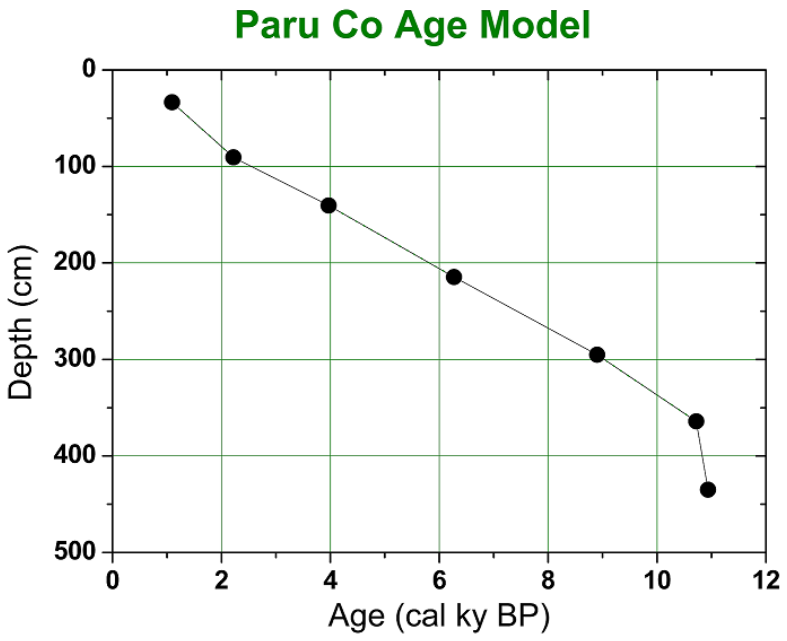

Figure 3.3: Age Model obtained for Lake Paru Co.

Relative total organic matter (%TOM) and total carbonate (%TC) were then determined by weight loss after ignition at 550 ^{o}C (4h) and 1000 ^{o}C (2h), respectively. Biogenic silica and lithic abundances were also calculated at the Indiana University-Purdue University by Prof. Bird and its research team.

Test samples 11 test samples were available in order to assess the potential interest of the core in paleofire reconstruction. The test sediment samples cover equidistantly and uniformly the depth of the core and their weight ranged from 0.32 to 1.31 g of dried material. These samples were extracted with PLE^{TM} (Pressurized Liquid Extraction, FMS, fluid managment sistem Inc., Watertown, MA, USA) only with MeOH as solvent at temperatures of 150 ^{o}C and pressures of 1500 psi. After extraction, the samples were filtered with PTFE filters (pore size 0.2 μm), dried under a stream of N_2 with TurboVap II® system (Caliper Life Science, Hopkinton, MA, USA), dissolved in 0.5 ml of ultra-pure water and sonicated to avoid any adsorption of MAs to the walls of the evaporation glass tubes. Finally, the samples were centrifuged (5 min, 14000 rpm) and transferred to the measurement vials. A blank was extracted every batch of 5 samples.
Final analyses were performed according to Kirchgeorg et al. [29] with IC-MS equipped with CarboPac PA1^{TM} and CarboPac PA10^{TM} columns (Thermo Scientific, each 2 mm x 250 mm) and an AminoTrap column (2 x 50 mm) to trap amino acids, that allowed to obtain a good separation of the isomers. The injection volume was 50 μL. MeOH/NH_4OH was added post-column (0.025 mL min^{-1}) to improve ionization of the aqueous eluent before entering the ESI (electrospray ionization) source used in negative ionization mode. Analytes (m/z 161) were quantified with response factors' calibration curve of levoglucosan, mannosan and galactosan, with increasing concentration of the natives from 1 to 1000 ppb - as well as levoglucosan ^{13}C labelled internal standard (m/z 167) at 200 ppb. The retention times were 4.8, 6.4 and 9.1 min (Figure 3.4, (B)) and the estimated overall method uncertainty was 4.7%, 9.9% and 8.7% for levoglucosan, mannosan and galactosan, respectively. Instrumental LOD and LOQ were estimated to be 4.5 and 14.5 ppb for the three isomers. For the full method details see Kirchgeorg et al., 2014 [29].

Complete record The complete MAs record of Paru Co consists of 72 samples sub-sampled from the core at intervals of 5 cm. The time resolution of this record is about 130 years on average, and spans from 1300 to 10900 cal y BP. For the analyses of these samples a new method was applied to combine MAs analyses with PAHs, FeSts and n-alkanes. The 72 Paru Co samples were extracted with a mixture DCM:MeOH 9:1 v/v with Thermo Scientific Dionex ASE 350 (Accelerated Solvent Extractor system), in the way to extract both non-polar and polar fractions, and then purified with three steps to get the PAHs/n-alkanes fraction, the FeSts fraction and the MAs fraction.
In each steel ASE cell (22 mL total volume) were inserted a cellulose filter, diatomaceous earth, the sample, 1 spoon of Na_2SO_4 and 1 spoon of activated copper and the internal standards: 100 μL of levoglucosan ^{13}C labelled at 1 ppm of concentration, 100 μL of hexatriacontane at 40 ppm, 100

μL of a mixture of PAHs ^{13}C labelled (Acenaphthylene, Phenanthrene and Benzo[a]pyrene) at 1 ppm, 100 μL of cholesterol-3,4-$^{13}C_2$. The extractions were performed with three cycles of static, at 100 ^{o}C, 1000 psi and a rinse volume of 60% for every cycle.
The purification of the samples was needed to separate the diverse analytes in different fractions, in the way to detect them with the proper analytical methods. The clean-up technique that we settled is a reworking and combination of different published methodologies [29, 128, 129, 130]. This method involves the use of 12 mL Solid-Phase Extraction cartridges (SPE DSC-Si Tube; 12 mL; 52657 Supelco, Sigma-Aldrich) packed with 2 g of silica gel (particle size 50 μm) and installed on Visiprep^{TM} (SPE Vacuum Manifold standard, Sigma-Aldrich) to accelerate the purification. For the conditioning of the cartridge 30 mL of DCM and 30 mL of Hex were used. The first non-polar fraction F1, containing PAHs and n-alkanes, was eluted using 40 mL of a mixture (Hex:DCM=9:1). Then, the second polar fraction F2, containing FeSts, was separated with 70 mL DCM. This fraction was needed to be derivatized at least for 1 h at 70 ^{o}C with 100 μL of BSTFA (sylilation reaction) to increase volatility and detectability of the compounds for analysis with GC-MS. Finally, the third polar fraction F3, that contains MAs, was separated with 20 mL of MeOH.
MAs were detected with IC-MS [29] at the same instrumental conditions as the test samples, except for the column. In this case CarboPac MA1^{TM} was used instead of PA1 and PA10, with a better separation and retention times of 6.2, 9.6 and 16.0 min for levoglucosan, mannosan and galactosan respectively (Figure 3.4, (C)).
PAHs, n-alkanes and FeSts were analysed with GC-MS [128, 130, 131, 132, 133] with three different oven programs but with the same capillary column (HP5-MS (5%-phenyl)-methylpolysiloxane, Agilent Technologies, Santa Clara, CA, USA). The conditions were a split/splitless injection volume of 2 μL (split valve open after 1.5 min) and He as a carrier gas (1 mL min^{-1}). The MS instrument was equipped with an electronic impact (EI) source used in positive ionisation mode (70 eV). The analytes were quantified according to specific mass to charge ratios (Table 3.1, Table 3.2) and with response factors containing both natives and labelled molecules. Response factors concentration were 10 ng μL^{-1} for n-alkanes, 1 ng μL^{-1} for PAHs and 1 ng μL^{-1} for FeSts.

The obtained values for the limit of detection (LOD) and limit of quantification (LOQ) (Table 3.1, Table 3.2) were calculated by the mean of the blanks plus three times the standard deviation, and mean of the blanks plus five or ten times the standard deviation, respectively, while the overall method uncertainty was estimated about 15/20% of the amount obtained for each class of biomarker analysed.

Table 3.1: Mass to charge ratios, LOD and LOQ for PAHs and FeSts expressed in ng.

	Compounds	**m/z**	**Retention time**	**LOD**	**LOQ**
PAHs	Naph	128	11.55	16.0	27.2
	Acy	152	19.33	8.4	12.6
	Ace	154	20.91	17.8	37.4
	Flu	166	25.38	8.7	17.4
	Phe	178	33.73	21.4	27.9
	Ant	178	34.13	19.3	19.3
	Fl	202	43.80	11.1	14.5
	Pyr	202	45.50	19.4	20.7
	BaAnt	228	55.26	-	-
	Chr	228	55.56	-	-
	Ret	234	48.62	-	-
	BbFl	252	63.23	-	-
	BkFl	252	63.40	-	-
	BaPyr	252	65.33	15.8	28.1
	BePyr	252	66.20	-	-
	BghiPer	276	72.47	-	-
	IPyr	276	74.13	-	-
	DBahAnt	278	72.72	-	-
FeSts	CoP	215	36.16	-	-
	e-CoP	215	36.40	-	-
	Chl	370	38.88	100.4	124.8
	5α-Ch	355	39.17	-	-
	5α-Sit	215	44.80	0.5	0.8
	Sit	215/396	44.46	2.3	3.5

Table 3.2: N-alkanes LOD and LOQ, expressed in ng.

m/z = 71	**LOD**	**LOQ**
C10	170.3	253.4
C11	361.7	552.2
C12	1936.9	3018.7
C13	3376.4	5188.2
C14	5326.3	8194.5
C15	8663.0	13074.0
C16	7149.5	10853.4
C17	2607.9	4026.6
C18	10980.8	16561.5
C19	2661.4	4162.6
C20	11307.4	17281.9
C21	1511.8	2353.1
C22	11050.9	17030.1
C23	1079.8	1572.5
C24	3149.3	4428.2
C25	4697.3	6931.1
C26	1359.4	1984.1
C27	1905.6	2861.1
C28	2334.6	3469.3
C29	898.3	1331.6
C30	719.6	1044.6
C31	696.3	1011.3
C32	807,0	1175.5
C33	565.7	804.6
C34	1089.3	1641.2
C35	1933.4	2953.8

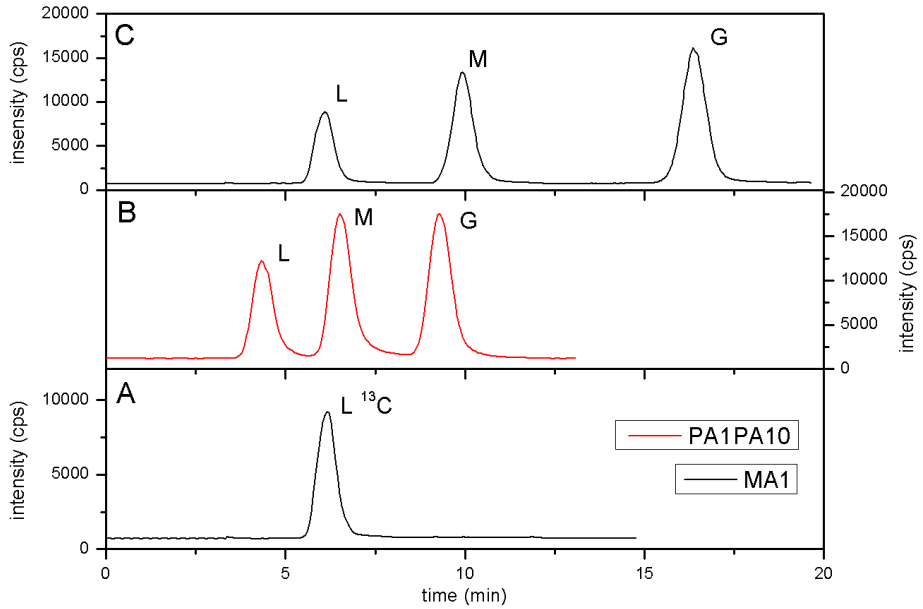

Figure 3.4: Standard mixture of MAs with 200 ppb of ^{13}C labelled internal standard analysed with MA1 column (A) and 250 ppb of natives analytes analysed with PA1PA10 columns (B) and MA1 column (C).

3.2.3 Hala Hu's method

The sampling campaign of Hala Hu H11 core was conducted within a field campaign that retrieved 12 cores in total and that lasted from winter 2010 to summer 2012 [13, 126]. Eight radiocarbon dates on bulk organic matter and extracted plant remains from core H11 were dated with AMS ^{14}C at Poznan Radiocarbon Laboratory, Poland, and the obtained age model was published by Yan and Wünnemann [13]. The topmost sample from core H11 (2 cm depth) with an age of 860 $\pm$ 30 yr BP was subjected to reservoir correction prior to calibration, and, even if it remains unknown whether the reservoir error was constant through time, it was applied to all other dates, discarding 3 dates that were not in line with other ages, perhaps due to higher reservoir errors than what was calculated for the entire core [13]. The final age model of the studied core is nearly constant, with a sedimentation rate of about 0.14-0.48 mm y^{-1} and an associated error between 15 and 71 years (Figure 3.5).

Elemental analysis of the core was performed by Prof. Bernd Wünnemann (from Institute of Geographical Sciences, Freie Universität Berlin, Germany) using high-resolution XRF line scan (2 mm) using an Avaatech XRF core

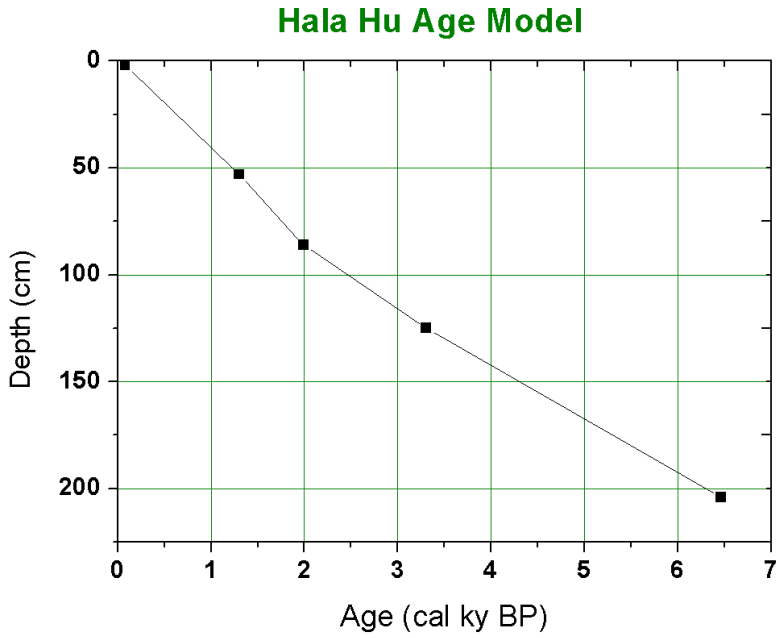

Figure 3.5: Age Model obtained for Lake Hala Hu.

scanner with line-scan camera for RGB color and multiple elements (10, 30, 50 keV, 2 mA, 15 s count time). Organic matter (OM) in 2 cm intervals was determined by Loss On Ignition (LOI), combusted under 550 ^{o}C temperature for 3 h in a burning oven.
The time resolution of this record is about 75 years on average and the samples weight ranged between 1 and 13 g of dried sediment. The methodological approach for biomarkers analysis consisted in 2 phases of extractions with ASE 350, firstly using DCM (2 cycles of static at 100 ^{o}C, 1000 psi) and then using MeOH (2 cycles at 100 ^{o}C and 1000 psi). The DCM total lipid extract (DCM-TLE) was then purified using Pasteur pipettes filled with silica gel and glass fibre filters (Figure 3.6). The 3 steps clean-up were made up by Hex firstly, to obtain the hydrocarbons (F1), DCM secondly to separate the alkenones (F2) and DCM:MeOH 1:1 v/v to get diols and glycerol dialkyl glycerol tetraethers (F3). Copper columns were run to remove sulphur from F2 and F3. All these proxies data will be needed in order to evaluate ecological (i.e. vegetation and precipitation) and temperature changes happened in the lake during the Holocene. These 3 fractions will be analysed with GC-MS by GFZ researchers in the near future and are not included in the results of this thesis.

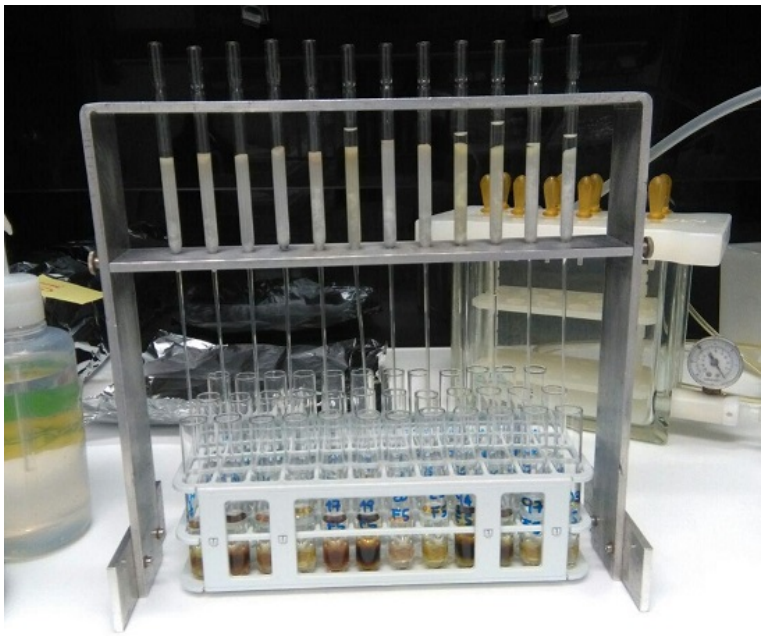

Figure 3.6: Clean-up of Hala Hu DCM-TLE with Pasteur pipettes filled with silica gel.

The MeOH-TLE containing the pyromarkers was treated as Paru Co's samples. Therefore the extracts were dried, water dissolved and centrifuged. In addition, the samples were purified with Maxi-Clean^{TM} C18 columns (W. R. Grace & Co.-Conn.) because of particulates and dirtiness observed in the solutions, prior to be analysed in IC-MS according to Kirchgeorg et al. [29].

3.2.4 Composite analysis of charcoal data

In this study, charcoal analysis was not performed because of samples and lack of time. However, charcoal data from the GCD were considered to infer some interpretation on past biomass burning events in the Tibetan Plateau. The R library called *paleofire: Analysis of Charcoal Records from the Global Charcoal Database* [134] is usually adopted to utilize version 3 of this database [69]. Data need to be firstly standardised, in fact, the range of metrics used to quantify charcoal (e.g., influx, concentration, charcoal/pollen ratios, gravimetric, image analysis, etc.) results in individual data values that vary over 13 orders of magnitude among and within sites [64]. The utilized standardization protocol to obtain the *charcoal index* [64, 68] included: (1) rescaling the values using a minimax transformation to allow comparisons among sites, (2) transforming and homogenising the variance using the Box–Cox transformation, and (3) rescaling values once more to z scores. Then, selecting different latitude and longitude ranges the analysis of the regional contribution of charcoal to the global fire signal was facilitated and then compared with other records and proxies.

Chapter 4

Results and discussion

4.1 Study of the Lake Paru Co

4.1.1 Paleoclimatic framework and lake's dynamics

Bird et al. [125] worked on lake Paru Co B11 core and the obtained results indicate the occurrence of the intense Indian summer monsoon (ISM) rainfall between 10.1 and 5.2 ka BP, when five-century-long high lake levels were recorded. Then, the ISM trended toward drier conditions to the present, with the exclusion of a pluvial event centred at 0.9 ka BP. Elevated sedimentation rate and dry bulk density (ρ_{dry}) in Paru Co likely reflect glacial sedimentation during the early Holocene from 10.9 to 10.7 ky BP. After 10.7 ky BP, significant reductions in the stabilization of sedimentation rates and ρ_{dry} suggest that glacial activity ended in the lake. In general, sediment deposition only occurs during the Boreal Summer when the lake is unfrozen. Therefore, after 10.7 ky BP, sedimentological variability is linked to summer climatic conditions and variations in ISM rainfall. Variability in almost all sections of Paru Co's sediment core is considered to reflect climatic, not glacial processes [125, 135]. The % of total organic matter (%TOM) showed a small variability with an increasing trend throughout the Holocene, indicating that Paru Co's depositional environment is influenced by the contribution of clastic material into the lake. The contribution of summer (90%) over winter (10%) precipitation indicates that ISM rainfall was enhanced from 10.1 to 7.1 ky BP and then decreased to a minimum between 7.1 and 3.4 ky BP. ISM increased during the late Holocene between 3.4 and 1.9 ky BP, and decreased again after 0.3 ky BP [125].

A weakening of the ISM around 4.2 ky BP possibly caused severe drought conditions which have also been observed in the western Tibetan Plateau, the Mesopotamian plain in Western Asia and Western Africa and Mexico regions, which have been considered to harshly hinder the development of ancient civilization in these areas [136].

Results acquired from Paru Co B11 resemble other paleoclimate records throughout the Tibetan Plateau, reflecting millennial-scale ISM dynamics. These millennial variations largely follow gradual decreases in orbital insolation, the southward migration of the ITCZ, decreasing zonal Pacific SST gradients and cooling surface air temperatures on the Tibetan Plateau. Centennial ISM and lake-level variability at Paru Co closely follow reconstructed surface air temperatures on the Tibetan Plateau, but may also reflect Indian Ocean Dipole events, particularly during the early Holocene when ENSO variability was reduced [125].

4.1.2 Preliminary Results

MAs obtained concentrations (ng g^{-1}) were then expressed in fluxes (ng cm^{-2} y^{-1}), calculated using density, water content and sedimentation rate data [137], in order to avoid the influence that different sedimentation rates can have on the data. Test results were indicative of a general pattern (Figure 4.1) and from these only few considerations can be inferred.
Levoglucosan concentration seemed to be higher in the deeper samples. The two samples with the highest fluxes are toward the bottom of the core, around 11 ky BP, when evidence for a weakened monsoon was observed [125]. Taking into account that the studied site is located at 4845 m a.s.l., above the alpine horizon that parts the alpine tundra, made of grass and little shrubs, from the conifer forests, and considering levoglucosan's catchment area, till hundreds km from the fire source [34], it could be stated that finding high levoglucosan concentrations in Paru Co sediments could be due to past regional fires of conifer wood.

Table 4.1: MAs ratios values for Paru Co B11 test samples.

cal yr BP	**L/M**	**L/(M+G)**
1809	1.4	0.8
3297	4.9	4.9
3967	7.0	7.0
5341	1.5	1.1
6257	1.3	0.8
8067	5.7	5.7
8774	6.8	6.8
10430	1.6	1.0
10781	0.4	0.3
10882	NA	NA
10934	3.2	1.6

Observing the values of the ratios L/M and L/(M+G) (Table 4.1), some abrupt changes in the trend of the two considered ratios may correlate

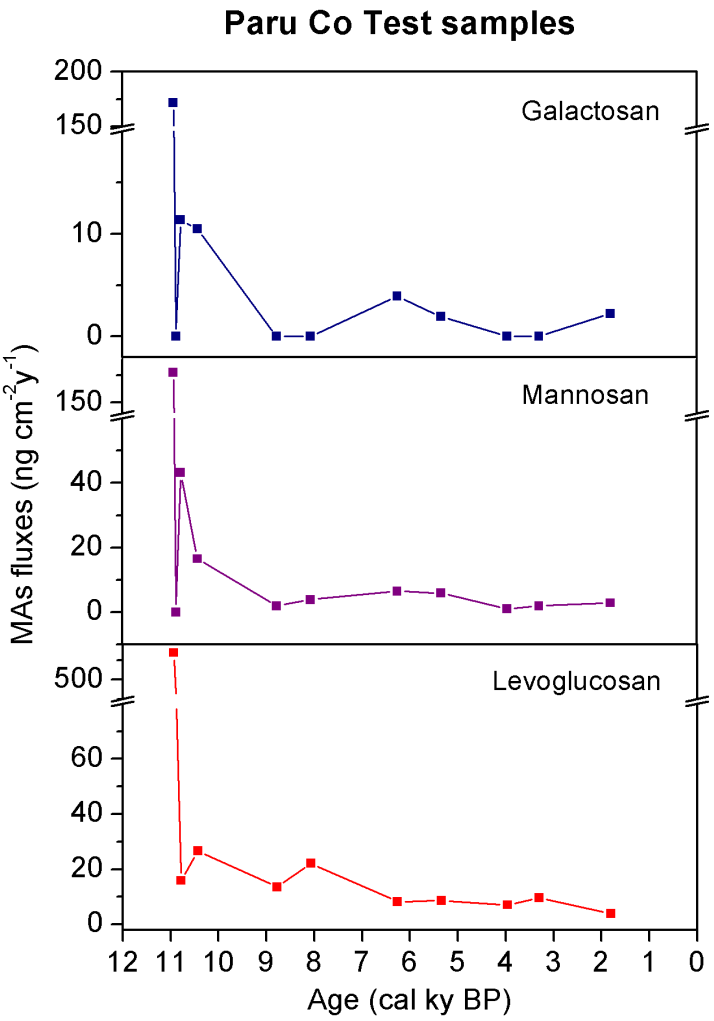

Figure 4.1: Galactosan, mannosan and levoglucosan results from Paru Co test samples in fluxes (ng cm^{-2} y^{-1}).

with changes in vegetation, where a possible explanation is the variation in environmental conditions due to forest clearance. The majority of MAs ratios, according the values published by Fabbri et al. [36], seemed to come from softwoods (conifers), except for 2 samples that showed their grass derivation (3967 and 8774 ky BP). However, these ratios values are still uncertain and their explanation can not leave other proxies out of consideration.
To proceed in further interpretations, the analysis of the entire Paru Co core is needed. The complete record (subsection 4.1.3) is in agreement with the results of the 11 test samples, because both trends show very high concentration of the samples located at the bottom of the core i.e. the oldest samples, where the sedimentation rate was 10 times higher than the rest of the core. Because of different methodological approaches, the 2 dataset were not merged.

4.1.3 Paleofire reconstruction

MAs record from Paru Co spans from 1.3 and 10.9 ky BP and it shows the same trend as the preliminary results (subsection 4.1.2), with high fluxes of monosaccharide anhydrides in the samples coming from the early Holocene, and then a long term decreasing trend towards the present, with a sharp decrease up to 7.5 ky BP. All the amounts were corrected for the sedimentation rate and transformed in fluxes, ranging from 5 to 2500, from 0.7 to 162 and from 0.9 to 531 ng cm^{-2} y^{-1} for levoglucosan, mannosan and galactosan respectively (Figure 4.2, Figure 4.3, Figure 4.4).

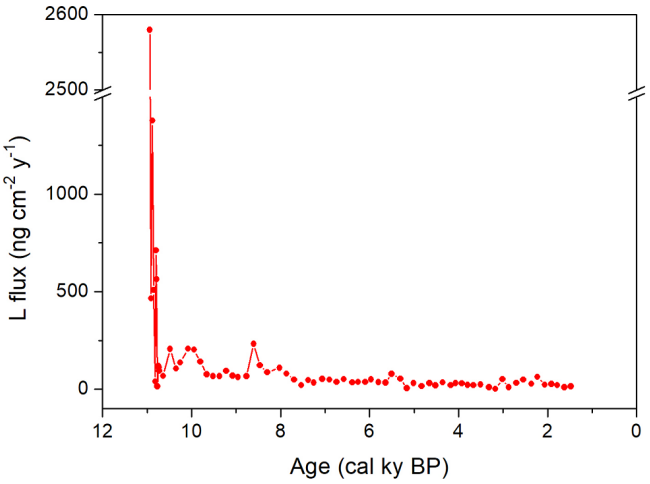

Figure 4.2: Levoglucosan results from Paru Co in fluxes (ng cm^{-2} y^{-1}).

MAs values for the oldest samples still remained very high in the period 10.8-10.9 cal ky BP, where the sedimentation rate was also very high, sug-

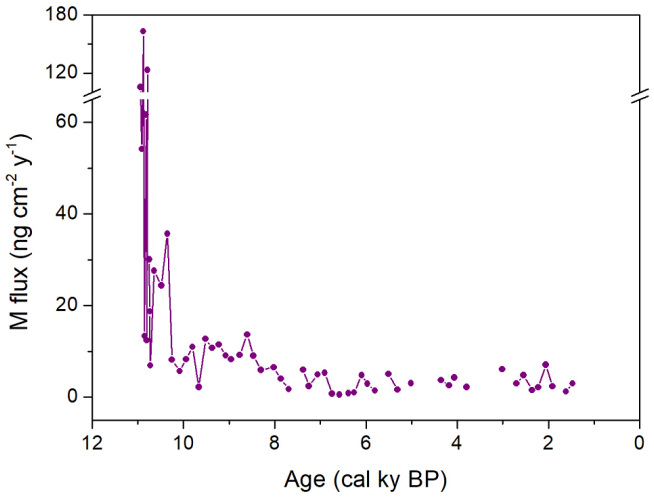

Figure 4.3: Mannosan results from Paru Co in fluxes (ng cm^{-2} y^{-1}).

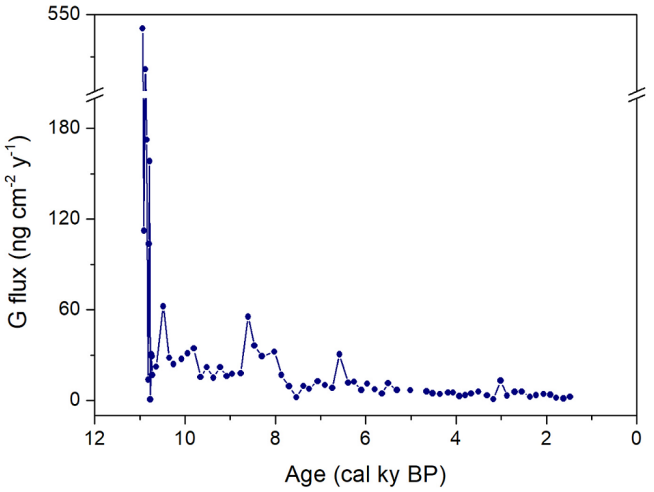

Figure 4.4: Galactosan results from Paru Co in fluxes (ng cm^{-2} y^{-1}).

gesting that MAs could have been better preserved inside the high quantity of sediment transported into the lake in that period. To better visualize MAs trends, the deepest samples were removed to plot the graphs of Figure 4.5, in which the fire peaks around 10, 8.6, 5.6 and 2.5 cal ky BP can be easily identified.

In general, mannosan and galactosan concentrations are always lower than levoglucosan's concentration, due to the different thermal stability of their anhydrosugar precursors, hemicellulose and cellulose [30, 35]. This fact can be clearly seen in the results plotted in Figure 4.5, and in addition, higher similarity was observed between levoglucosan and galactosan trends respect

to the mannosan one, which appear to have concentration's peaks slightly different from the other two isomers.

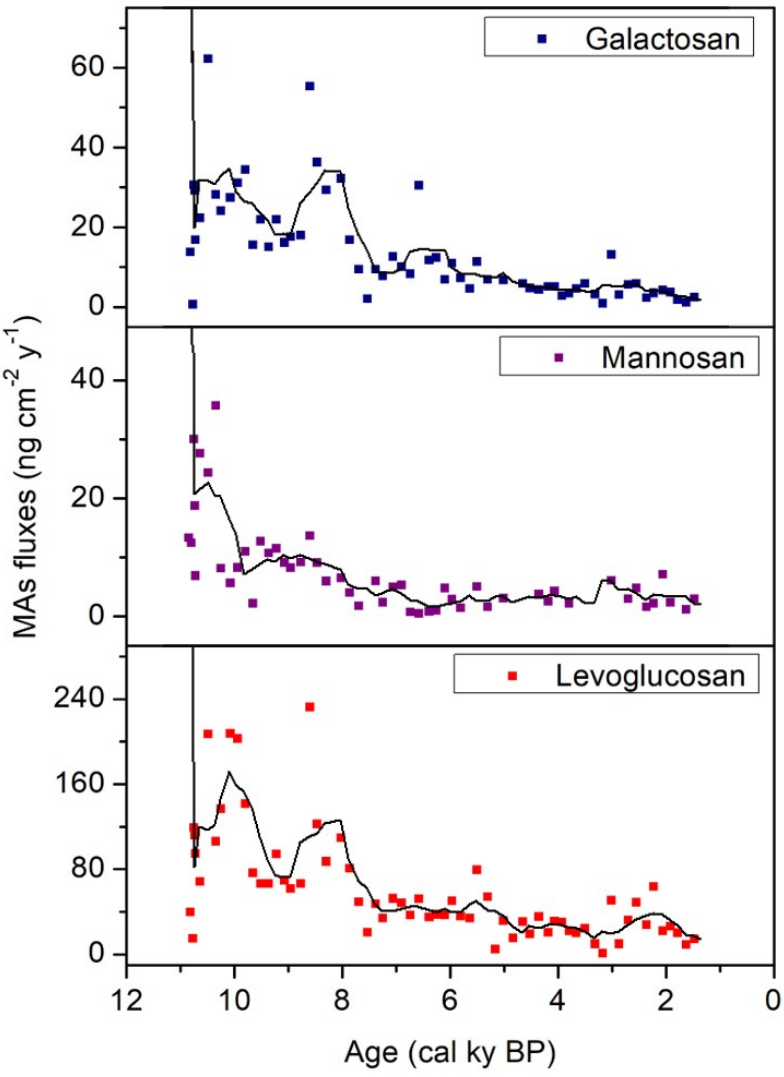

Figure 4.5: MAs results from Paru Co in fluxes (ng cm^{-2} y^{-1}).

Fluxes of PAHs, which can come from biogenic, pyrogenic, petrogenic or diagenetic sources, were calculated in the same way as for MAs. For each sample, by multiplying sedimentation rate, wet density and concentration (ng g^{-1}) of the respective analytes, fluxes values were obtained (Figure 4.6). Again, by removing the deepest and oldest samples, much more concentrated, variations of the PAHs fluxes during the Holocene are noticeable in very noisy trends (Figure 4.7, Figure 4.8). Within PAHs, Naphthalene, Fluorene, Fluoranthene, Phenanthrene and Benzo[e]pyrene reach the highest concentrations throughout the Holocene, mainly between 10.9 and 10.7 ky BP, similar to MAs record, ranging between 0 and 70 ng cm^{-2} y^{-1}. The other PAHs presented very low concentrations.

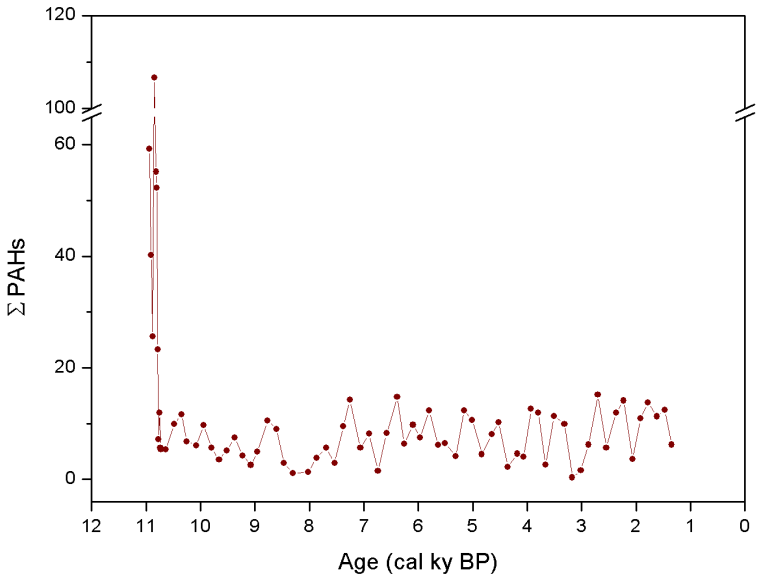

Figure 4.6: Sum of PAHs analysed in Paru Co.

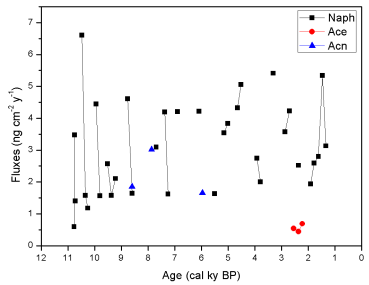

(a) *Naph, Acy and Ace*

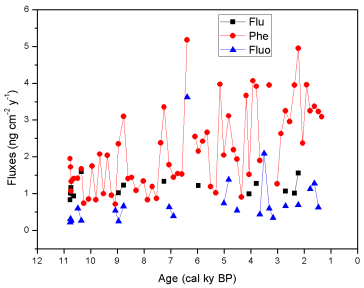

(b) *Flu, Phe and Fl*

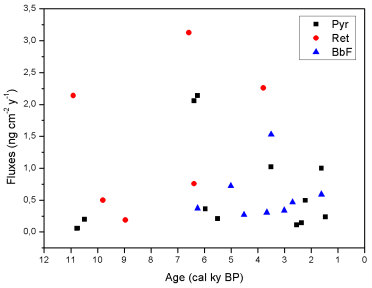

(c) *Pyr, Ret and BaFl*

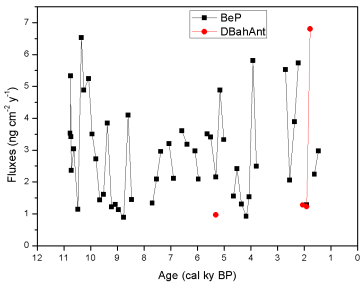

(d) *BePyr and DBahAnt*

Figure 4.7: PAHs results from Paru Co in fluxes.

MAs and PAHs were plotted together with biogenic silica (BSi), total organic matter and their trends (5 points moving averages) in the Figure 4.8. Pearson's correlation were calculated between MAs and % of BSi and between MAs and % of TOM with negative results, -0.76 and -0.54 respectively. This anti-correlation can also be visually observed in Figure 4.8 and indicates the non-dependence between MAs quantities and the organic content of the sediments. TOM presented small variability but slightly increasing trend across the Holocene, while BSi signal reflected the ISM, registered to be intense, with warmer and wetter climate between 11 to 5 ky BP, and subsequently leaked with cooler and drier conditions [125, 138].

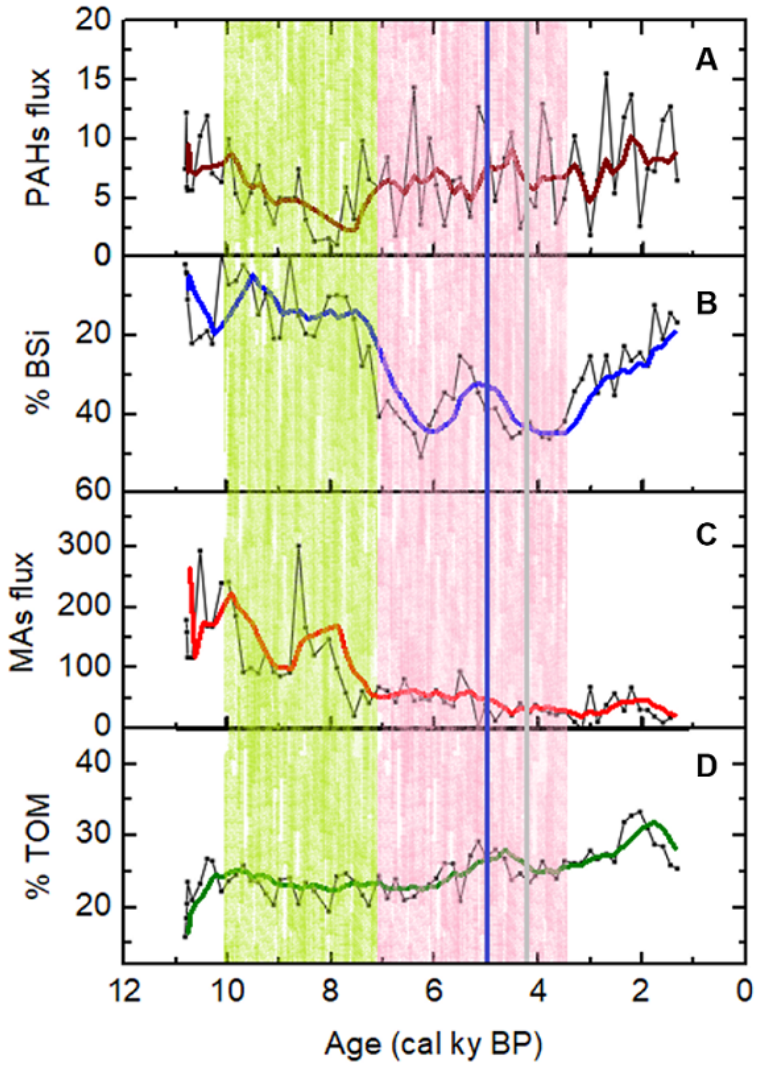

Figure 4.8: Results from Paru Co showing (A) ΣPAHs; (B) %BSi; (C) ΣMAs; (D) %TOM. Green box: ISM rainfall increased from 10.1 to 7.1 ky BP. Pink box: decrease of ISM rainfall to a minimum between 7.1 and 3.4 ky BP. Grey line: weakening of the ISM around 4.2 ky BP. Blue line: division between warmer/wetter ISM and successive cooler/drier conditions.

A long-term decreasing trend for MAs (which signal is mainly due to levoglucosan) but not for PAHs was observed. Throughout the Holocene, the sum of the obtained data for PAHs and MAs are not correlated (r = 0.16) and the same happened for their trends, obtained with a 5 points moving average (r = 0.30). However, dividing their Holocene trends into two periods, the first 11-8.7 ky BP and the second 8.7-1.3 ky BP, positive and negative correlations appear, with r = 0.69 and r = -0.82 for the first and second period respectively. Therefore, it is likely to deduce that the contribution of PAHs as well as MAs in the oldest period could be derived from local wildfires, while after 8.7 ky BP PAHs input may have had different origin, i.e. biogenic due to the fact that TOM and PAHs show increasing trends from 8 to 1.3 ky BP. Considering that MAs catchment area varies from m to hundreds km, the highest fluxes found in the Early Holocene could be explained with local fire activity, better preservation and bigger amounts in the sediments.

Therein PAHs, Yang et al. [139] affirm that high percentage of 4-6 ring PAHs generally suggests the contribution of local high-temperature combustion sources as predominant. In Paru Co, BePyr presents the second highest concentration and it is highly resistant to oxidation processes, as well as BbFl, found only in few samples from the middle Holocene to late Holocene, with very low concentrations. BaPyr was not found, maybe due to the fact that it usually disappears in severe weathering conditions; in general, low amounts of BaAnt and BaPyr could be also due to solubilisation or biodegradation in an oxic water column, or to prolonged exposure in an oxic bottom environmental condition. Concentrations and distributions of PAHs in sedimentary basins depend on the rate of sedimentation, as well as their source and diagenesis, with variable sediment dilution effects among river/lacustrine and marine environments. The relative proportions of PAHs derived from land areas are generally independent of sedimentation rate [39]. Therefore, the relative composition of the PAHs could record information of terrigenous/land environment in the Paru Co succession [135].

Dry conditions in Asia around 10.5 ky BP are consistent with the observed high levels of fire recorded in Paru Co. Subsequently, biomass burning activity registered after 10 ky BP could be associated with insolation-induced intensification of the Asian monsoon in the region, showing wettest conditions (ca 10-6 ky BP) that can provide more vegetation growth and hence biomass source for fire [7, 125]. The general decreasing fire pattern observed in Paru Co can be associated with a regional cooling trend reconstructed from Lake Zigetang with the pollen ratio *Artemisia*/Cyperaceae, a semi-quantitative measure for summer temperature, that indicates a general cooling trend throughout the Holocene [140]. Moreover, according to Liu et al. [95], summer monsoon retreated across the Qinghai-Tibetan Plateau during the middle Holocene. Relatively humid periods occurred at 2700–2200, 1500–800, and 600–80 yr BP, probably as a result of neoglacial cooling. Again, from a sedge-dominated

fen peatland in the central Zoige Basin on the eastern Tibetan Plateau, Zhao et al. [141] observed that the organic matter content was high between 10-3 ky and showed large-magnitude fluctuations in the last 3 ky in parallel with ash-free bulk density (proxy of peat decomposition and peatland surface moisture conditions) that fluctuated around a mean value of 0.1 g cm^{-3}, with low values at 6.5 4.7 ky BP, reflecting a wet interval, and an increasing trend from 4.7 to 2 ky BP, suggesting a drying trend.

The PC fire peaks at 8-8.5 ky BP can be easily associated with an abrupt climate event happened about 8200 years ago [142, 143]. This sudden event brought generally cold and dry conditions largely to northern-hemisphere regions especially in wintertime, subsequently to a huge outburst flood that freshened the North Atlantic [144]. Regarding Tibetan area, a dry interval at Shumxi Co (34^o N, 81^o E), probably correlative with the 8k event, is indicated by pollen and diatom records [145]. A peak in eolian silt in northwestern China (Lop Nur, Xinjiang, northwestern China; 40.51^o N, 90^o E) was associated with the 8k event [146], that was also correlated with a cold interval in pollen diagrams from Qinghai Lake (Koko-nur) at 37^o N, 100^o E [143, 147].

4.1.4 Inferences on past vegetation

Using and interpreting MAs and n-alkanes ratios, past vegetation reconstruction in the area is conceivable.
Paru Co's L/M and L/(M+G) ratios range from 0.6 to 100 and 0.5 to 11.1, respectively (Figure 4.9). Their oscillation throughout the Holocene, with the highest L/M value of 100 and a very low L/(M+G) value of 1.7 in 6.6 ky BP, may indicate the degradation of M and G due to their lower thermal stability. Higher combustion temperature (300 ^{o}C) and longer combustion duration result in higher L/M and L/(M+G) ratios, regardless of plant species. This "combustion effect" is probably due to the higher thermal lability of mannosan and galactosan compared to that of levoglucosan [35]. According to these information and considering ratios values classification [36], predictions about the burnt vegetation can be attempted. The data suggest that grasses (GR) dominated the area from the beginning of Paru Co's core and softwood (SW) began to grow in the region after 10.74 ky BP. Successively GR, SW and hardwood (HW) oscillated until 8.6 ky BP, when the vegetation was dominated by HW until 7.7 ky BP. Then, vegetation fluctuated again having the predominance of GR. However, no standard literature data on the L/M and/or L/(M+G) ratios for any kind of fuels is available and it is quite difficult to precisely predict the vegetation type throughout the Holocene [135]. Trying to improve the interpretation, the obtained data were compared with other Tibetan records.

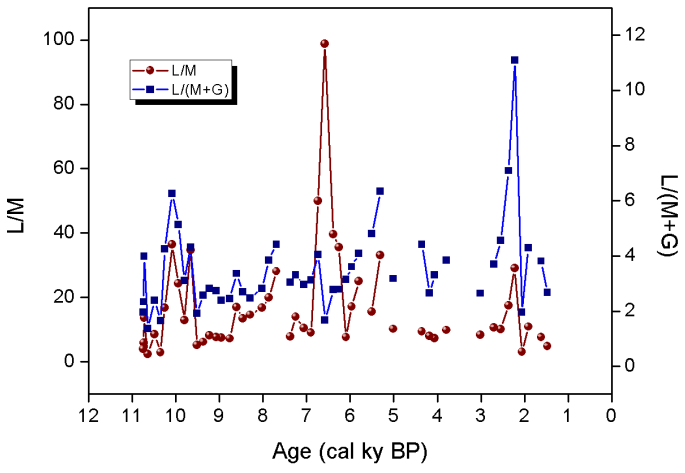

Figure 4.9: Results from Paru Co showing L/M and L/(M+G) ratios.

Pollen record obtained from the nearby Hidden Lake shows the vegetation fluctuations in the area during the Holocene (Figure 4.10, B). The climate

shifted from cold-dry of the Late Pleistocene to warm-humid during the early Holocene when meadow-forest began to grow, until circa 5 ky BP, when temperature and precipitation decreased linearly leading to cold and dry conditions and favouring steppe vegetation [115]. The major changes happened around 8 ky BP (probably associable with the 8 ky climatic change event) when meadow began to be replaced by SW and then between 5.3 to 3 ky BP, with the substitution of conifer with steppe. Comparing these pollen data with the L/M trend (5 points moving averages), a similarity could be seen (Figure 4.10, A). Reviewing isotopic and pollen information from surrounding lakes, these climatic variations from cold-dry Early Holocene to warm-humid middle-late Holocene can be confirmed [148, 149, 150, 151] in accordance with Paru Co's results, highlighting that the early Holocene climatic characteristics were mainly affected by the ISM, which contributed with the inferred vegetation provided by MAs ratios and pollen records.

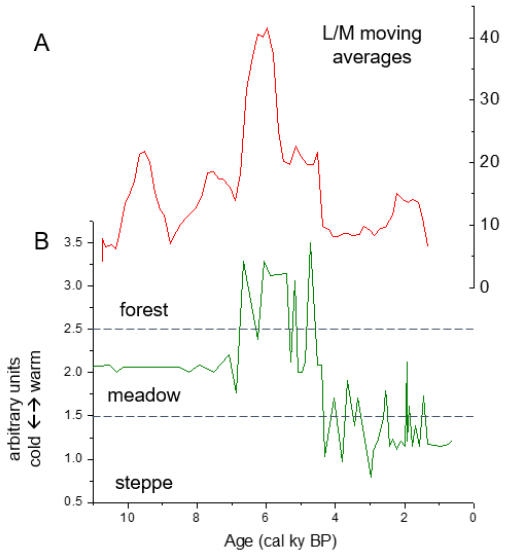

Figure 4.10: Results from Paru Co showing (A) trend of L/M ratio and (B) vegetation changes inferred from Hidden Lake pollen data [115].

Nam Co and Taro Co lakes, located in the same vegetation zone as Paru Co, recorded the influence of the westerlies during the late Holocene. From 5.6 to 0.9 ky BP, Paru Co's $\delta D_w ax$ increased suggesting a weakening in the ISM and a possible influence by the westerlies as well [125, 151, 152].

Past vegetation changes can be derived by variations in n-alkanes and their ratios too. Several different ratios were found in the literature (see subsection 1.3.1) and were applied to Paru Co data. For example, ATR and TAR

ratios were not calculable due to the absence or scarcity of n-alkanes C_{15-19} in the Paru Co sediment samples, due to the algae derivation of this group of alkanes. Average chain length was calculated using different ranges of alkanes chain length (15-33, 21-33, 25-33). In Figure 4.11 ACL_{21-33} and P_{aq} are plotted together, with y axis of P_{aq} inverted, to visualize their highly negative correlation (r = -0.87). Higher values of ACL_{21-33} could be associated to lower presence of submerged aquatic plants in the period 10.9-10 ky BP. Then, 10-5.5 ky BP could be identified with prevalence of submerged aquatic plants and lower ACL values. After 5.2 ka, lake levels decreased probably causing opposite fluctuations in both ACL and P_{aq}, with the Holocene minimum at 1.4 ky BP, suggesting diminished ISM rainfall and reduced clastic deposition and lowered lake levels, which led to an invasion of the littoral zone on the core site and an increase in sand deposition [125].

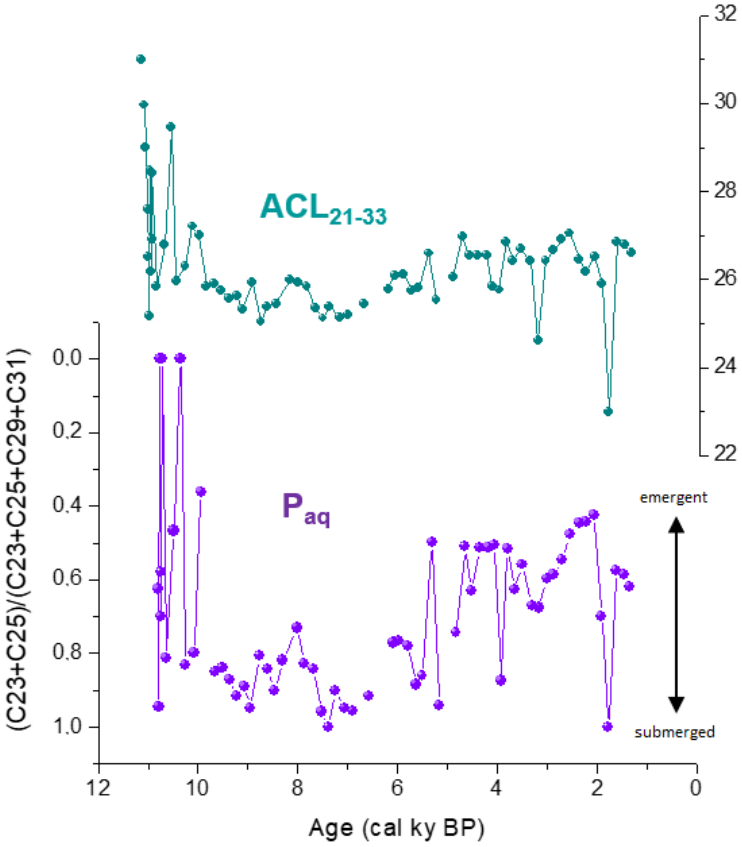

Figure 4.11: Comparison between ACL and P_{aq} data. These parameters are negatively correlated, with r = -0.87.

Carbon preference index was calculated using different ranges of chain length

(15-33, 21-33, 25-33). In Figure 4.12 Paru Co Holocene variations of CPI_{21-33} are plotted against the ratios aquatic/terrestrial and trees/(grass+shrubs). Some data are absent due to missing or very low values of some n-alkanes. The correlations of these parameters are positive and high: $r_{CPI-T/(G+S)} = 0.76$, $r_{CPI-A/T} = 0.67$ and $r_{A/T-T/(G+S)} = 0.83$ (correlations are significant at the 0.01 level - 2-tailed). In contrast with the parameters of Figure 4.11, where the majority of fluctuations are highlighted in the period 5.2-1.3 ky BP, here oscillations are enhanced between 10 and 5.2 ky BP, period in which five century-scale high lake stands alternated with low levels periods were registered in Paru Co [125].
Cui et al. [73] studied the leaf n-alkanes in modern plant from Qingjiang (Hubei province, China) and discovered that an identical plant species show invariability in the carbon number distribution and the dominant carbon number; instead, a remarkable seasonal variation is observed in their CPI and ACL values. During warmer months, the CPI values of all the plant species decrease gradually due to the fading process of the leaves. The ACL values are greater in middle summer than in May and November, inferring the temperature influence. In comparison with the fresh leaves, the defoliated leaves have the elevated abundance of the n-alkanes, probably due to the degradation of microorganisms and the biotransformation [73]. From this considerations we can infer that inside the sediments biotransformation of fresh leaves happens, increasing the quantities of these biomarkers, detected in very high abundances in Paru Co samples. Moreover, because of the fact that the climate of the Nyainqentanglha Mountains is dominated by the ISM and deposition only occurs at Paru Co during the boreal summer, when the lake is ice-free, the interpretation of sedimentological, and maybe also n-alkanes, variability reflects summer climatic changes.

Relationship between recorded fire and biomarkers distribution can be inferred according to the study of Knicker et al. [153], who noticed that prolonged charring reduced the average chain length of n-alkanes by up to four carbons and shifted the characteristic odd/even predominance of fresh plants towards a balanced odd/even distribution. Furthermore, the saturated fatty acids are less prone to heat degradation than the unsaturated counterparts, making them visible also in intense fire activity periods. However, in Paru Co record no correlations were observed between fire proxies and n-alkanes ratios.

Grass to wood prevalence can be observed with the 3 similar ratios shown in Figure 4.13, that evidenced alternate period of grass predominance over woody plants. Comparing these data with MAs ratios, different oscillations in their trends can be observed. Diversity in the pattern of these 2 ratios can be deduced due to their different provenance. MAs have a regional transport pattern and are fire-/markers, while n-alkanes are more local and can originate also from living plants. Moreover, angiosperms produce much more

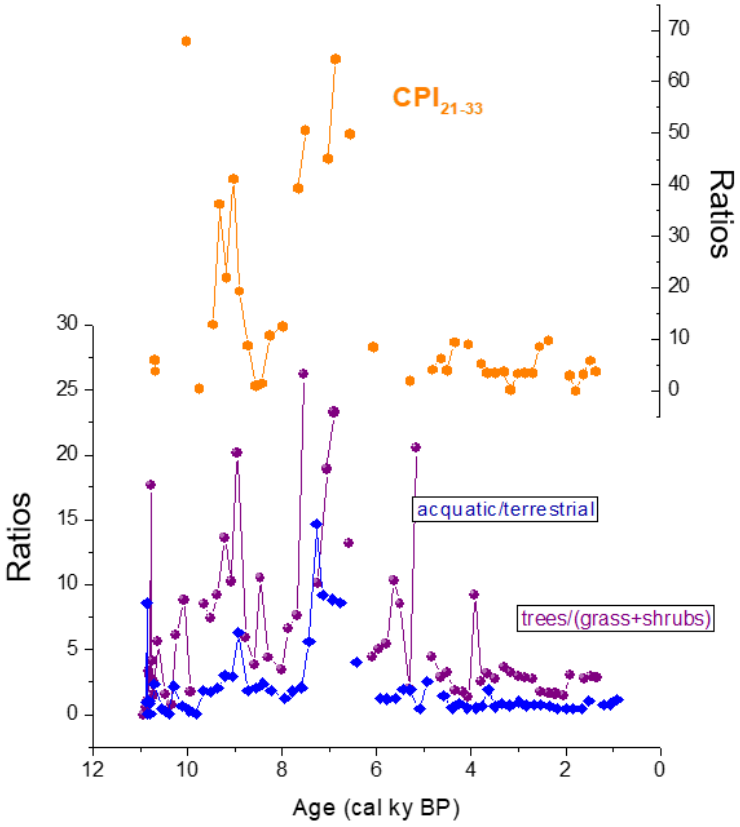

Figure 4.12: Confrontation between CPI, T/(G+S) and Aquatic/Terrestrial ratios. These parameters are positively correlated with $r_{CPI-T/(G+S)} = 0.76$, $r_{CPI-A/T} = 0.67$ and $r_{A/T-T/(G+S)} = 0.83$.

n-alkanes than gymnosperms do. That is the probable reason why grass/wood prevalence registered with n-alkanes is different from the one recorded by MAs ratios and pollens of Figure 4.10. MAs and pollen transport range is quite huge, so that their variations prevalently reflect regional environmental modifications respect to n-alkanes, which registered vegetation changes in the surroundings of Paru Co, probably derived by lake levels variations.
FeSts were not found in Paru Co samples, except for sitostanol and sitosterol, that were present at very low concentrations. Despite this, they could be compared with Norm31 ratio, showing similar shifting trends and indicating alternating vegetation during the Holocene (Figure 4.14). These two compounds from the FeSts group are very highly correlated (r = 0.93) due to the degradation path of sitosterol into sitostanol.
From a general point of view, vegetation changes can be explained not only by climatic factors but also by human and grazing animals activities thanks

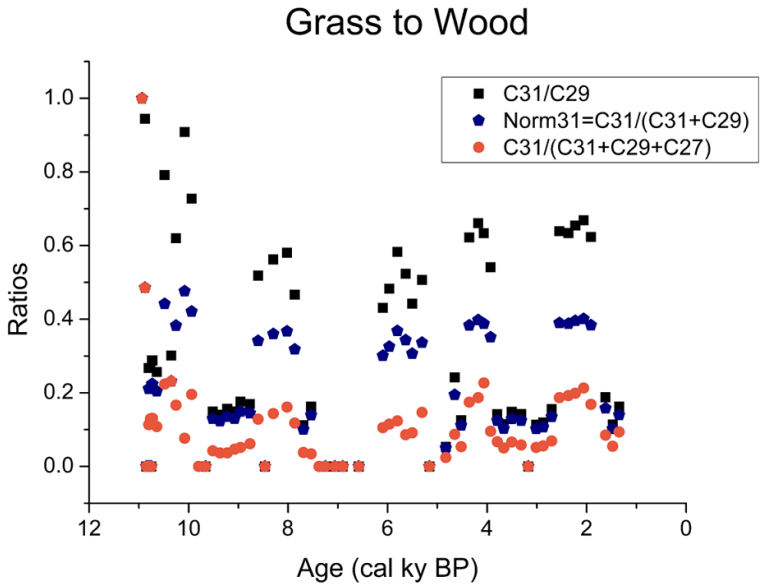

Figure 4.13: Confrontation between different ratios expressing the "grass to wood" quotient. They show similar trends, with alternate periods of grass and wood major proportions, and high correlation (r = 0.99).

to the FeSts analyses. In Paru Co case study, due to the absence of human/animals indicators, the variations in fire regimes and vegetation changes are supposed to be only climate driven, regarding the local fire activity. However, considering the regional diffusion basin of MAs, it can be excluded the potential human influence on fire from the Tibetan region. The majority of biomarkers trends, indices and ratios calculated with Paru Co data shows bimodal behaviour, with differences between the first and the second half of the core, maybe following the dramatic climate variation occurred in the Middle Holocene at 4-6 ky BP, reported by many studies [95, 122, 125].
A study on pollen assemblages in different lakes from 2 transects (East-West and North-South) in TP was performed by Li et al. [124]. In the east-west transect the pollen assemblages before 12 ky BP indicated sparse vegetation with very low pollen concentrations. During 12-7.5 ky BP a rise in pollen concentrations of *Artemisia*, *Ephedra* and Poaceae was observed, indicating *Artemisia*-Cyperaceae alpine steppe. During 7.5-1 ky BP, peaks of pollen concentration suggested dense steppe vegetation dominated by *Artemisia* and Cyperaceae in response to relatively abundant monsoonal precipitation during the mid-to late Holocene. In the north-south transect predominant elements of regional steppe vegetation changed from *Artemisia*, during the first half of the Holocene, to Cyperaceae in the latter half. Altitudinal vegetation belts on the mountain regions shifted downwards in elevation during the Holocene, in response to the reduced temperatures. This synthesis on changes

in Holocene vegetation suggests that variations of monsoonal precipitation and insolation-driven temperature are the predominant driving forces for changes in alpine vegetation in the central TP [124].
Eendorsements of Tang's work on Hidden Lake [115] (Figure 4.10, B) are given by other different studies. Herzschuh et al. [140] found the establisment of alpine steppes with desert elements (mainly Cyperaceae, Poaceae, Chenopodiaceae, and characteristic high-alpine herb families) during the second half of the Holocene (4.4–0 ky BP). Furthermore, dense temperate steppe vegetation and maximum desert plant withdrawal were used as indicators of a suitable balance of wet and warm conditions for optimum vegetation growth, during the middle Holocene (7.3–4.4 ky BP). They also confirmed severe Early Holocene cold events for 8.7–8.3 and 7.4 ky, found by other studies [120, 121]. Zhao et al. [141] detected a change from meadow to forest in the Eastern Tibet in the Early Holocene, with peaks in tree pollens (mainly *Picea*, SW) during the mid-Holocene at 6.5 ky BP, and then a decreasing trend until 2 ky BP.
Another work considered pollen and charcoal content as markers to detect vegetation, climate, and human activity changes on the South-Eastern Tibetan Plateau (SETP) since the Pleistocene–Holocene transition (11.7 cal ky BP) [149]. The results explained are in accordance with Paru Co paleoreconstructions. Samples from Lake Naleng were found to be strongly affected by extra-regional pollen transport, probably due to the steep elevation gradients and pronounced local wind systems.
Spreading of *Salix* and *Betula* at the beginning of the Holocene marked the transition to a mosaic shrub and meadow vegetation due to warmer conditions. From 10.7 to 4.4 cal ky BP open *Abies–Betula* forests were found, probably reflecting a stronger (in respect to the present) summer monsoon and an upward shift of treeline. Temperature range reconstructions appeared to be about 2-3 ^{o}C warmer and the treeline position was 400–600 m higher than today. A severe climate deterioration with temperatures about 1-2 ^{o}C colder than before was documented by retreating forests between 8.1 and 7.2 ky BP, while subalpine *Rhododendron* shrubs spread around Lake Naleng, indicating colder conditions with temperatures 1-2 ^{o}C below early and mid Holocene levels and treeline moving downwards [149]. The forest decline from 4.4 ky BP at Lake Naleng, with rapid changes after 3.4 ky BP and increasing domination of meadow and shrub vegetation of Cyperaceae, was observed in several sites in the TP even if not synchronous everywhere [154, 155, 156]. This event is considered to reflect climatic conditions as low concentrations of charcoal particles found in this period exclude human-induced fires as reason for the forest retreat. However, grazing indicators (increases of *Rumex*, *Sanguisorba* and Apiaceae pollen), found about 1000 year after the beginning of the forest decline, imply human influence on the environment since 3.4 ky BP around Lake Naleng. According to Miehe et al. [100], slashing and burning of woodland around Lhasa (SETP) were used to obtain free lands.

Moreover, another study does indeed suggest a link between fire activity and forest clearance in Southern and SETP during the late Holocene [157, 158]. It appears that the extent of human activity on the TP vegetation during the Holocene has not yet been satisfactorily resolved. Paru Co's paleofire and FeSts records seem not to indicate human induced fires.

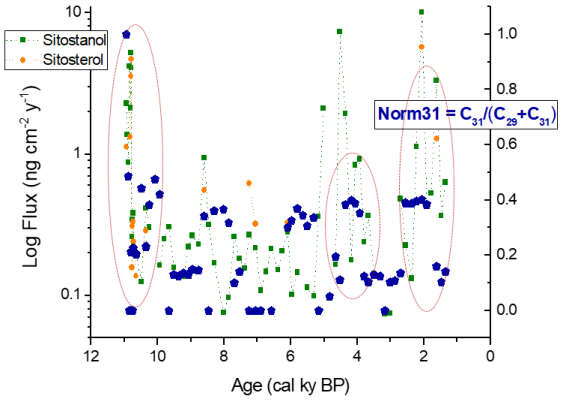

Figure 4.14: Sitostanol and sitosterol log fluxes detected in Paru Co compared with n-alkanes Norm31 ratio.

4.1.5 Statistical Analysis

Pearson correlation matrix (Figure 4.15) attests the correlations some of what were already shown and discussed in the previous sections, such as high correlations of fire proxies with BSi and TOM and between G/W ratios. Few correlations are highlighted and this poor interdependence between the variables and the samples will be also shown with the multivariate analysis performed with the principal component analysis (PCA).

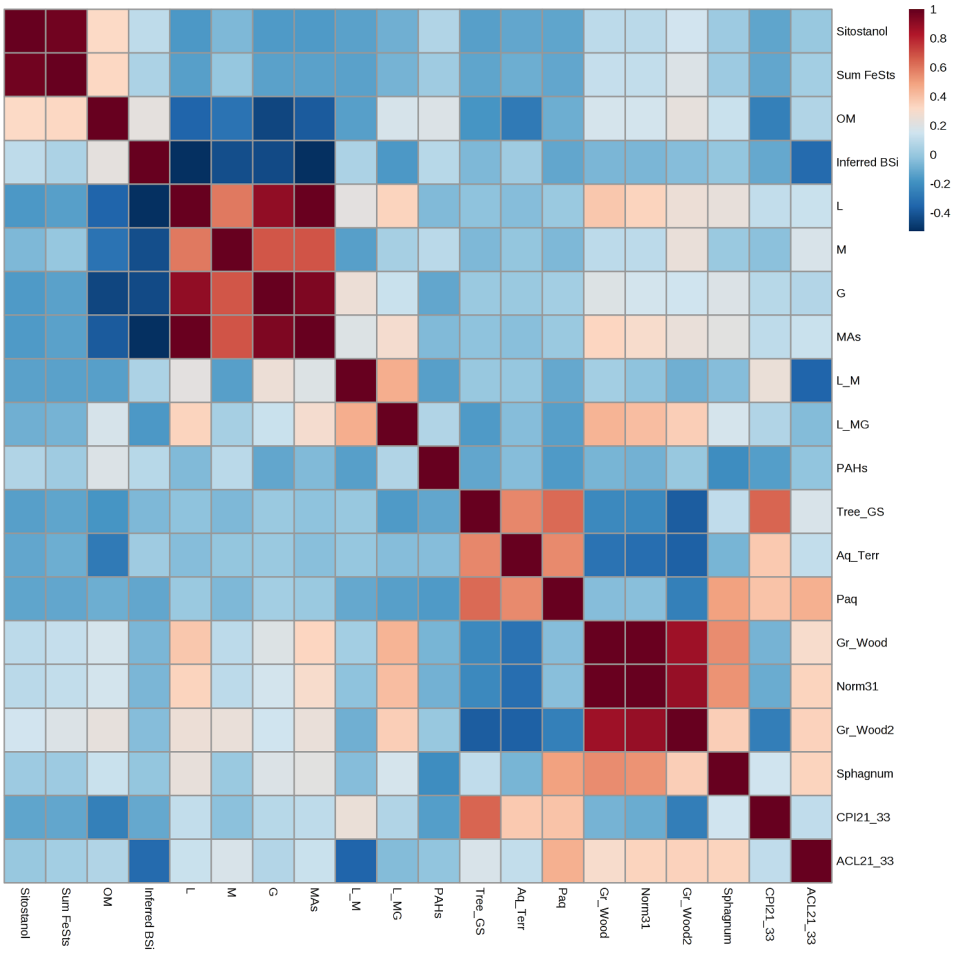

Figure 4.15: Pearson correlation matrix for Paru Co dataset.

In order to perform the PCA, the dataset was partitioned into 4 groups of samples according to the major differences between periods derived both by Paru Co data and literature findings. The chosen groups are visible in the scores plot of Figure 4.17: 10.7-10 ky BP (number 4, light blue), 10-8 ky BP (number 3, blue), 8-4.5 ky BP (number 2, green), 4.4-1.3 (number 1, red) ky BP.

Then, the normalization of the dataset was achieved with a range scaling (mean-centred and divided by the range of each variable) [127].
The obtained values of the explained variance are 31.3% for PC1, 19.8% for PC2, 13.7% for PC3 (Figure 4.16). Looking at the variables loadings, absolute values above 0.25 are evidenced in bold in Table 4.2. It is possible to explain that PC1 is mainly due to the prevalence of grass to wood specific n-alkanes that have negative loadings, while PC2 can be associated mostly with fire markers, with negative loadings for levoglucosan, galactosan and ΣMAs, but also for CPI, P_{aq}, T/(G+S) and a positive loading for biogenic silica. PC3, instead, is better identified mainly by submerged versus terrestrial n-alkanes ratio, with P_{aq}'s negative loading but also from ACL, CPI, Norm31 and T/(G+S) negative loadings.

Table 4.2: PCA loadings for Paru Co variables.

Variables	**PC1**	**PC2**	**PC3**
ACL21-33	-0.13	-0.13	**-0.30**
Aq/Terr	0.12	-0.17	-0.18
CPI21-33	0.08	**-0.28**	**-0.26**
G/W	**-0.50**	0.19	-0.09
G/W2	**-0.47**	0.08	-0.22
Inferred BSi	0.13	**0.39**	-0.15
L	-0.23	**-0.34**	0.20
L/(M+G)	-0.15	-0.01	0.02
L/M	-0.01	-0.05	0.07
M	-0.14	-0.23	0.23
G	-0.16	**-0.33**	0.23
MAs	-0.23	**-0.35**	0.23
Norm31	**-0.52**	0.11	**-0.26**
OM	-0.03	0.24	-0.11
PAHs	0.02	0.11	0.13
Paq	0.10	**-0.34**	**-0.57**
Sitostanol	-0.02	0.11	-0.02
Sum FeSts	-0.03	0.09	-0.02
T/(G+S)	0.14	**-0.26**	**-0.33**

Observing the scores plot of Figure 4.17, a clear separation between groups 1 and 3 is shown according to PC2, thus, mostly in dependence of fire markers and biogenic silica, that behaves oppositely, as it can be seen also from Figure 4.18. Group number 2 is evidently in between 1 and 3, while number 4 is maybe characterized by less samples to be well explained. Group 1 is identified by low values of fire markers as the fire activity in the period 4.4-1.3 ky BP was very low, and high values of BSi. In contrast, group 3 (10-8 ky BP) can be described by high biomass burning events and low values of BSi. In conclusion, it can be affirmed that the PCA performed on Paru Co dataset revealed results that are in accordance with the interpretations proposed in the previous sections.

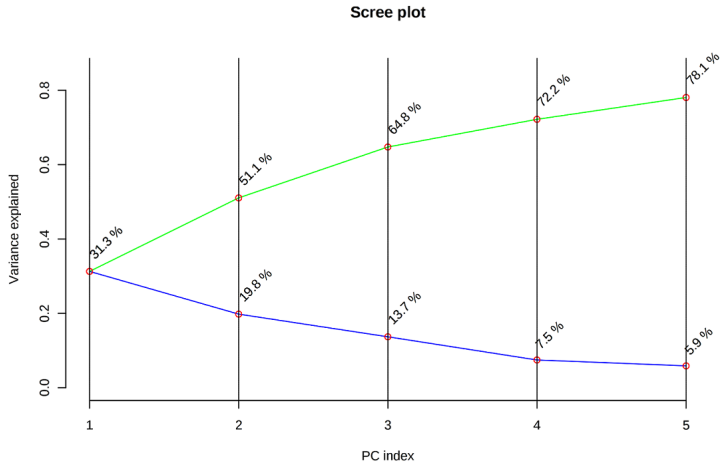

Figure 4.16: Scree plot of PCA analysis for Paru Co dataset.

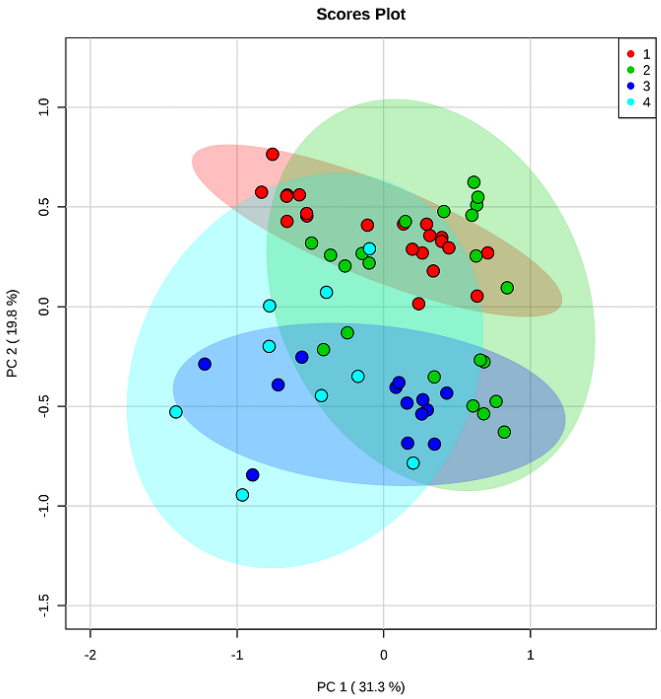

Figure 4.17: Scores plot of PCA analysis for Paru Co dataset.

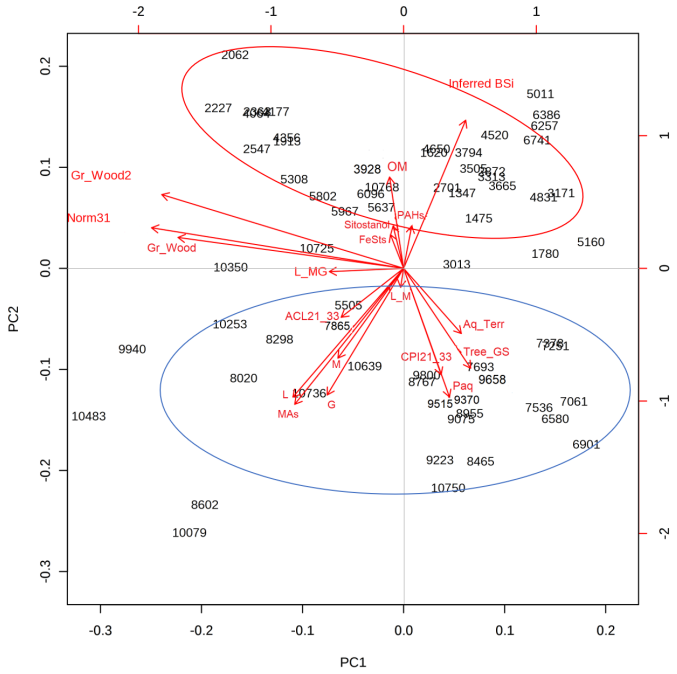

Figure 4.18: Biplot of PC1 and PC2 of PCA for Paru Co dataset.

4.2 Study of the Lake Hala Hu

4.2.1 Paleoclimatic framework and lake's dynamics

The study area is highly interesting due to its location on the NETP which is characterized by a relatively well examined settlement history. The great potential of this record is due to the possible combination of biomass burning indicators with temperature and hydrological sensitive proxies, to get an integrative picture about human, climate and fire interactions.
The position of the lake is between the influence of the summer monsoon and westerly-driven effective moisture, suggesting that the lake sediment may preserve a record of the impact of both air masses on the environment through time. A mean annual air temperature of -1.5 ^{o}C is estimated for Hala Lake, and mean annual precipitation is calculated at 228 mm of which about 48 % falls between July and September, when the summer monsoon reaches northern latitudes in China, while the lake is frozen from December to March. Vegetation around the lake is extremely sparse and influenced by grazing. Mean total salinity of the surface water is about 17–18%, with slightly lower values at major depth. [13, 126].
An algae layer is present between 25 and 32 m of water depth and it is considered responsible for the oxygen oversaturation at this depth, followed by a decline to anoxic conditions in the deep zone due to rapid degradation of organic matter during summer time [13]. The lake is frozen from December to March, that is the reason why precipitation recorded are considered to be derived mainly from summer, as in Paru Co.

H11 core studied for the paleofire reconstruction is associated to H7 core, both retrieved from the centre of the lake. Studying OM, carbonate and XRF parameters of this core (visible in Figure 4.19), the reconstruction of past environmental conditions of the area was possible. A filling phase started at the beginning of the Holocene and the lake reached a similar level as it is today. This lake level rise can be explained by strong climate warming and increased moisture availability at the beginning of the Holocene. It seems that the East Asian Summer Monsoon (EASM) had by this time reached the area. The rise in OM in the bottom part of the cores is related to the amelioration of climatic conditions between 9.5 and 7.6 ky BP and permitted the development of aquatic plants and macrophytes. Despite maximum insolation and thermal land-ocean contrast during the early Holocene, which are considered to be the main triggers for summer monsoon strength in northern latitudes [159], Hala Lake remained less affected than the Qinghai Lake region (200 km south-east). The lowstand in Hala Lake at around 8.1 kyr BP perhaps coincides with a mass flow layer observed in three records (H7, H11 and H12). The highest carbonate content, however, reflects either formation in the littoral and downslope area, or detrital input from the

catchment. High variations of OM, detrital fluxes (Ti and Si, XRF counts), carbonate (Ca, XRF counts) and Sr/Ca (salinity) all support the assumption of sediments that were formed at near-shore locations. A possible source for this material is located at the northern side of the lake basin, where a steep terrace circa 10 m is identified as an ideal site for the initiation of a large-scale slope movement [13, 126].

In the period 7.6–6 ky BP constant detrital input, high carbonate values and relatively steady OM were recorded. This could be explained as a period of balanced hydrological and climate conditions, followed by a precise modification to a negative water budget and feebly decreasing OM until about 4.5 ky BP [126]. All data denote a huge decline in melt water amount, potentially increased by diminished summer rainfall, favouring carbonate precipitation at the near-shore location under conditions of low lake stand [126]. Strong carbonate precipitation may have also been related to abrupt modifications in water supply from other sub-catchments, providing more Ca^{+2} cations for biogenic precipitation. This supposition is based on the fact that the increase in carbonate at 6 ky BP was sudden and unique within the profile [126]. The general slightly declining trends in OM and carbonate from 4.5 ky BP to today are interpreted to be possibly coincident with cooling climate, as revealed by pollen data from the central TP [140]. The 3 ky period of mainly positive water balance (high lake levels, deeper lake) between 7.8 and 4.6 ky BP has also been recorded from the north-eastern, southern and central TP, despite a general decreasing trend of monsoonal impact [13]. Moreover, wet phases during the mid-Holocene are reported from Bosten Lake (7-4 kyr BP [160]; 6.4-5.1 ky BP [161]), Balikun Lake (7.9-4.3 ky BP [162]), Wulungu Lake (after 6.7 ky BP [163]) contradicting records from Hurleg Lake (south of Hala Lake) where unstable and mainly dry climate conditions prevailed [164]. However, lakes in highly elevated regions, such as Hala Lake, may have received locally higher precipitation, thereby maintaining a positive water balance.

During the Late Holocene (4.0 ky BP to present) rapid fluctuations in water depth were observed, perhaps more frequently controlled by westerly-driven effective moisture supply, and related to detrital fluxes. No detrital input was recorded between 4 and 3.0 ky BP, in contrast to the high fluxes of 1.8-1 ky BP, at H7/H11 site. Then, from about 1.5 ky BP, a clear trend toward the lake's present level was recorded [13].

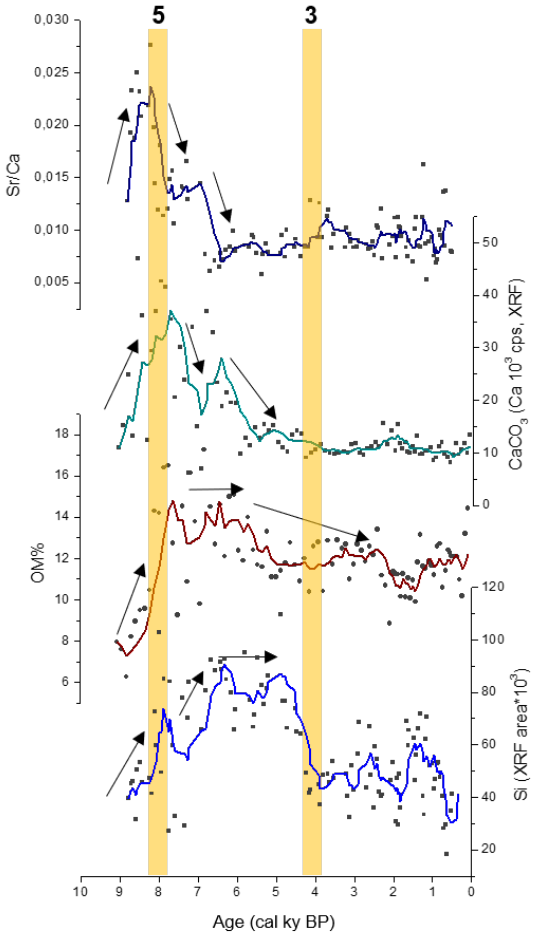

Figure 4.19: H11 results for Si (detrital input), OM%, Ca ($CaCO_3$), Sr/Ca (salinity), unpublished data. Yellow bars indicate dramatic drying events of circa 8 and 4 ky BP (Bond events 5 and 3).

4.2.2 Paleofire reconstruction

MAs fluxes values ranged between 0.3 and 6.1 ng cm^{-2} y^{-1}, with low values for mannosan and especially for galactosan. This high difference respect to Paru Co MAs fluxes is probably due to the very diverse size of the 2 lakes, 0.1 km^2 Paru Co and 590 km^2 Hala Hu. Thus, in the bigger Hala Hu biomarkers occur to be more diluted. The results are nevertheless comparable because the calculated signal/noise ratio is circa the same, 10/1.

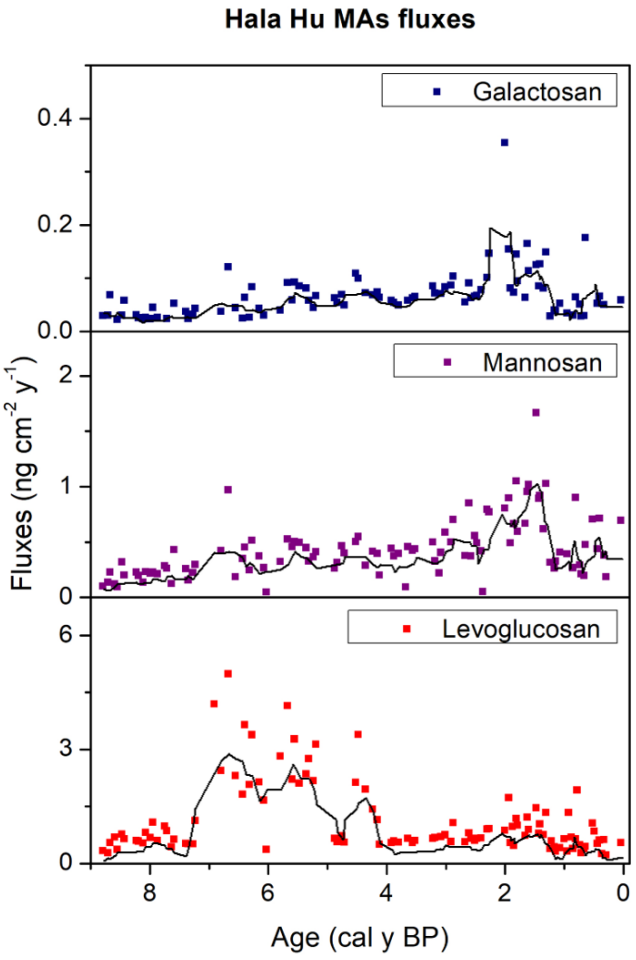

Figure 4.20: MAs results from Hala Hu in fluxes (ng cm^{-2} y^{-1}).

Different trends in mannosan and galactosan (slightly increasing towards the present) respect to the one of levoglucosan are due to their different thermal stability and consequently much easier degradation of M and G during the fire event. As shown in Figure 4.20, the majority of fire activity is recorded by levoglucosan in the middle Holocene between 7 and 4 ky BP, with 3 major

groups of fire activity at 7.1-6.1, 5.8-5.2 and 4.5-4.1 ky BP. Subsequently, biomass burning can be identified by smaller peaks between 2 and 0.8 ky BP, and in this case the contribution of mannosan and galactosan is higher than in the middle Holocene, maybe because of different combustion conditions and type of vegetation burned.
In fact, looking at the ratios L/M and L/(M+G) plotted in Figure 4.21, three diverse combustion conditions periods can be identified: 1) from 9 to 7 ky BP quite low but unstable ratio values probably due to the changing climatic conditions of the period and not stable mass flow inputs and variable lake levels; 2) higher ratios from 7 to 4 ky BP in parallel with high fire activity; 3) low and stable ratios from 4 to 0 ky BP could indicate more stable burning conditions. Comparing the obtained ratios values with the published ones [36] a lot of overlapping interpretations are derived, again confirming that this classification is not totally reliable as categorization method for the type of vegetation burned. Notwithstanding, an attempt of interpretation based on the ratios in the Early Holocene could point out GR and SW derivation; the higher middle Holocene values could be indicative of GR, SW, aerosols and smoke particles; the lower values at 4-0 ky BP seem to mainly come from SW.

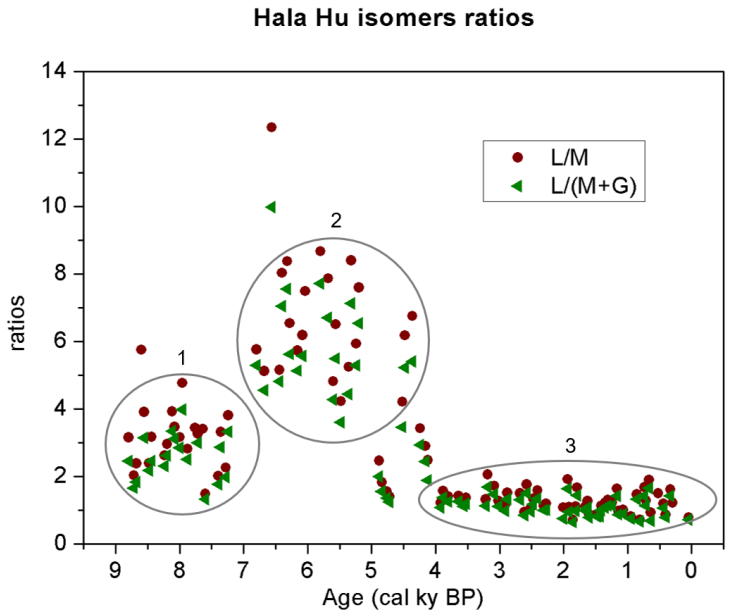

Figure 4.21: MAs isomers ratios results from Hala Hu lake, distinguished in 3 periods.

The occurrence of a peak value with the highest average elemental carbon abundance in the Holocene, studied on a loess and paleosol sequence from the

Lingtai section on the Chinese Loess Plateau by Zhou et al. [11], may reflect a major climate event at 6 ky BP, and, according to the author, may also be partly due to more frequent anthropogenic fire usages. In Hala Hu these event could have been recorded by levoglucosan, but shifted to 6.2-6.4 ky BP. The highest elemental carbon peak at 6 ky BP is also coincident with higher magnetic susceptibility, which implies a stronger summer monsoon climate with widespread growth of vegetation and accumulation of biomass [165], and it slightly postdates the commencement of Neolithic civilization in central China, which occurred in the first half of the 7^{th} millennium BP, detected due to pottery found in the region [166]. In general, given sufficient fuel, the risks of fires increase during high temperature and dry conditions. However, humidity and temperature also affect biomass, the major source of fuel and prerequisite for the paleofires [11], that is one of the probable explanation for 7-4 ky BP period of fires recorded in H11. In northern China, an abrupt climatic shift at around 4 ky BP was recorded in the eastern margin of the TP [122] and this event could have been displayed also by Hala Hu fire record, with a clear diminished MAs signal exactly from 4 ky BP.
A study on biomass burning reconstruction on a slope sedimentary section in Gonghe Basin (350 km south-east from Hala Hu) using charcoal was published by Miao et al. [9]. This fire record can be seen in Figure 4.22. The explanation for the fire registered during the past 10000 years is due to paleoclimatic factors, with lower fire frequency in the warm/humid period of the middle Holocene and higher fire frequency in the colder/drier periods of the early and late Holocene, that seems to be the opposite of what is registered in Hala Hu. However, the super-high fire frequency event at 3.6 ky BP was explained as the result of the Bronze Age's rapid human colonization in high elevation areas of the TP [167], which was accompanied by frequent use of fire. Comparing this plot with Hala Hu's fire record few similarities are present, such as the fire peak around 5.5 ky BP and the fire activity of the 2-1 ky BP period, which are explained as climate induced by Miao et al. [9].

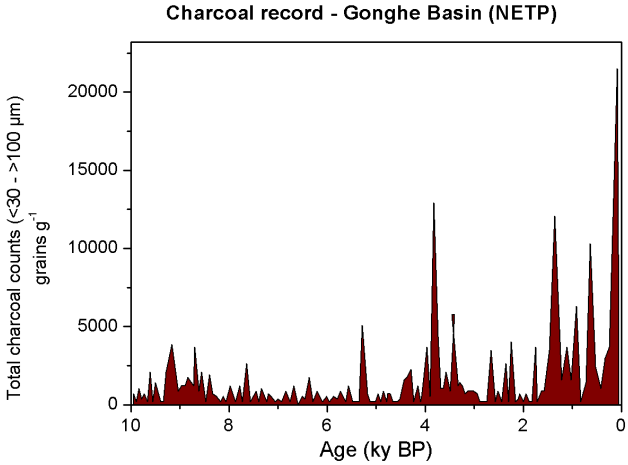

Figure 4.22: Charcoal record from Gonghe Basin in the NETP, from Miao et al. [9].

4.2.3 Statistical Analysis

Considering both paleofire and XRF data of Hala Hu H11, pearson's correlation matrix was calculated. Some areas of positive high correlations can be seen as red coloured in Figure 4.23. Interesting positive correlation is revealed between MAs, whose signal is mainly due to levoglucosan, and the elements Al, K and Si. In order to better understand these relation, PCA was performed.

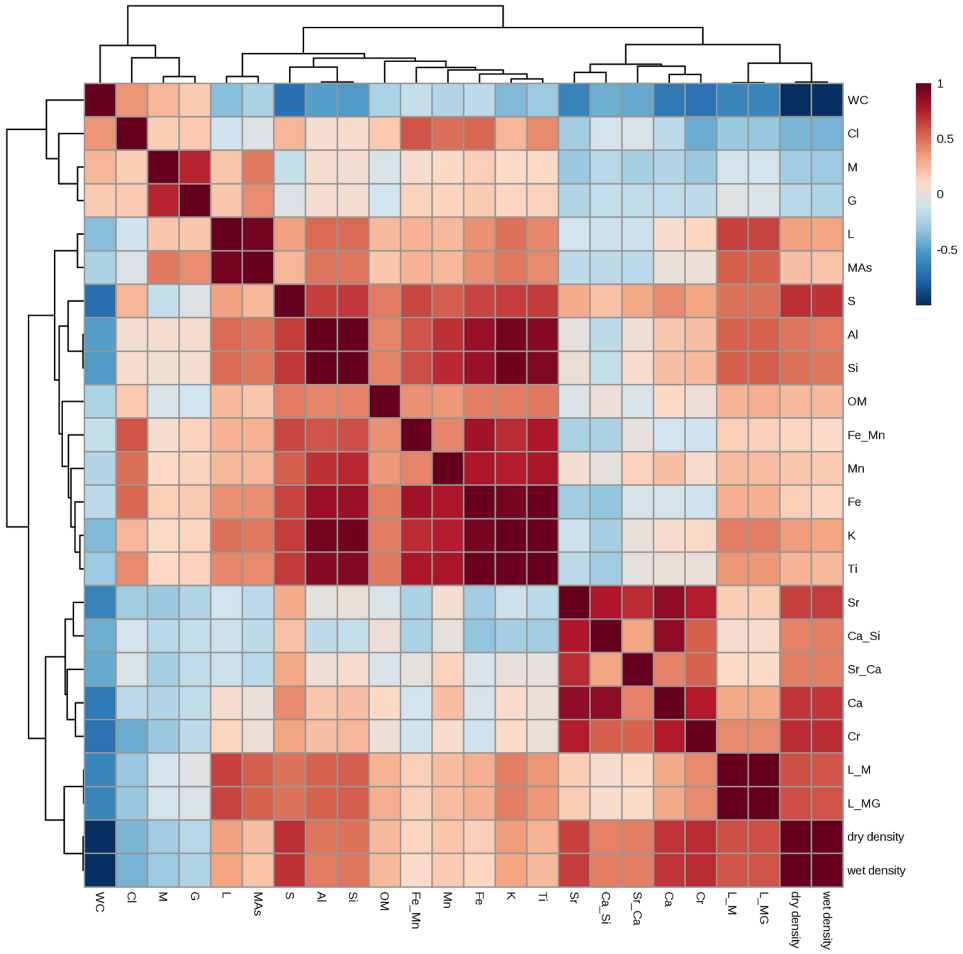

Figure 4.23: Pearson correlation matrix for Hala Hu dataset.

Hala Hu dataset was partitioned into 3 groups of samples according to the major differences registered by MAs. The chosen groups are are visible in the scores plot of Figure 4.25: 8.8-7.2 ky BP (number 3, blue), 7.1-4.1 ky BP (number 2, green), 4.1-0 (number 1, red) ky BP.
Then, the normalization of the dataset was achieved with an auto scaling

(mean-centred and divided by the standard deviation of each variable) [127]. The obtained values of the explained variance are 38.1% for PC1, 25% for PC2, 10.8% for PC3 (Figure 4.24). Looking at the variables loadings, absolute values above 0.25 are evidenced in bold in Table 4.3.

Table 4.3: PCA loadings for Hala Hu variables.

Variables	**PC1**	**PC2**	**PC3**
L	0.20	-0.08	**0.38**
L/M	0.24	0.06	**0.30**
L/(M+G)	0.24	0.07	**0.30**
M	-0.02	-0.19	0.21
G	0.00	-0.16	0.18
MAs	0.17	-0.13	**0.41**
Al	**0.29**	-0.12	-0.01
Ca	0.15	**0.29**	-0.11
Ca/Si	0.04	**0.30**	-0.14
Cl	0.01	-0.24	**-0.37**
Cr	0.16	**0.29**	0.01
Fe	0.24	**-0.26**	-0.16
Fe/Mn	0.18	-0.22	-0.20
K	**0.28**	-0.19	-0.07
Mn	0.21	-0.14	-0.23
S	**0.28**	0.02	-0.18
Si	**0.30**	-0.12	-0.02
Sr	0.09	**0.34**	-0.15
Sr/Ca	0.09	0.22	-0.22
Ti	**0.26**	-0.22	-0.13
WC%	**-0.25**	-0.23	-0.04
OM%	0.16	-0.08	-0.10
dry density	**0.25**	0.24	0.04
wet density	0.24	0.24	0.03

Therefore, it is possible to explain that PC1 is mainly due to the inorganic elements indicators of detrital influx, which are Al, K, Si, Ti and S with positive loadings. In fact, especially Si is considered to be a proxy for lithologic boundaries and changes in detrital flux [126].
In addition, quite significant loadings for PC1 are shown by MAs and their ratios. PC2 can be associated positively with Ca, Cr, Sr, Sr/Ca and negatively with Fe. PC3, then, is well identified with ΣMAs and levoglucosan positively, with Cl negatively.

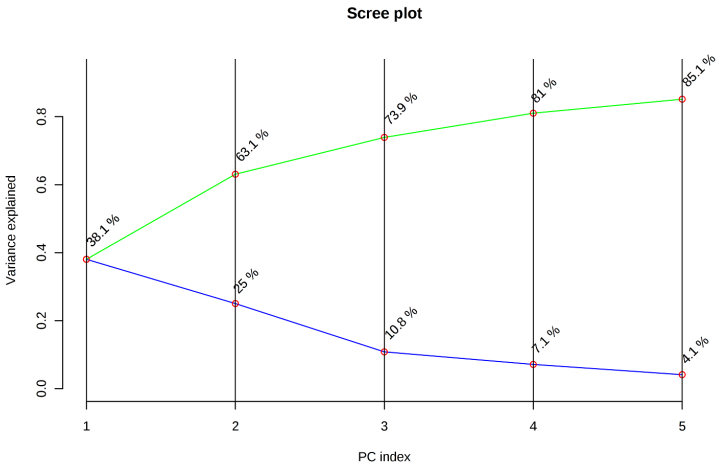

Figure 4.24: Scree plot of PCA analysis for Hala Hu dataset.

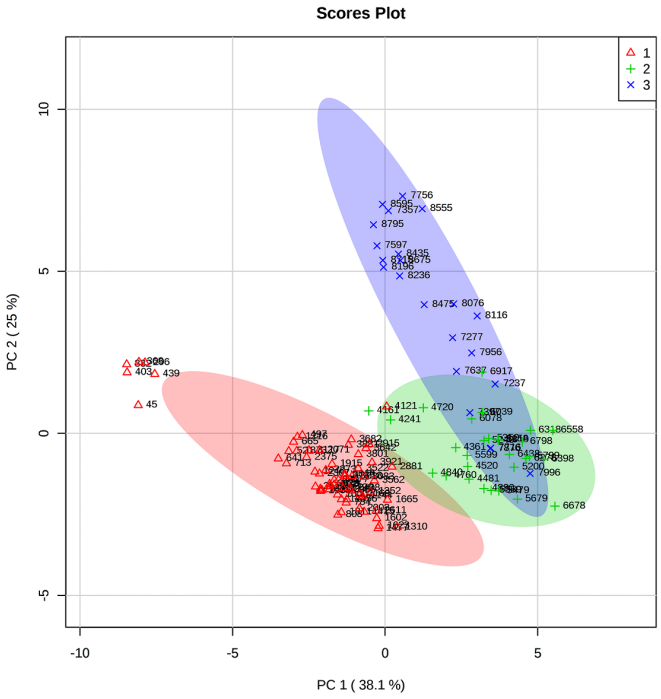

Figure 4.25: Scores plot of PCA analysis for Hala Hu dataset.

Observing the scores plot, both in Figure 4.25 and Figure 4.26, the 3 groups can be quite well divided according to the 3 major principal components:

- PC1 separates group 1 from 2-3;
- PC2 separates group 3 from 1-2;
- PC3 separates group 2 from 1-3.

To be noticed that the small set of samples that belong to group 1 but it is graphically split by it, has a different behaviour due to fair quantity of missing values.
As consequences of these divisions, group 3 (8.8-7.1 Ky BP) can be associated with higher values of salinity and carbonates, derived mostly by the variables Ca and Sr/Ca, and some medium values for detrital input proxies. Group 2 (4.1-7.1 ky BP) is well identified by high values of MAs and also of detrital fluxes, indicating that the intense fire peaks recorded in this warm and humid period could be associated with increased detrital supply and high lake levels. Finally, the variables that characterise group 1 (0-4.1 ky BP) are low quantities of detrital influx and of fire markers, except for few samples belonging to the period of discrete fire activity between 1 and 2 ky BP.

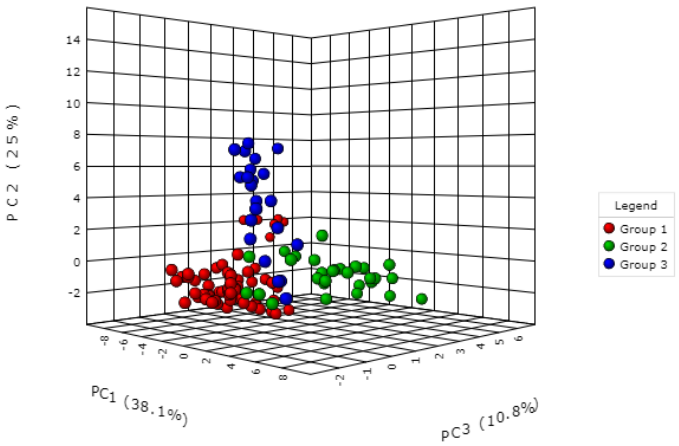

Figure 4.26: 3D scores plot of PCA analysis for Hala Hu dataset.

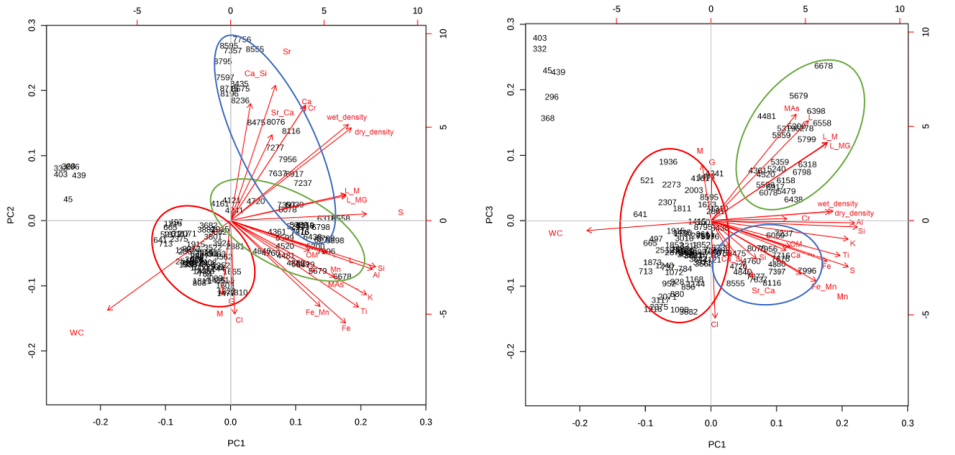

Figure 4.27: Biplots of PC1 vs PC2 and PC1 vs PC3 of PCA for Hala Hu dataset.

At this point, in order to visualize the patterns of fire and of detrital influx proxies at Hala Hu, Figure 4.28 must be observed. It is clearly noticeable the correlation between these parameters during the whole H11 record, except for the oldest samples, in which evidences of detrital inputs were found, while fire activity was not recorded.
According to this fact and to some similarities evidenced in the previous section between Hala Hu fire reconstruction and others NETP records, the issue whether levoglucosan signal in H11 is due to human invasions of the area with "slash and burn" activities or to climatic drivers is still to be evaluated. Moreover, the post-depositional effects on levoglucosan are still needed to be further assessed and no literature studies were found on this topic. Nevertheless, the secondary deposition process can be excluded as explanation for these results, because, despite levoglucosan can be quite easily degraded in water [168], its preservation is enhanced when attached to sediment and aerosol particles [62, 168, 169], assuring its deposition and burial, and then its power as paleofire proxy.

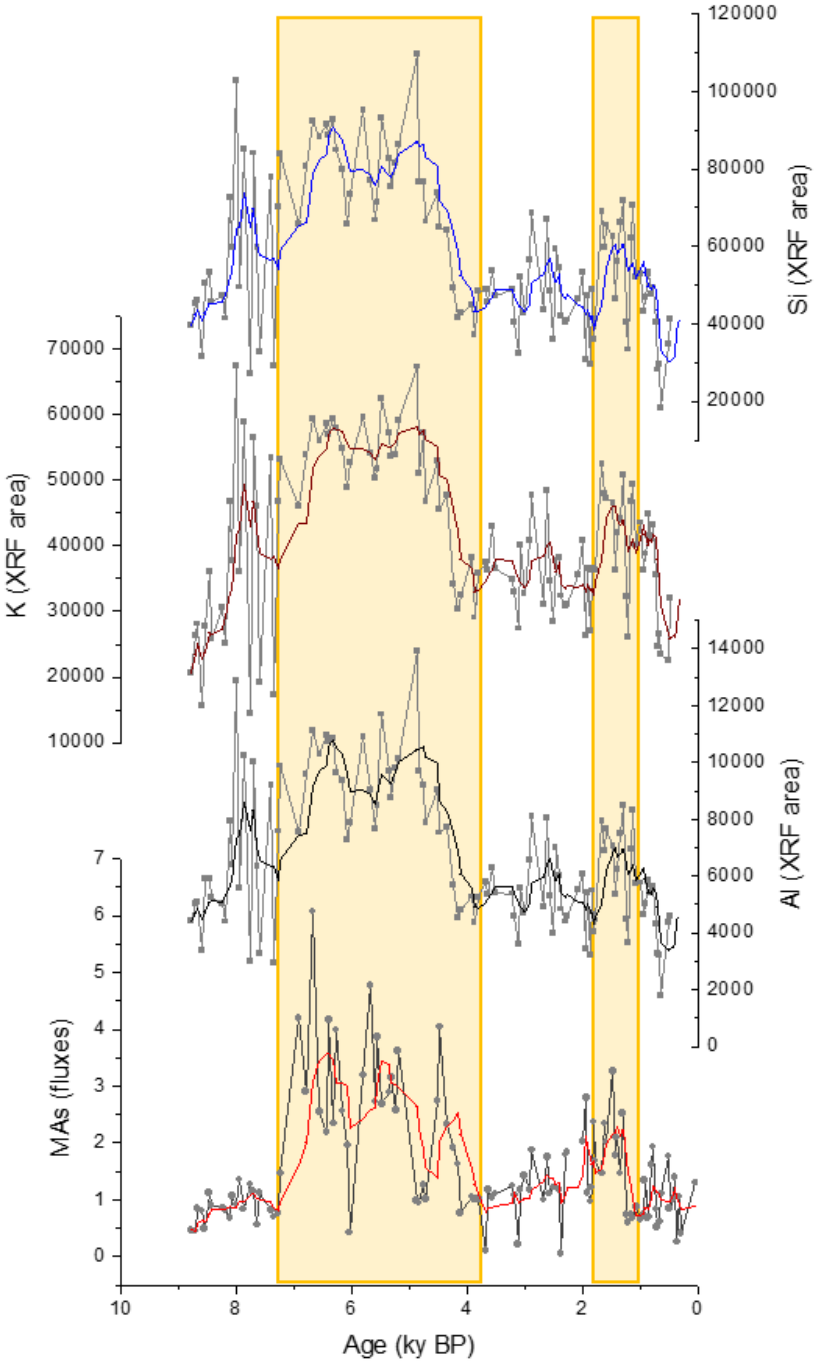

Figure 4.28: Results from Hala Hu showing ΣMAs and XRF data for Al, K, Si. Orange boxes indicate the periods with clear evidence of association between intense fire activity and high concentrations of these elements.

4.3 Composite analysis of charcoal data

Looking at the GCD version 3 and interpolating its data from multiple series to a unique one using *paleofire* R package, it is possible to infer some considerations about Holocene fire events in the Asiatic region.
Taking into account that the GCD does not include charcoal records located in the Tibetan Plateau, the consideration of other records coming from the surrounding territories was needed, in order to compare their composite signal with Paru Co and Hala Hu fire records. In fact, considering that MAs catchment area goes from few to hundreds kilometres, this intercomparison is possible. The period between 0 and 12 ky BP and the entire Chinese area, containing 43 sites, were firstly selected (Figure 4.29, Figure 4.30); then, different ranges of latitudes and longitudes were explored, dividing the records around the TP into 3 groups according to cardinal points (Figure 4.31, Figure 4.32, Figure 4.33). The North-Eastern, South-Eastern and North-Western charcoal record groups included 31, 34 and 20 sites, respectively, and, despite the scarcity of available sites, were used to infer considerations about the geographical provenance of the fire signal. Concerning the South-Western part of the TP, the nearest sites come from East Africa, subjected to different climatic drivers and probably too far to be used for the data computation and interpolation.

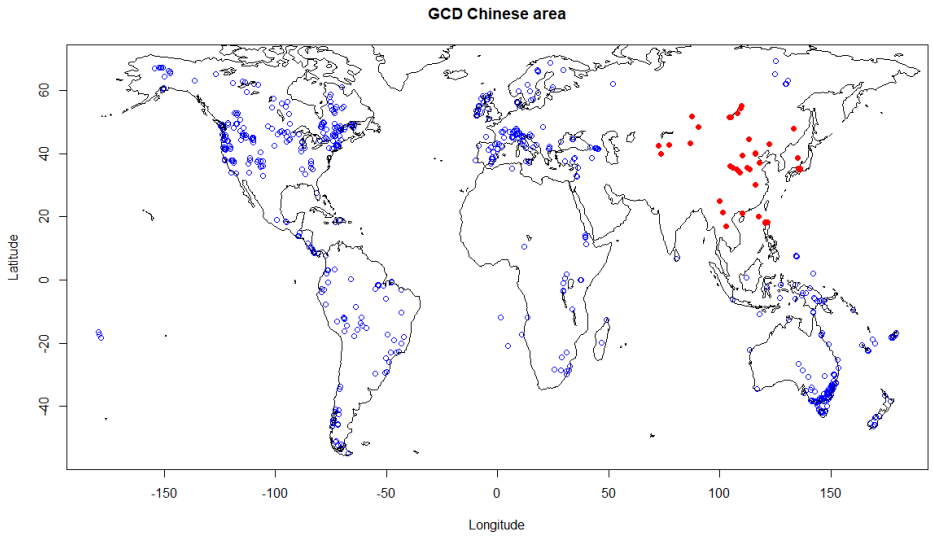

Figure 4.29: Map with selected site in red from the GCD, Chinese area.

Comparing charcoal composite record with Paru Co and Hala Hu fire records, it is possible to observe how MAs signals match or differ with the charcoal index (Figure 4.34). Looking at the three reconstructions at a millennial

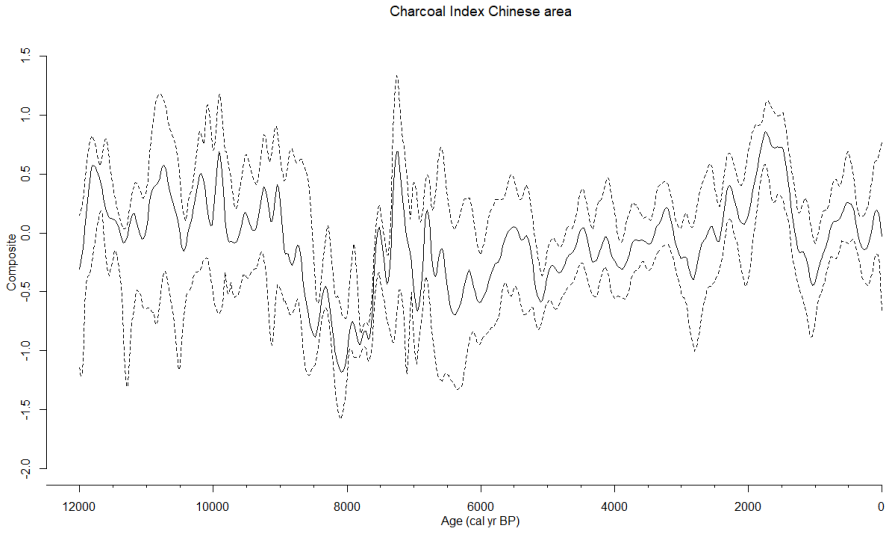

Figure 4.30: Charcoal Index: charcoal data transformation, background estimation and homogenisation from multiple series to a unique one from the Chinese area.

scale, the trends appear very different. However, examining the short-term variability, some similarities in fire pattern are recognizable, highlighted with coloured bars in Figure 4.34. All the following considerations have been drawn taking into account the different burning temperatures and transport patterns of charcoal and MAs. Currently, most paleofire researchers analyse macroscopic charcoal particles (> 100 μm) sampled contiguously from sediment cores to produce fire-history records that are spatially and temporally precise [69] because macrocharcoal generally travels few kilometres from its source and it is burnt at temperature between 250 and 550 ^{o}C, while levoglucosan its mainly produced at 250 ^{o}C and can travel up to hundreds kilometres. In addition to this, the dating uncertainties among the different records and the composite charcoal index can be source of misinterpretation. Firstly, the Chinese area composite series seems to show, despite the bias, high fire activity during the Early Holocene with two main peaks, as in Paru Co. Then, a decreasing biomass burning period around 8 ky BP and then again a slight increasing trend towards the present. This is verified by Marlon et al. [7], who reported that Eastern Asia exhibits the characteristic response of regional biomass burning: biomass burned increased non-linearly with temperature, growing more rapidly at higher temperatures, and increased non-linearly with decreasing moisture. In the monsoon areas of Asia and Australasia and also in Africa, burning is higher in the early and late Holocene than in the mid-Holocene. However, Asia was marked by very low biomass

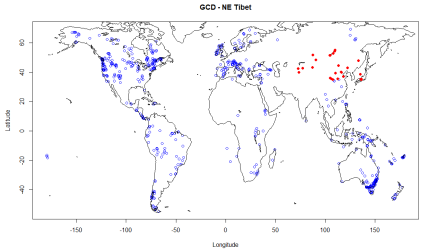

(a) *Map with selected sites in red*

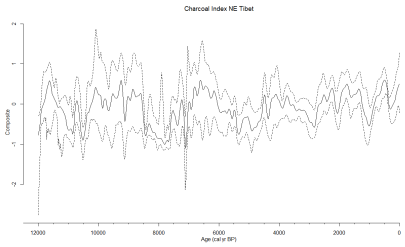

(b) *Charcoal Index*

Figure 4.31: Charcoal data transformation, background estimation and homogenisation from multiple series to a unique one from the North-Eastern area outside the Tibetan Plateau.

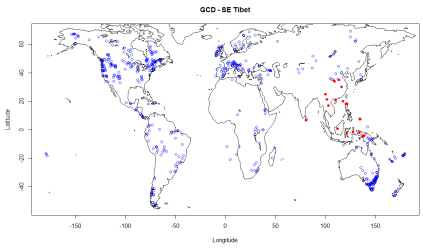

(a) *Map with selected sites in red*

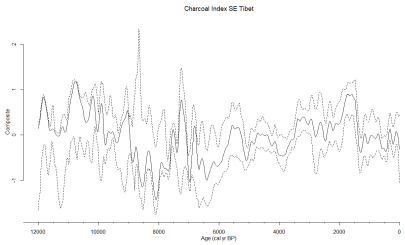

(b) *Charcoal Index*

Figure 4.32: Charcoal data transformation, background estimation and homogenisation from multiple series to a unique one from the South-Eastern area outside the Tibetan Plateau.

burning ca 9-8 ky BP, while the opposite happened in Australasia at the same time [7]. Paru Co's high fire activity in the early Holocene is in accordance with the charcoal composite record around 10 ky BP, but intense biomass burning recorded in Paru Co around 8 ky BP is not explained by charcoal, very low in that period, neither registered in Hala Hu. The fire peaks visible in Hala Hu between 7 and 4 ky BP are not clearly associated with charcoal's trend, where some peaks are visible but a flat pattern seems to prevail. Intense fire activity can be observed between 6 and 5 ky BP in Hala Hu, Paru Co and somehow in the charcoal index, and was recorded also in the charcoal record from lake Nam Co [58]. Then, smaller fire peaks could be seen in Paru Co between 3 and 2 ky BP, slightly in accordance with the general increase in fire. Again, high fire activity observed in Hala Hu between 2 and 1 ky BP is matching the regional trend.
Many regions during the Early Holocene were characterized by high fire, owing to local conditions, e.g. decreasing ice-sheet size, vegetation changes, and rising sea-surface temperature and sea level [7, 67].

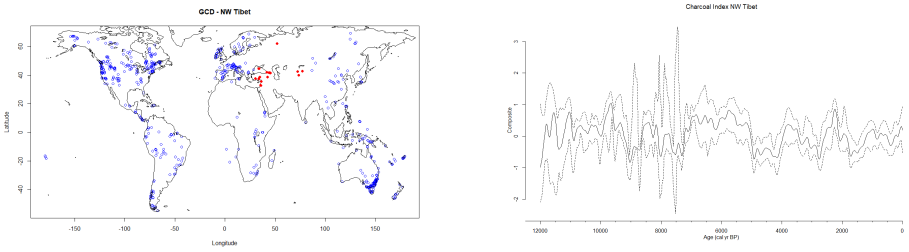

(a) *Map with selected sites in red* (b) *Charcoal Index*

Figure 4.33: Charcoal data transformation, background estimation and homogenisation from multiple series to a unique one from the North-Western area outside the Tibetan Plateau.

Recent studies have shown that the climatic change at 5.5 ky BP (Bond event 4) was one of the most prominent climatic events that occurred all over the world in the Holocene [170, 122]. The marked increase in fire between 6 and 5 ky BP, identified in individual records of charcoal, has been attributed to an increase in ENSO activity [7]. These informations might be consistent with the 5.5 ky BP increase in monosaccharide anhydrides concentration both in Paru Co and Hala Hu.
As far as the regional charcoal groups, high fire signals in the Early Holocene in Paru Co and in the period 7-6 ky BP in Hala Hu are more pronounced in the regional composite record from the North-Eastern area, as it could be seen in Figure 4.31. Moreover, intensive biomass burning activity around 10.5 and 2-1 ky BP can be associated with a South-Eastern signal (Figure 4.32). On the contrary, fire trend reconstructed using and North-Western (Figure 4.33) charcoal group is difficult to be interpreted. The explanation for this hurdle could be most certainly due to the number of sites, not enough to perform a significant statistical study.

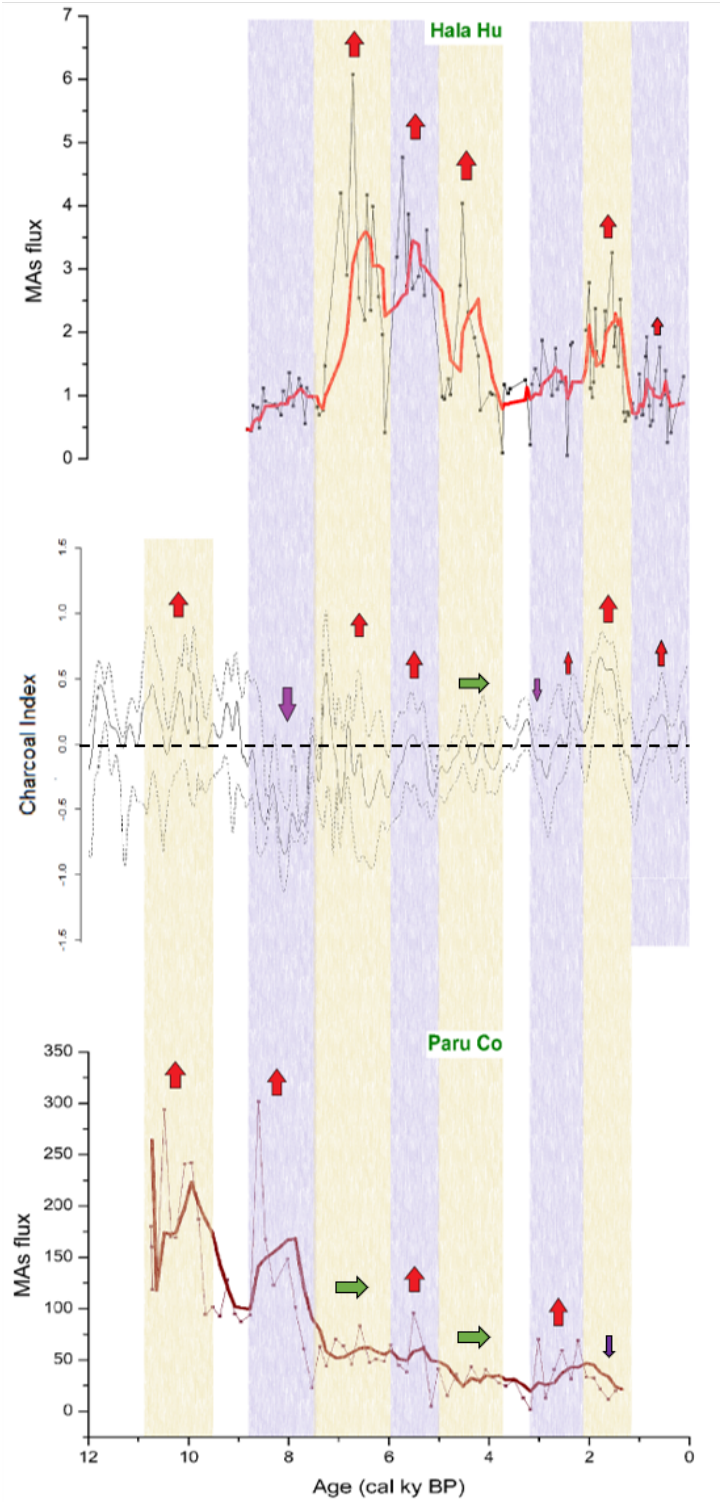

Figure 4.34: Charcoal data composite record from the Chinese region, compared to Hala Hu and Paru Co MAs record.

4.4 Relationship with other climatic records

A conjunct interpretation of fire records from Paru Co and Hala Hu is not immediately neither clearly feasible and it needs comparisons with other records from the TP. The locations are settled within high mountains ridges that from one side can act as natural barriers to block the transport of smoke aerosols to the TP, and from the other side contain glaciers and lakes, which mainly act as receptors of biomass burning emissions from surrounding regions [171]. The climatic systems that act on Paru Co and Hala Hu are mainly southern monsoons and westerlies, respectively, and these could have act as major transport ways for levoglucosan associated to particles in the two analysed sediment cores. In fact, Wang et al. [104] studied the black carbon (BC) patterns and reported that the Northern Tibetan Plateau is controlled by the westerlies during all year, and the airborne BC is dominated by the transport from the arid and semi-arid region on the north TP and Central Asia, while in the Southern TP BC was transported by the air masses from the North-Eastern India and Bangladesh in both winter and spring, influenced by regional monsoon precipitation.
Moreover, the two studied records differ in time span, which is 10.9-1.3 ky BP for Paru Co and 8.9-0 ky BP for Hala Hu, and in time resolution, higher for Hala Hu. Must be taken into account that fire events might have been missed because of sub-sampling resolution.
The diversities between the two records must be also settled into the feedback responses mechanisms of the environments, that can lead to asynchronicities, for example in the middle to late-Holocene climate transitions. Indeed, it is not expected that different past ecosystems supporting different cultures should have responded to the dramatic climatic transition absolutely synchronously, even if the climate change happened more or less synchronous on regional and hemispheric scales [122].
Association between asian monsoon (AM) and fire events can be made in both lakes because, according to Tang et al. [115] the summer monsoon enforced apparently at 10 ky BP and reached its maximum in SETP at 8 ky BP, and the time range 10-8 ky BP indicates a lot of fires in Paru Co; thereafter, 7 ky BP it reached the summit in NW-NETP and it was followed by a gradually weakened monsoon system from 6 ky BP to the present, and rightly at 7 ky BP started to be registered fire activity at Hala Hu. In agreement with Colombaroli et al. [172], fire peaks at medium levels of moisture balance are possible, and the response of fire to spatial/temporal climate variability fluctuation can be considered as a deterministic process.
According to Wang et al. [173], the long gradual weakening in AM intensity through the Holocene correlates well with other northern low-latitude records and results directly from the orbitally induced lowering of summer insolation, affecting ITCZ position and low-latitude precipitation patterns. Meantime, the short-term variability of AM is also characterized by events that correlate

with changes in oceanic and atmospheric circulation [173, 174]. Can be evidenced that the history of the AM during the Holocene broadly follows summer insolation and it is punctuated by eight weak monsoon episodes lasting from 1 to 5 centuries, in correspondence of the abrupt climate changes phenomena known as "Bond events" (0.5, 1.6, 2.7, 4-4.4, 5.5, 6.3, 7.2 and 8-8.3 ky BP) [173, 175, 174]. Bond events 7 to 0 appear in coincidence with weakening periods of the AM and in particular the 8.2 ky event is the more prominent together with the 4 ky event, that correlates with the collapse of the Chinese Neolithic culture [122, 173]. Most of the other events are associated with North Atlantic ice-rafting events [173, 174].
The integration between these events and biomass burning reconstruction in Paru Co and Hala Hu is shown in Figure 4.35. In order to identify interconnections between Bond events and fire activity, specific statistical software would be needed and improved, besides the mere visual interpretation of Figure 4.35. Regarding Paru Co, Bond events 7, 6 and 5 are settled in the period of the major fire activity recorded by this lake, that corresponds also to minor quantities of biogenic silica. Then, due to the decreasing trend of fire, no associations can be visualised, except for the fire peak at around 5.5 ky, present also in Hala Hu, both in fire and Si. In Hala Hu the 7.2 ky event is located right at the starting point of increasing trend of Si and fire. Also, Bond events 4, 3 and 1 seem to correspond with high fire peaks. The issue whether this correlation is significant or not would need further investigations.

Looking at other climatic records from the surroundings of the TP can be seen that the Pleistocene-Holocene transition was characterized by increasing temperatures until circa 8.2 ky BP, when a dramatic change was documented in different regions (i.e. Bond event 5) [176]. After Bond event 5, the summertime temperature in the northern high latitudes has decreased almost linearly until the last millennium [122]. The higher average summer SSTs are consistent with a stronger summer monsoon during the Middle Holocene, characterized indeed by warm and wet climate [141, 170]. ENSO variability in the mid-Holocene was weaker than that in the modern records, and the SST record with the highest summer temperatures from circa 6.46 ky BP to 6.50 ky BP shows no robust ENSO cycle. This agrees with other studies indicating that stronger summer monsoon circulation may have been associated with suppressed ENSO variability during the mid-Holocene [170]. The timing is consistent with paleo-monsoon records from southern China and with the idea that the interplays between summer insolation and other large-scale boundary conditions, including SST and sea-level change, control regional climate [141]. Afterword, a drying trend during the past 6000 years was abundantly documented in many records from the northern subtropics and tropics [122]. The cooling trend after the Holocene Climatic Optimum (6.5-4.7 ky BP) was correlated with decreasing solar insolation [141] and was the cause of a progressive southward shift of the Northern Hemisphere summer position of

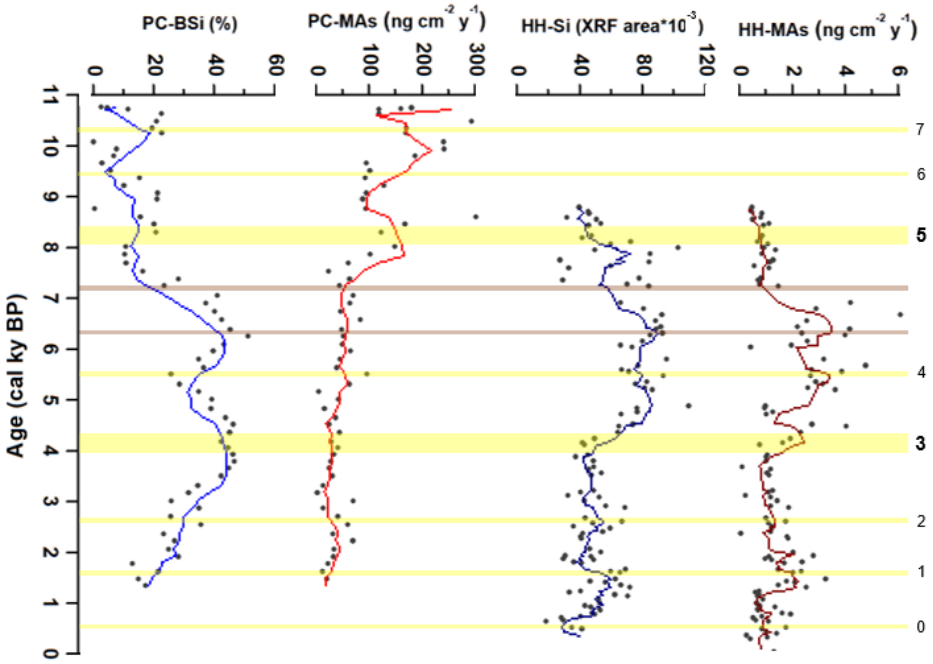

Figure 4.35: Holocene Bond events 0 to 7 (yellow bars) within fire and silica proxies in Paru Co and Hala Hu. Grey bars indicate other two events of lowering of the Asian Monsoon, according to Bond et al. and Wang et al. [173, 174].

the ITCZ, resulting in a decreasing strength of the monsoon systems in both Asia and Africa, making the climate even drier through the negative feedbacks of "air-land interactions". The lowered solar activities during Bond event 3 finally turned the climate into a more dramatic drying mode at circa 4.2 ky BP, directly or indirectly leading to the observed collapses of many Chinese Neolithic cultures [122, 173]. During the past 750 years in the Altai region precipitation changes controlled fire-regime and vegetation shifts, and the high sensitivity of ecosystems to occasional decal-scale drought events may, in the future, trigger unprecedented environmental reorganizations under global-warming conditions [177].
Regional synthesis of five pollen records along a south-north transect indicates that this climate pattern can be recognized all across the eastern Tibetan Plateau [141] and so Paru Co and Hala Hu paleoreconstructions can be setted in this pattern as well. Considering pollen potentiality as proxies for precipitation (positive correlation) an temperature (negative correlation) and thus as indicators of moisture availability and vegetation density [95], the comparison of pollen data with Hala Hu and Paru Co is very useful. Vegetation density and productivity increased during the early to middle

Holocene, as suggested by relatively high pollen concentrations in the Dunde ice cap (north TP) during ca. 10–4.8 ky BP, only interrupted by the already mentioned abrupt return to dry conditions during 8.0–7.7 ky BP [95]. Pollen data are consistent with the oxygen isotope record showing a gradual ^{18}O enrichment throughout the Holocene with a warm period centred at 8–6 ky BP. Then, progressive drying of the climate with maximum aridity at circa 4.0–3.0 ky BP was linked with the Northern Hemisphere summer insolation, and the cold events at 8.2–7.4, 5.8–5.3, 3.4–2.9 and 1.8–1.3 ky BP reflect the high-latitude influence of the winter monsoon [121]. Finally, the intervals 2.7–2.2, 1.5–0.8 and 0.6–0 ky BP were comparatively humid periods with higher vegetation density and productivity, with characteristic pollen taxa of alpine meadow (Cyperaceae, *Polygonum*) [95].
From the above data, it can be suggested that increased biomass availability as fire fuel was the pivotal driver for the kindling of intense fire activity periods in both lakes, firstly in Paru Co and then in Hala Hu. The ending of Paru Co high burning stage at circa 8 ky BP might have been caused by Bond event 5, which, with about 1 ky delay, can be addressed also as the primer event for the starting of fires recorded by Hala Hu, that lasted until 4 ky BP during increasing drying conditions (evidenced by declining *Artemisia*/Chenopodiaceae pollen ratio [95]). Samples from ca. 790–620 yr B.P. (A.D. 1200– 1370) contain abundant dust particles but very low pollen concentrations suggesting an interval with warm, dry summers and very windy conditions coincident with part of the Medieval Warm Period (MWP) [95]. These data can be associated with the medium-low fire events registered in the same period at Hala Hu. Holocene landscape and vegetation changes in TP are, therefore, derived by the interactions between monsoonal activity and a not clearly quantifiable human influence (possible deforestation) [58].
In the KE section, Gonghe Basin, studied by Miao et al. [121], the percentages of woody plants and herbs were high during the early-mid Holocene (8.2–4.2 ky BP), and obviously decreased after 3 ky BP; this compares well with the arboreal pollen percentages from the neighbouring DLH core [178], Qinghai Lake and Zigetang Lake [140, 155, 156] (Figure 4.36). These similar long-term trends of climate change are considered to be the result of the consistent influence of insolation forcing on vegetation and climate changes in high alpine environments [140, 179]. This means that during warm stages the monsoonal system brings and will bring more effective precipitation into the NETP as well as to other Asian monsoon regions, indicating insolation-driven temperature changes as the key climate driving force for the Holocene vegetation successions in the central Tibetan Plateau [124].

Holocene climatic trends in the TP were also studied thanks to data-model comparisons. The reconstructions with models primarily identify decreasing summer monsoon precipitation and changes in the temperature of the warm season as the responsible mechanisms for the vegetation shift [182]. The

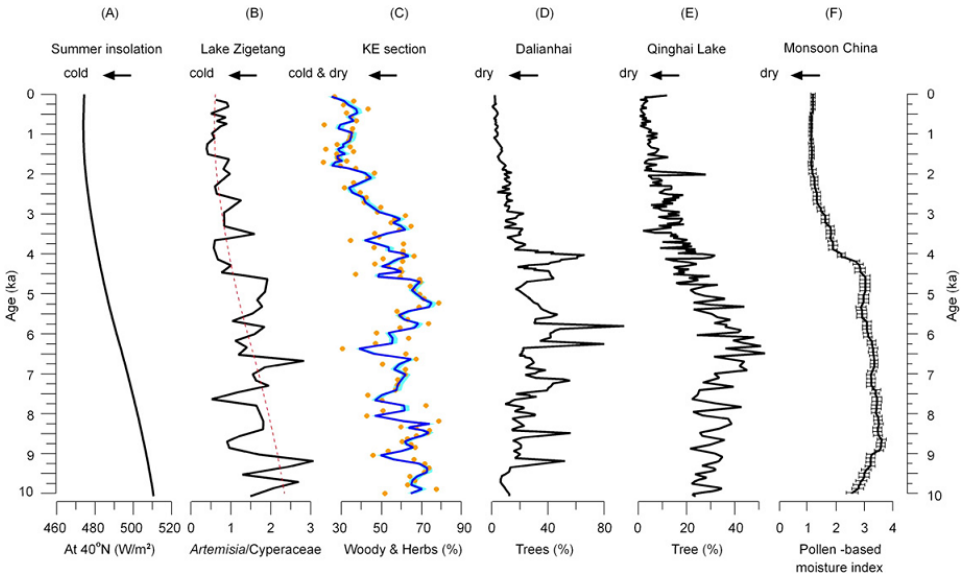

Figure 4.36: Comparison of KE section climate evolution with other selected proxy records from the neighboring area during the last 10 ky: (A) summer insolation at 40^{o}N [180]; (B) ratio of *Artemisia*/Cyperaceae at the Zigetang Lake [140]; (C) percentages of woody and herbaceous plants at the KE section [121]. Percentages of the arboreal pollen at the (D) Dalianhai Lake [178] and (E) Qinghai Lake [155]; (F) pollen-based moisture index in monsoonal China [181]. Image source: [121].

averaged forest fraction on the Plateau shrank by almost one-third from mid-Holocene (41.4%) to present (28.3 %). Shrubs, instead, are quadrupled at present-day (12.3 %), replacing most of this forest. Grass fraction increased from 38.1% during the mid-Holocene to the 42.3% of now. This land cover change was documented also by Lu et al. [183], with SETP forest decline contrasted to shrubs increase from 6 ky to now.

Finally, concerning dust records in the TP, with the aim to compare them with fire peaks to find some similarities, scarcity of intense dust transport was observed throughout the Holocene, except for the rapid decrease in dust deposition at the Last Glacial Stage - Holocene transition. This dust increase could reflect substantial change in the prevailing climatic conditions that limited the capability of the atmosphere to transport dust [184]. Qiang et al. [185] studied dust layers in Genggahai Lake (NETP) and discovered that aeolian activity was weak from 10.3 to 6.3 ky BP, which may be a response to increased vegetation cover due to the strengthened Asian summer monsoon. In contrast, in central Asia (Lake Zhuyeze, [176]) the 8.2 ky event started the increased mobility of aeolian sands which gradually caused the degradation of vegetation because of burial and led to massive and widespread aeolian sand transportation, up to 7.5 ky when the vegetation recovered. Then, the

overall intensification of aeolian activity in NETP between 11.6 and 10.3 ky BP and after 6.3 ky BP would be associated with the reduced vegetation cover. Dust layers occurred episodically when the summer monsoon weakened in the periods 5.5-6, 4-4.6, 1.4-1.8 and 0.2 ky BP and these abrupt events of sand mobility were associated with enhanced wind strength, probably in response to cooling events at high latitudes [185]. An hypothesis regarding these increased wind events is that they might have had an influence on MAs transport to the analysed lakes, allowing the finding of the evidences of fire peaks at Hala Hu (5.8-5.2, 4.5-4.1, 1.6 ky BP) and Paru Co (5.6 ky BP).

Chapter 5

Conclusions

In this work the reconstruction of biomass burning history on the Tibetan Plateau was performed with the analyses of more common used proxies, i.e n-alkanes and charcoal, was combined with MAs, PAHs and FeSts analyses. The achieved results confirm the appropriate usefulness of lacustrine sediments as key storage materials, recommend the suitability of this multi-biomarkers approach, endorse the general applicability of MAs as firemarkers and propose a wider diffusion of their adoption.
The utility of these proxies as indirect indicators of past climate and ecosystem changes is confirmed, but still has its limitations due to low concentrations levels e.g. for FeSts and PAHs. Moreover, the less used MAs add consistent information to the climatic scenarios and their applicability is recommended within a paleoclimatic reconstruction. However, to overcome their limitations such as doubtful sources and uncertain degradation pattern, MAs are therefore suggested to be included in multi-proxy studies, together with PAHs, n-alkanes and FeSts. This last group of molecules, when found, is clearly indicative of human/animal presence and thus it allow a fair identification of human induced fires.
The paleofire reconstructions performed during this research revealed Holocene biomass burning events and related vegetation changes in the Tibetan Plateau. The two selected lakes, Paru Co (NETP) and Hala Hu (SETP) showed different periods of fire activity during the past 11 ky. These fire events were mostly related to the climatic systems which act on the Tibetan Plateau, especially Westerlies for the Northern Tibet and Southern Monsoons for the Southern Tibet.
A general synthesis of the obtained results can be finalized putting them into the regional paleoclimatic framework of the TP. According both to fire signals and climatic variations, the three periods of Early-Middle-Late Holocene can be described as follows.

1. Early Holocene: 10.9-7.5 ky BP
   The period 10.9-10.7 ky BP was characterized by increasingly warming and drying climate due to the transition from the Pleistocene, then followed by an intensification phase of the ISM up to the Middle Holocene. These conditions probably favoured vegetation growth that led to fire activity recorded in Paru Co both by MAs and PAHs, in a decreasing trend. High biomass burning in the Chinese region is also registered by charcoal from 12 up to 9 ky BP. The paleofire at Paru Co about 9-7.5 ky BP, instead, neither in Hala Hu nor in the charcoal synthesis is observed, suggesting that it could be ascribed to local fires, subsequently lowered and interrupted maybe by the dramatic dry event of circa 8 ky BP, known as Bond event 5. MAs ratios and pollen records indicated meadow as prevalent vegetation in Paru Co, confirmed at some points also by grass/wood ratio of n-alkanes. Softwood forests were likely prevalently settled around Hala Hu, due to favourable humid climate.

2. Middle Holocene: 7.5-3.8 ky BP
   While the 8 ky event could have caused the sharp decline in Paru Co fire record, its reverberations on the northern TP arrived at around 7 ky BP, when intense fire activity started in Hala Hu, lasting circa 3000 years. During this period 3 main peaks of fire are visible at 6.5, 5.8-5.2 and 4.5 ky BP and MAs ratios values could indicate combustion of grass and softwood, with smoke and aerosol particles. Extensive forest presence is confirmed by numerous pollen records in the NETP, indicating that the humid climate was favouring vegetation growth and its subsequent availability as kindling for fire. Increased forest vegetation cover due to the strengthened Asian and Indian Summer Monsoons is observed also in Paru Co, leading to the 5.6 ky BP fire event as the unique one recorded in this core in the Middle Holocene. This event is registered in Hala Hu and charcoal composite record too, probably indicating a regional source of fire, as it can be likewise associated with enhanced aeolian activity most likely related to drying and cooling events. At around 6 ky BP a general drying climatic pattern is observed, reaching the maximum at circa 4.2 ky BP, with very cold climate as well (Bond event 3). At this point, fire activity in Hala Hu was stopped and the forest decline started. This period coincides with the expansion of Bronze Age civilizations that could have had an impact on landscape changes.

3. Late Holocene: 3.8-0 ky BP
   The past few thousands years were characterized by low fire activity both in Hala Hu and Paru Co, with some exceptions at 1.6 ky BP in Hala Hu, when even elevated detrital input into the lake and high wind

activity were reported. Vegetation prevalence of steppe and grasses were documented in both sites, due to the weaker summer insolation and lesser precipitations.

Some research perspectives could be gained from this work and implemented in the near future. First, take into account the methodological process both from the experimental design and from the innovative analytical procedure points of view, as the basis for future paleo-/ecological reconstructions. Then, starting from the major strength of the work, i.e. the combination of new and established indicators in a multi-proxy approach, establish an ultimate and standardised working scheme that can reduce the analytical errors and improve the reliability of this kind of studies. Moreover, try to set up and apply new statistical methods to gain more insights about the significance of correlations among the diverse parameters. Finally, expand the area of interest, investigating new cores from the same lakes and including new lakes nearby Paru Co and Hala Hu, in order to confirm the obtained results and enhance the knowledge about the paleoclimate of the Tibetan Plateau.

References

[1] Juli G Pausas and Jon E Keeley. "A burning story: The role of rire in the history of life". In: *BioScience* 59.7 (2009), pp. 593–601. ISSN: 0006-3568. DOI: 10.1525/bio.2009.59.7.10.

[2] I. J. Glasspool, D. Edwards, and L. Axe. "Charcoal in the Silurian as evidence for the earliest wildfire". In: *Geology* 32.5 (2004), pp. 381–383. ISSN: 00917613. DOI: 10.1130/G20363.1.

[3] W.J. Bond. "Fires, Ecological Effects of". In: *Encyclopedia of Biodiversity, Volume 3*. Second Edi. 2013, pp. 435–442. ISBN: 9780128096338. DOI: 10.1016/B978-0-12-809633-8.02098-7. URL: http://www.sciencedirect.com/science/article/pii/B9780128096338020987.

[4] Paul J Crutzen and Meinrat O Andreae. "Biomass burning in the tropics: impact on atmospheric chemistry and biogeochemical cycles". In: *Science* 250.4988 (1990).

[5] William F. Ruddiman. "The Anthropocene". In: *Annual Review of Earth and Planetary Sciences* 41.1 (2013), pp. 45–68. ISSN: 0084-6597. DOI: 10.1146/annurev-earth-050212-123944. URL: http://www.annualreviews.org/doi/abs/10.1146/annurev-earth-050212-123944.

[6] William F Ruddiman. "The Anthropogenic Greenhouse Era Began Thousands of Years Ago". In: *Climatic Change* 61 (2003), pp. 261–293. ISSN: 0165-0009. DOI: 10.1007/s10584-005-7278-0.

[7] Jennifer R. Marlon et al. "Global biomass burning: A synthesis and review of Holocene paleofire records and their controls". In: *Quaternary Science Reviews* 65 (2013), pp. 5–25. ISSN: 02773791. DOI: 10.1016/j.quascirev.2012.11.029.

[8] William J. Bond. "Fires in the Cenozoic: a late flowering of flammable ecosystems". In: *Frontiers in Plant Science* 5.January (2015), p. 749. ISSN: 1664-462X. DOI: 10.3389/fpls.2014.00749. URL: http://journal.frontiersin.org/article/10.3389/fpls.2014.00749/abstract.

[9] Yunfa Miao et al. “Holocene fire on the northeast Tibetan Plateau in relation to climate change and human activity”. In: *Quaternary International* (2016). DOI: 10.1016/j.quaint.2016.05.029.

[10] D. W. Woodcock and P. V. Wells. “The burning of the new world: The extent and significance of broadcst burning by early humans”. In: *Chemosphere* 29.5 (1994), pp. 935–948. ISSN: 00456535. DOI: 10.1016/0045-6535(94)90161-9.

[11] Bin Zhou et al. “Elemental carbon record of paleofire history on the Chinese Loess Plateau during the last 420 ka and its response to environmental and climate changes”. In: *Palaeogeography, Palaeoclimatology, Palaeoecology* 252.3-4 (2007), pp. 617–625. ISSN: 00310182. DOI: 10.1016/j.palaeo.2007.05.014.

[12] Bernd Zolitschka et al. “Varves in lake sediments – a review”. In: *Quaternary Science Reviews* 117 (June 2015), pp. 1–41. ISSN: 02773791. DOI: 10.1016/j.quascirev.2015.03.019. URL: http://linkinghub.elsevier.com/retrieve/pii/S0277379115001262.

[13] Dada Yan and Bernd Wünnemann. “Late Quaternary water depth changes in Hala Lake, northeastern Tibetan Plateau, derived from ostracod assemblages and sediment properties in multiple sediment records”. In: *Quaternary Science Reviews* 95 (2014), pp. 95–114.

[14] Robert M. D’Anjou et al. “Climate impacts on human settlement and agricultural activities in northern Norway revealed through sediment biogeochemistry.” In: *Proceedings of the National Academy of Sciences of the United States of America* 109.50 (2012), pp. 20332–20337. ISSN: 1091-6490. DOI: 10.1073/pnas.1212730109.

[15] Anders R. Johnsen, Lukas Y. Wick, and Hauke Harms. “Principles of microbial PAH-degradation in soil”. In: *Environmental Pollution* 133.1 (2005), pp. 71–84. ISSN: 02697491. DOI: 10.1016/j.envpol.2004.04.015.

[16] Simon Schüpbach et al. “Combining charcoal sediment and molecular markers to infer a Holocene fire history in the Maya Lowlands of Petén, Guatemala”. In: *Quaternary Science Reviews* 115 (2015), pp. 123–131. ISSN: 02773791. DOI: 10.1016/j.quascirev.2015.03.004.

[17] Dario Battistel et al. “Fire and human record at Lake Victoria , East Africa , during the Early Iron Age : Did humans or climate cause massive ecosystem changes during the Early Iron Age in East Africa?” In: *The Holocene* (2016). ISSN: 0959-6836. DOI: 10.1177/0959683616678466.

[18] M O Andreae and P Merlet. “Emission of trace gases and aerosols from biomass burning”. In: *Global Biogeochemical Cycles* 15.4 (2001), pp. 955–966.

[19] Bärbel Langmann et al. "Vegetation fire emissions and their impact on air pollution and climate". In: *Atmospheric Environment* 43 (2009), pp. 107–116. ISSN: 13522310. DOI: 10.1016/j.atmosenv.2008.09.047. URL: http://www.sciencedirect.com/science/article/pii/S135223100800900X.

[20] M. Wang et al. "Carbonaceous aerosols recorded in a southeastern Tibetan glacier: Analysis of temporal variations and model estimates of sources and radiative forcing". In: *Atmospheric Chemistry and Physics* 15.3 (2015), pp. 1191–1204. ISSN: 16807324. DOI: 10.5194/acp-15-1191-2015.

[21] D.M.J.S. Bowman et al. "Fire in the Earth system." In: *Science* 324.5926 (2009), pp. 481–4. ISSN: 1095-9203. DOI: 10.1126/science.1163886. URL: http://www.ncbi.nlm.nih.gov/pubmed/19390038.

[22] IPCC. *Summary for Policymakers*. Ed. by R.K. Pachauri Core Writing Team and L.A. Meyer (eds.) Geneva, 2014, p. 151. ISBN: 9789291691432. DOI: 10.1017/CBO9781107415324. arXiv: arXiv:1011.1669v3.

[23] Pete Smith et al. *Agriculture, forestry and other land use (AFOLU)*. Tech. rep. Cambridge, 2014, pp. 811–922. DOI: 10.1104/pp.900074. arXiv: /www.ipcc-nggip.iges.or.jp/public/2006gl/pdf/4{_}Volume4/V4{_}04{_}Ch4{_}Forest{_}Land.pdf [http:].

[24] Peter McKendry. "Energy production from biomass (part 1): overview of biomass". In: *Bioresource Technol* 83.1 (2002), pp. 37–46. ISSN: 09608524. DOI: 10.1016/S0960-8524(01)00118-3. arXiv: arXiv:1011.1669v3. URL: http://dx.doi.org/10.1016/S0960-8524(01)00118-3.

[25] Haiping Yang et al. "In-Depth Investigation of Biomass Pyrolysis Based on Three Major Components: Hemicellulose, Cellulose and Lignin". In: *Energy & Fuels 2006,* 20.17 (2006), pp. 388–393. ISSN: 08885885. DOI: 10.1021/ie1025453.

[26] Munna Verma et al. "Drying of biomass for utilising in co-firing with coal and its impact on environment - A review". In: *Renewable and Sustainable Energy Reviews* 71.February 2015 (2017), pp. 732–741. ISSN: 18790690. DOI: 10.1016/j.rser.2016.12.101.

[27] Haiping Yang et al. "Characteristics of hemicellulose, cellulose and lignin pyrolysis". In: *Fuel* 86.12-13 (Oct. 2007), pp. 1781–1788. ISSN: 00162361. DOI: 10.1016/j.fuel.2006.12.013. URL: http://linkinghub.elsevier.com/retrieve/pii/S001623610600490X%20http://www.ncbi.nlm.nih.gov/pubmed/18296047.

[28] B.R.T. Simoneit et al. "Levoglucosan, a tracer for cellulose in biomass burning and atmospheric particles". In: *Atmospheric Environment* 33.2 (1999), pp. 173–182. ISSN: 13522310. DOI: 10.1016/S1352-2310(98)00145-9. URL: http://www.sciencedirect.com/science/article/pii/S1352231098001459.

[29] T. Kirchgeorg et al. "Method for the determination of specific molecular markers of biomass burning in lake sediments". In: *Organic Geochemistry* 71 (2014), pp. 1–6. ISSN: 01466380. DOI: 10.1016/j.orggeochem.2014.02.014.

[30] Bernd R T Simoneit. *Biomass burning - A review of organic tracers for smoke from incomplete combustion*. Vol. 17. 3. 2002, pp. 129–162. DOI: 10.1016/S0883-2927(01)00061-0.

[31] Ting Zhang et al. "Identification and estimation of the biomass burning contribution to Beijing aerosol using levoglucosan as a molecular marker". In: *Atmospheric Environment* 42.29 (2008), pp. 7013–7021. ISSN: 13522310. DOI: 10.1016/j.atmosenv.2008.04.050.

[32] Natalie Kehrwald. "Decadal-scale changes in East African fire activity for the past 4000 years". In: *Quaternary International* 279-280.2012 (2012), p. 239. ISSN: 10406182. DOI: 10.1016/j.quaint.2012.08.545.

[33] Ping Yao et al. "Levoglucosan concentrations in ice-core samples from the Tibetan Plateau determined by reverse-phase high-performance liquid chromatography-mass spectrometry". In: *Journal of Glaciology* 59.216 (2013), pp. 599–612. ISSN: 00221430. DOI: 10.3189/2013JoG12J157.

[34] P. Zennaro et al. "Fire in ice: Two millennia of boreal forest fire history from the Greenland NEEM ice core". In: *Climate of the Past* 10.5 (2014), pp. 1905–1924. ISSN: 18149332. DOI: 10.5194/cp-10-1905-2014.

[35] Li Jung Kuo, Patrick Louchouarn, and Bruce E. Herbert. "Influence of combustion conditions on yields of solvent-extractable anhydrosugars and lignin phenols in chars: Implications for characterizations of biomass combustion residues". In: *Chemosphere* 85.5 (2011), pp. 797–805. ISSN: 00456535. DOI: 10.1016/j.chemosphere.2011.06.074.

[36] Daniele Fabbri et al. "Levoglucosan and other cellulose and lignin markers in emissions from burning of Miocene lignites". In: *Atmospheric Environment* 43.14 (2009), pp. 2286–2295. ISSN: 13522310. DOI: 10.1016/j.atmosenv.2009.01.030.

[37] Guenter Engling et al. "Determination of levoglucosan in biomass combustion aerosol by high-performance anion-exchange chromatography with pulsed amperometric detection". In: *Atmospheric Environment* 40.SUPPL. 2 (2006), pp. 299–311. ISSN: 13522310. DOI: 10.1016/j.atmosenv.2005.12.069.

[38] Ivan Kourtchev et al. "The use of polar organic compounds to estimate the contribution of domestic solid fuel combustion and biogenic sources to ambient levels of organic carbon and PM2.5 in Cork Harbour, Ireland". In: *Science of the Total Environment* 409.11 (2011), pp. 2143–2155. ISSN: 00489697. DOI: 10.1016/j.scitotenv.2011.02.027.

[39] H. M. Zakir Hossain, Yoshikazu Sampei, and Barry P. Roser. "Polycyclic aromatic hydrocarbons (PAHs) in late Eocene to early Pleistocene mudstones of the Sylhet succession, NE Bengal Basin, Bangladesh: Implications for source and paleoclimate conditions during Himalayan uplift". In: *Organic Geochemistry* 56 (2013), pp. 25–39. ISSN: 01466380. DOI: 10.1016/j.orggeochem.2012.12.001.

[40] Ana Lúcia C. Lima, John W. Farrington, and Christopher M. Reddy. "Combustion-Derived Polycyclic Aromatic Hydrocarbons in the Environment—A Review". In: *Environmental Forensics* 6.2 (2005), pp. 109–131. ISSN: 1527-5922. DOI: 10.1080/15275920590952739.

[41] Ki-Hyun Kim et al. "A review of airborne polycyclic aromatic hydrocarbons (PAHs) and their human health effects." In: *Environment international* 60 (Oct. 2013), pp. 71–80. ISSN: 1873-6750. DOI: 10.1016/j.envint.2013.07.019. URL: http://www.sciencedirect.com/science/article/pii/S0160412013001633.

[42] Hussein I Abdel-shafy and Mona S M Mansour. "A review on polycyclic aromatic hydrocarbons : Source , environmental impact , effect on human health and remediation". In: *Egyptian Journal of Petroleum* 25.1 (2016), pp. 107–123. ISSN: 1110-0621. DOI: 10.1016/j.ejpe.2015.03.011. URL: http://dx.doi.org/10.1016/j.ejpe.2015.03.011.

[43] Chunqing Jiang et al. "Polycyclic aromatic hydrocarbons in ancient sediments and their relationships to palaeoclimate". In: *Organic Geochemistry* 29.5-7 -7 pt 2 (1998), pp. 1721–1735. ISSN: 01466380. DOI: 10.1016/S0146-6380(98)00083-7.

[44] Jacopo Gabrieli et al. "Post 17th-century changes of european pah emissions recorded in high-altitude alpine snow and ice". In: *Environmental Science and Technology* 44.9 (2010), pp. 3260–3266. ISSN: 0013936X. DOI: 10.1021/es903365s.

[45] Mark B. Yunker et al. "PAHs in the Fraser River basin: A critical appraisal of PAH ratios as indicators of PAH source and composition". In: *Organic Geochemistry* 33.4 (2002), pp. 489–515. ISSN: 01466380. DOI: 10.1016/S0146-6380(02)00002-5. arXiv: arXiv:1011.1669v3.

[46] D.S. Page et al. "Pyrogenic Polycyclic Aromatic Hydrocarbons in Sediments Record Past Human Activity: A Case Study in Prince William Sound, Alaska". In: *Marine Pollution Bulletin* 38.4 (1999), pp. 247–260. ISSN: 0025326X. DOI: 10.1016/S0025-326X(98)00142-8. URL: http://www.sciencedirect.com/science/article/pii/S0025326X98001428.

[47] Elizabeth H. Denis et al. "Polycyclic aromatic hydrocarbons (PAHs) in lake sediments record historic fire events: Validation using HPLC-fluorescence detection". In: *Organic Geochemistry* 45 (2012), pp. 7–17. ISSN: 01466380. DOI: 10.1016/j.orggeochem.2012.01.005.

[48] Marco Conedera et al. "Reconstructing past fire regimes: methods, applications, and relevance to fire management and conservation". In: *Quaternary Science Reviews* 28.5-6 (2009), pp. 555–576. ISSN: 02773791. DOI: 10.1016/j.quascirev.2008.11.005.

[49] Efstathios Stogiannidis and Remi Laane. "Source Characterization of Polycyclic Aromatic Hydrocarbons by Using Their Molecular Indices: An Overview of Possibilities". In: *Reviews of Environmental Contamination and Toxicology*. Vol. 234. 2015, pp. 49–133. DOI: DOI10.1007/978-3-319-10638-0_2.

[50] Diane Saber, David Mauro, and Tanita Sirivedhin. "Environmental Forensics Investigation in Sediments near a Former Manufactured Gas Plant Site". In: *Environmental Forensics* 7.December 2014 (2006), pp. 65–75. ISSN: 1527-5922. DOI: 10.1080/15275920500506881.

[51] Mohamad Pauzi Zakaria et al. "Distribution of polycyclic aromatic hydrocarbons (PAHs) in rivers and estuaries in Malaysia: A widespread input of petrogenic PAHs". In: *Environmental Science and Technology* 36.9 (2002), pp. 1907–1918. ISSN: 0013936X. DOI: 10.1021/es011278+. arXiv: es011278+ [10.1021].

[52] S. D. Killops and M. S. Massoud. "Polycyclic aromatic hydrocarbons of pyrolytic origin in ancient sediments: evidence for Jurassic vegetation fires". In: *Organic Geochemistry* 18.1 (1992), pp. 1–7. ISSN: 01466380. DOI: 10.1016/0146-6380(92)90137-M.

[53] M. I. Bird. "RADIOCARBON DATING / Charcoal". In: *Encyclopedia of Quaternary Science* 2001 (2007), pp. 2950–2958. DOI: 10.1016/B0-44-452747-8/00046-6.

[54] Rudolf Jaffé et al. "Global charcoal mobilization from soils via dissolution and riverine transport to the oceans." In: *Science (New York, N.Y.)* 340.6130 (2013), pp. 345–7. ISSN: 1095-9203. DOI: 10.1126/science.1231476. URL: http://www.ncbi.nlm.nih.gov/pubmed/23599492.

[55] Cathy Whitlock and Chris P. S. Larsen. "Charcoal as a Fire Proxy". In: *Tracking Environmental Change Using Lake Sediments.* Vol. Volume 3. Dordrecht, The Netherlands: Kluwer Academic Publishers, 2001. Chap. 5, pp. 557–578. ISBN: 978-94-007-2744-1. DOI: 10.1007/978-94-007-2745-8. URL: http://link.springer.com/10.1007/978-94-007-2745-8.

[56] William A. Patterson, Kevin J. Edwards, and David J. Maguire. "Microscopic charcoal as a fossil indicator of fire". In: *Quaternary Science Reviews* 6 (1987), pp. 3–23. ISSN: 02773791. DOI: 10.1016/0277-3791(87)90012-6.

[57] X Gao et al. "Organic Geochemistry Organic geochemical approaches to identifying formation processes for middens and charcoal-rich features". In: *ORGANIC GEOCHEMISTRY* 94 (2016), pp. 1–11. ISSN: 0146-6380. DOI: 10.1016/j.orggeochem.2016.01.007.

[58] Mark Herrmann et al. "Reconstructing Holocene vegetation and climate history of Nam Co area (Tibet), using pollen and other palynomorphs". In: *Quaternary International* 218.1-2 (2010), pp. 45–57. ISSN: 10406182. DOI: 10.1016/j.quaint.2009.05.007.

[59] Sd Mooney and W Tinner. "The analysis of charcoal in peat and organic sediments". In: *Mires and Peat* 7 (2011), pp. 1–18. URL: http://pixelrauschen.de/wbmp/media/map07/map%7B%5C_%7D07%7B%5C_%7D09.pdf.

[60] Willy Tinner et al. "Pollen and charcoal in lake sediments forest fires in southern Switzerland". In: 1.1998 (2014), pp. 31–42.

[61] Florian Thevenon et al. "Combining charcoal and elemental black carbon analysis in sedimentary archives: Implications for past fire regimes, the pyrogenic carbon cycle, and the human-climate interactions". In: *Global and Planetary Change* 72.4 (2010), pp. 381–389. ISSN: 09218181. DOI: 10.1016/j.gloplacha.2010.01.014.

[62] Vladimir O. Eliasl et al. "Evaluating levoglucosan as an indicator of biomass burning in Carajás, Amazônia: A comparison to the charcoal record". In: *Geochimica et Cosmochimica Acta* 65.2 (2001), pp. 267–272. ISSN: 00167037. DOI: 10.1016/S0016-7037(00)00522-6.

[63] Li Jung Kuo, Bruce E. Herbert, and Patrick Louchouarn. "Can levoglucosan be used to characterize and quantify char/charcoal black carbon in environmental media?" In: *Organic Geochemistry* 39.10 (2008), pp. 1466–1478. ISSN: 01466380. DOI: 10.1016/j.orggeochem.2008.04.026.

[64] M. J. Power et al. "Fire history and the global charcoal database: A new tool for hypothesis testing and data exploration". In: *Palaeogeography, Palaeoclimatology, Palaeoecology* 291.1-2 (2010), pp. 52–59. ISSN: 00310182. DOI: 10.1016/j.palaeo.2009.09.014.

[65] A. L. Daniau et al. "Predictability of biomass burning in response to climate changes". In: *Global Biogeochemical Cycles* 26.4 (2012), pp. 1–12. ISSN: 08866236. DOI: 10.1029/2011GB004249.

[66] A. L. Daniau, S. P. Harrison, and P. J. Bartlein. "Fire regimes during the Last Glacial". In: *Quaternary Science Reviews* 29.21-22 (2010), pp. 2918–2930. ISSN: 02773791. DOI: 10.1016/j.quascirev.2009.11.008.

[67] M. J. Power et al. "Changes in fire regimes since the Last Glacial Maximum : an assessment based on a global synthesis and analysis of charcoal data". In: *Climate Dynamics* 30.7-8 (2008), pp. 887–907. DOI: 10.1007/s00382-007-0334-x.

[68] J.R. Marlon et al. "Climate and human influences on global biomass burning over the past two millennia." In: *Nature geoscience* 1 (2008), pp. 697–702. ISSN: 1752-0894. DOI: 10.1038/ngeo468. URL: http://centaur.reading.ac.uk/29663/.

[69] J. R. Marlon et al. "Reconstructions of biomass burning from sediment charcoal records to improve data-model comparisons". In: *Biogeosciences Discussions* 12.22 (2016), pp. 18571–18623. ISSN: 1810-6285. DOI: 10.5194/bgd-12-18571-2015. URL: http://www.biogeosciences-discuss.net/12/18571/2015/.

[70] Sheperd T. and Griffiths D.W. "The effects of stress on plant cuticular waxes". In: *New Phytologist* 171 (2006), pp. 469–499. DOI: 10.1111/j.1469-8137.2006.01826.x.

[71] Jens Mingram et al. "The Huguang maar lake-a high-resolution record of palaeoenvironmental and palaeoclimatic changes over the last 78,000 years from South China". In: *Quaternary International* 122.1 SPEC. ISS. (2004), pp. 85–107. ISSN: 10406182. DOI: 10.1016/j.quaint.2004.02.001.

[72] Dirk Sachse et al. "Molecular paleohydrology: interpreting the hydrogen-isotopic composition of lipid biomarkers from photosynthesizing organisms". In: *Annual Review of Earth and Planetary Sciences* 40 (2012), pp. 221–249. ISSN: 0084-6597. DOI: 10.1146/annurev-earth-042711-105535.

[73] JingWei Cui, JunHua Huang, and ShuCheng Xie. "Characterstics of seasonal variations of leaf n-alkanes and n-alkenes in modern higher plants in Qingjiang, Hubei Province, China". In: *Chinese Science Bulletin* 53.17 (2008), pp. 2659–2664. ISSN: 10016538. DOI: 10.1007/s11434-008-0194-8.

[74] Rosemary T. Bush and Francesca A. McInerney. "Leaf wax n-alkane distributions in and across modern plants: Implications for paleoecology and chemotaxonomy". In: *Geochimica et Cosmochimica Acta* 117 (Sept. 2013), pp. 161–179. DOI: 10.1016/j.gca.2013.04.016.

[75] J Han and M Calvin. "Hydrocarbon distribution of algae and bacteria, and microbiological activity in sediments." In: *Proceedings of the National Academy of Sciences of the United States of America* 64.Table 1 (1969), pp. 436–443. ISSN: 0027-8424. DOI: 10.1073/pnas.64.2.436.

[76] Joan Grimalt and Joan Albaigés. "Sources and occurrence of C12-C22n-alkane distributions with even carbon-number preference in sedimentary environments". In: *Geochimica et Cosmochimica Acta* 51.6 (June 1987), pp. 1379–1384. DOI: 10.1016/0016-7037(87)90322-X. URL: http://linkinghub.elsevier.com/retrieve/pii/001670378790322X.

[77] K.J. Ficken et al. "Glacial/interglacial variations in carbon cycling revealed by molecular and isotope stratigraphy of Lake Nkunga, Mt. Kenya, East Africa". In: *Organic Geochemistry* 29.5-7 (Nov. 1998), pp. 1701–1719. ISSN: 01466380. DOI: 10.1016/S0146-6380(98)00109-0. URL: http://linkinghub.elsevier.com/retrieve/pii/S0146638098001090.

[78] Bernhard Aichner, Ulrike Herzschuh, and Heinz Wilkes. "Influence of aquatic macrophytes on the stable carbon isotopic signatures of sedimentary organic matter in lakes on the Tibetan Plateau". In: *Organic Geochemistry* 41.7 (2010), pp. 706–718. ISSN: 01466380. DOI: 10.1016/j.orggeochem.2010.02.002.

[79] J Poynter and G Eglinton. "Molecular composition of three sediments from hole 717C: The Bengal fan". In: *Proceedings of the Ocean Drilling Program, Scientific Results* 116 (1990), pp. 155–161. DOI: 10.2973/odp.proc.sr.116.151.1990. URL: http://www-odp.tamu.edu/Publications/116%7B%5C_%7DSR/VOLUME/CHAPTERS/sr116%7B%5C_%7D14.pdf.

[80] Yi Duan and He Jinxian. "Distribution and isotopic composition of n -alkanes from grass , reed and tree leaves along a latitudinal gradient in China". In: *Geochemical Journal* 45 (2011), pp. 199–207.

[81] Philip A. Meyers and Ryoshi Ishiwatari. "Lacustrine organic geochemistry—an overview of indicators of organic matter sources and diagenesis in lake sediments". In: *Organic Geochemistry* 20.7 (Sept. 1993), pp. 867–900. ISSN: 01466380. DOI: 10.1016/0146-6380(93)90100-P. URL: http://www.sciencedirect.com/science/article/pii/014663809390100P.

[82] E.E Bray and E.D Evans. "Distribution of n-paraffins as a clue to recognition of source beds". In: *Geochimica et Cosmochimica Acta* 22.1 (Feb. 1961), pp. 2–15. ISSN: 00167037. DOI: 10.1016/0016-7037(61)90069-2. URL: http://linkinghub.elsevier.com/retrieve/pii/0016703761900692.

[83] R A Bourbonniere and P A Meyers. "Sedimentary geolipid records of historical changes in the watersheds and productivities of Lakes Ontario and Erie". In: *Limnology and Oceanography* 41.2 (1996), pp. 352–359. ISSN: 0024-3590. DOI: 10.4319/lo.1996.41.2.0352.

[84] Heinz Wilkes, Antje Ramrath, and J. F W Negendank. "Organic geochemical evidence for environmental changes since 34,000 yrs BP from Lago di Mezzano, central Italy". In: *Journal of Paleolimnology* 22 (1999), pp. 349–365. DOI: 10.1023%2FA%3A1008051821898.

[85] K. J. Ficken et al. "An n-alkane proxy for the sedimentary input of submerged/floating freshwater aquatic macrophytes". In: *Organic Geochemistry* 31.7-8 (2000), pp. 745–749. ISSN: 01466380. DOI: 10.1016/S0146-6380(00)00081-4.

[86] ENNO SCHEFUSS et al. "Carbon isotope analyses of n -alkanes in dust from the lower atmosphere over the central eastern Atlantic". In: *Geochimica et Cosmochimica Acta* 67.10 (2003), pp. 1757–1767. DOI: 10.1016/S0016-7037(02)01414-X.

[87] Nathalie Dubois and Jérémy Jacob. "Molecular Biomarkers of Anthropic Impacts in Natural Archives: A Review". In: *Frontiers in Ecology and Evolution* 4.August (2016), pp. 1–16. DOI: 10.3389/fevo.2016.00092.

[88] Christian G Daughton. "Real-time estimation of small-area populations with human biomarkers in sewage." In: *The Science of the total environment* 414 (2012), pp. 6–21. DOI: 10.1016/j.scitotenv.2011.11.015.

[89] C H Vane et al. "Sedimentary records of sewage pollution using faecal markers in contrasting peri-urban shallow lakes." In: *The Science of the total environment* 409.2 (2010), pp. 345–56. DOI: 10.1016/j.scitotenv.2010.09.033.

[90] Jingming Wu et al. "Determination of fecal sterols by gas chromatography – mass spectrometry with solid-phase extraction and injection-port derivatization". In: *Journal of Chromatography A* 1216 (2009), pp. 1053–1058. DOI: 10.1016/j.chroma.2008.12.054.

[91] Jago Jonathan Birk et al. "Faeces deposition on Amazonian Anthrosols as assessed from 5a-stanols". In: *Journal of Archaeological Science* 38.6 (2011), pp. 1209–1220. ISSN: 03054403. DOI: 10.1016/j.jas.2010.12.015. URL: http://dx.doi.org/10.1016/j.jas.2010.12.015.

[92] Ian D. Bull et al. "The Origin of Faeces by Means of Biomarker Detection". In: *Environment International* 27 (2002), pp. 647–654. DOI: S0160-4120(01)00124-6.

[93] Mitsugu Nishimura and Tadashiro Koyama. "The occurrence of stanols in various living organisms and the behavior of sterols in contemporary sediments". In: *Geochimica et Cosmochimica Acta* 41.3 (Mar. 1977), pp. 379–385. DOI: 10.1016/0016-7037(77)90265-4. URL: http://linkinghub.elsevier.com/retrieve/pii/0016703777902654.

[94] Hailiang Dong et al. "Impacts of environmental change and human activity on microbial ecosystems on the Tibetan Plateau, NW China". In: *GSA Today* 20.6 (2010), pp. 4–10. ISSN: 10525173. DOI: 10.1130/GSATG75A.1.

[95] K B Liu, Z J Yao, and L G Thompson. "A pollen record of Holocene climatic changes from the Dunde ice cap, Qinghai-Tibetan Plateau". In: *Geology* 26.2 (1998), pp. 135–138. DOI: 10.1130/0091-7613(1998)026<0135.

[96] Wenying Wang et al. "Distribution and species diversity of plant communities along transect on the northeastern Tibetan Plateau". In: *Biodiversity and Conservation* 15.5 (2006), pp. 1811–1828. ISSN: 09603115. DOI: 10.1007/s10531-004-6681-6.

[97] Ayako Shimono et al. "Patterns of plant diversity at high altitudes on the Qinghai-Tibetan Plateau". In: *Journal of Plant Ecology* 3.1 (2010), pp. 1–7. ISSN: 17529921. DOI: 10.1093/jpe/rtq002.

[98] Jin T. Zhang and Xiangcheng Mi. "Diversity and distribution of high-mountain meadows across elevation gradient in Wutai Mts. (North China)". In: *Polish Journal of Ecology* 55.3 (2007), pp. 585–593. ISSN: 15052249.

[99] Dorian Q Fuller et al. "The contribution of rice agriculture and livestock pastoralism to prehistoric methane levels: An archaeological assessment". In: *The Holocene* 21.5 (2011), pp. 743–759. DOI: 10.1177/0959683611398052.

[100] Georg Miehe et al. "Palaeoecological and experimental evidence of former forests and woodlands in the treeless desert pastures of Southern Tibet (Lhasa, A.R. Xizang, China)". In: *Palaeogeography, Palaeoclimatology, Palaeoecology* 242.1-2 (2006), pp. 54–67. DOI: 10.1016/j.palaeo.2006.05.010.

[101] DongJu Zhang et al. "History and possible mechanisms of prehistoric human migration to the Tibetan Plateau". In: *Science China Earth Sciences* August (2016). DOI: 10.1007/s11430-015-5482-x.

[102] Anne P. Underhill. "Current issues in Chinese Neolithic archaeology". In: *Journal of World Prehistory* 11.2 (1997), pp. 103–160. ISSN: 0892-7537. DOI: 10.1007/BF02221203.

[103] Alice Callegaro and Federico Dallo. "Paleomigrazioni e tracciati climatici". In: *OFFICINA** 13 (2016), pp. 34–37. URL: http://www.officina-artec.com/project/officina-13/.

[104] Mo Wang et al. "Two distinct patterns of seasonal variation of airborne black carbon over Tibetan Plateau". In: *Science of The Total Environment* 573 (2016), pp. 1041–1052. ISSN: 00489697. DOI: 10.1016/j.scitotenv.2016.08.184. URL: http://linkinghub.elsevier.com/retrieve/pii/S0048969716318885.

[105] Wu Yanhong et al. "Holocene climate development on the central Tibetan Plateau: A sedimentary record from Cuoe Lake". In: *Palaeogeography, Palaeoclimatology, Palaeoecology* 234 (2006), pp. 328–340. DOI: 10.1016/j.palaeo.2005.09.017.

[106] Xingqi Liu et al. "Late Holocene forcing of the Asian winter and summer monsoon as evidenced by proxy records from the northern Qinghai-Tibetan Plateau". In: *Earth and Planetary Science Letters* 280.1-4 (2009), pp. 276–284. DOI: 10.1016/j.epsl.2009.01.041.

[107] Stephan Opitz et al. "Late Glacial and Holocene development of Lake Donggi Cona, north-eastern Tibetan Plateau, inferred from sedimentological analysis". In: *Palaeogeography, Palaeoclimatology, Palaeoecology* 337-338 (2012), pp. 159–176. DOI: 10.1016/j.palaeo.2012.04.013.

[108] Elisabeth Dietze et al. "Early to mid-Holocene lake high-stand sediments at Lake Donggi Cona, northeastern Tibetan Plateau, China". In: *Quaternary Research (United States)* 79.3 (2013), pp. 325–336. DOI: 10.1016/j.yqres.2012.12.008.

[109] Chao You et al. "Method for determination of levoglucosan in snow and ice at trace concentration levels using ultra-performance liquid chromatography coupled with triple quadrupole mass spectrometry". 2016.

[110] S. D. Kaspari et al. "Recent increase in black carbon concentrations from a Mt. Everest ice core spanning 1860-2000 AD". In: *Geophysical Research Letters* 38.4 (2011), pp. 11–16. ISSN: 00948276. DOI: 10.1029/2010GL046096.

[111] Bai Qing Xu et al. "Deposition of anthropogenic aerosols in a southeastern Tibetan glacier". In: *Journal of Geophysical Research Atmospheres* 114.17 (2009), pp. 1–8. ISSN: 01480227. DOI: 10.1029/2008JD011510.

[112] J. Ming et al. "Black carbon record based on a shallow Himalayan ice core and its climatic implications". In: *Atmospheric Chemistry and Physics* 8.5 (2008), pp. 1343–1352. ISSN: 1680-7324. DOI: 10.5194/acp-8-1343-2008. URL: http://www.atmos-chem-phys.net/8/1343/2008/.

[113] Hou Shugui et al. "A 154 a high-resolution ammonium record from the Rongbuk Glacier, north slope of Mt. Qomolangma (Everest), Tibet-Himal region". In: *Atmospheric Environment* 37.5 (2003), pp. 721–729. ISSN: 13522310. DOI: 10.1016/S1352-2310(02)00582-4.

[114] Liping Zhu et al. "Environmental changes since 8.4 ka reflected in the lacustrine core sediments from Nam Co, central Tibetan Plateau, China". In: *The Holocene* 18 (2008), pp. 831–839. ISSN: 0959-6836. DOI: 10.1177/0959683608091801.

[115] Lingyu Tang et al. "Changes in South Asian monsoon : New high-resolution paleoclimatic records from Tibet , China". In: *Chinese Science Bulletin* 45.1 (2000), pp. 87–91.

[116] J. P. Severinghaus and E. J. Brook. "Abrupt Climate Change at the End of the Last Glacial Period Inferred from Trapped Air in Polar Ice". In: *Science* 286.October (1999), pp. 930–933. ISSN: 00368075. DOI: 10.1126/science.286.5441.930.

[117] Jeetendra Saini et al. "Climate variability in the past 19,000 yr in NE Tibetan Plateau inferred from biomarker and stable isotope records of Lake Donggi Cona". In: *Quaternary Science Reviews* 157 (2017), pp. 129–140. ISSN: 02773791. DOI: 10.1016/j.quascirev.2016.12.023.

[118] Xingqi Liu et al. "Evolution of Chaka Salt Lake in NW China in response to climatic change during the Latest Pleistocene-Holocene". In: *Quaternary Science Reviews* 27.7-8 (2008), pp. 867–879. ISSN: 02773791. DOI: 10.1016/j.quascirev.2007.12.006.

[119] Alexander A. Prokopenko et al. "Paleoenvironmental proxy records from Lake Hovsgol, Mongolia, and a synthesis of Holocene climate change in the Lake Baikal watershed". In: *Quaternary Research* 68.1 (2007), pp. 2–17. ISSN: 00335894. DOI: 10.1016/j.yqres.2007.03.008.

[120] Steffen Mischke and Chengjun Zhang. "Holocene cold events on the Tibetan Plateau". In: *Global and Planetary Change* 72.3 (2010), pp. 155–163. DOI: 10.1016/j.gloplacha.2010.02.001.

[121] Yunfa Miao et al. "Holocene climate change on the northeastern Tibetan Plateau inferred from mountain-slope pollen and non-pollen palynomorphs". In: *Review of Palaeobotany and Palynology* 221 (2015), pp. 22–31. DOI: 10.1016/j.revpalbo.2015.05.006.

[122] Fenggui Liu and Zhaodong Feng. "A dramatic climatic transition at ˜4000 cal. yr BP and its cultural responses in Chinese cultural domains". In: *The Holocene* 22.10 (2012), pp. 1181–1197. DOI: 10.1177/0959683612441839.

[123] Hui Wang et al. "Eco-environmental degradation in the northeastern margin of the Qinghai-Tibetan Plateau and comprehensive ecological protection planning". In: *Environmental Geology* 55.5 (2008), pp. 1135–1147. ISSN: 09430105. DOI: 10.1007/s00254-007-1061-7.

[124] Quan Li et al. "Vegetation successions in response to Holocene climate changes in the central Tibetan Plateau". In: *Journal of Arid Environments* 125 (2016), pp. 136–144. DOI: 10.1016/j.jaridenv.2015.07.010.

[125] Broxton W. Bird et al. "A Tibetan lake sediment record of Holocene Indian summer monsoon variability". In: *Earth and Planetary Science Letters* 399 (2014), pp. 92–102. ISSN: 0012821X. DOI: 10.1016/j.epsl.2014.05.017.

[126] Bernd Wünnemann et al. "Implications of diverse sedimentation patterns in Hala Lake, Qinghai Province, China for reconstructing Late Quaternary climate". In: *Journal of Paleolimnology* 48.4 (2012), pp. 725–749. ISSN: 09212728. DOI: 10.1007/s10933-012-9641-2.

[127] Jianguo Xia and David S. Wishart. "Using MetaboAnalyst 3.0 for Comprehensive Metabolomics Data Analysis". In: *Current Protocols in Bioinformatics* September (2016), pp. 14.10.1–14.10.91. DOI: 10.1002/cpbi.11.

[128] Dario Battistel et al. "GC-MS method for determining faecal sterols as biomarkers of human and pastoral animal presence in freshwater sediments". In: *Analytical and Bioanalytical Chemistry* 407.28 (2015), pp. 8505–8514. ISSN: 16182650. DOI: 10.1007/s00216-015-8998-2.

[129] Peter M J Douglas et al. "Aridity and vegetation composition are important determinants of leaf-wax dD values in southeastern Mexico and Central America". In: *Geochimica et Cosmochimica Acta* 97 (2012), pp. 24–45. DOI: 10.1016/j.gca.2012.09.005.

[130] Matteo Martino. "Sviluppo di un metodo per la determinazione di biomarker in campioni di torba". Master thesis. Ca' Foscari University of Venice, 2016, pp. 1–113. URL: http://dspace.unive.it/handle/10579/7916?show=full.

[131] R. Piazza et al. "Development of a method for simultaneous analysis of PCDDs, PCDFs, PCBs, PBDEs, PCNs and PAHs in Antarctic air". In: *Analytical and Bioanalytical Chemistry* 405.2-3 (2013), pp. 917–932. ISSN: 16182642. DOI: 10.1007/s00216-012-6464-y.

[132] E. Argiriadis et al. "Assessing the influence of local sources on POPs in atmospheric depositions and sediments near Trento (Italy)". In: *Atmospheric Environment* 98 (2014), pp. 32–40. ISSN: 18732844. DOI: 10.1016/j.atmosenv.2014.08.035.

[133] Elena Gregoris et al. "Gas-particle distributions, sources and health effects of polycyclic aromatic hydrocarbons (PAHs), polychlorinated biphenyls (PCBs) and polychlorinated naphthalenes (PCNs) in Venice aerosols". In: *Science of the Total Environment* 476-477 (2014), pp. 393–405. ISSN: 18791026. DOI: 10.1016/j.scitotenv.2014.01.036. URL: http://dx.doi.org/10.1016/j.scitotenv.2014.01.036.

[134] Olivier Blarquez et al. "paleofire: An R package to analyse sedimentary charcoal records from the Global Charcoal Database to reconstruct past biomass burning". In: *Computers and Geosciences* 72 (2014), pp. 255–261. ISSN: 00983004. DOI: 10.1016/j.cageo.2014.07.020. URL: http://dx.doi.org/10.1016/j.cageo.2014.07.020.

[135] Felipe Matsubara Pereira. "Paleofire activity reconstruction in the Tibetan Plateau". Master thesis. Università Ca' Foscari Venezia, 2017. URL: http://dspace.unive.it/handle/10579/10154?show=full.

[136] Y. T. Hong et al. "Correlation between Indian Ocean summer monsoon and North Atlantic climate during the Holocene". In: *Earth and Planetary Science Letters* 211.3-4 (2003), pp. 371–380. ISSN: 0012821X. DOI: 10.1016/S0012-821X(03)00207-3.

[137] B. Menounos. "The water content of lake sediments and its relationship to other physical parameters: an alpine case study". In: *The Holocene* 7.2 (1997), pp. 207–212. ISSN: 0959-6836. DOI: 10.1177/095968369700700208.

[138] B. W. Bird et al. "Late-Holocene Indian summer monsoon variability revealed from a 3300-year-long lake sediment record from Nirpa Co, southeastern Tibet". 2016. URL: http://hol.sagepub.com/cgi/doi/10.1177/0959683616670220.

[139] Ruiqiang Yang et al. "Sedimentary records of polycyclic aromatic hydrocarbons (PAHs) in remote lakes across the Tibetan Plateau". In: *Environmental Pollution* 214 (2016), pp. 1–7. ISSN: 02697491. DOI: 10.1016/j.envpol.2016.03.068. URL: http://linkinghub.elsevier.com/retrieve/pii/S0269749116302482.

[140] Ulrike Herzschuh et al. "A general cooling trend on the central Tibetan Plateau throughout the Holocene recorded by the Lake Zigetang pollen spectra". In: *Quaternary International* 154-155 (2006), pp. 113–121. ISSN: 10406182. DOI: 10.1016/j.quaint.2006.02.005.

[141] Yan Zhao, Zicheng Yu, and Wenwei Zhao. "Holocene vegetation and climate histories in the eastern Tibetan Plateau: Controls by insolation-driven temperature or monsoon-derived precipitation changes?" In: *Quaternary Science Reviews* 30.9-10 (2011), pp. 1173–1184. DOI: 10.1016/j.quascirev.2011.02.006.

[142] R B Alley et al. "Holocene climate variability: a prominent widespread event 8200 years ago". In: *Geology* 25.February 2009 (1997), pp. 483–486. DOI: 10.1130/0091-7613(1997)025<0483:HCIAPW>2.3.CO;2.

[143] Richard B. Alley and Anna Maria Ágústsdóttir. "The 8k event: Cause and consequences of a major Holocene abrupt climate change". In: *Quaternary Science Reviews* 24.10-11 (2005), pp. 1123–1149. DOI: 10.1016/j.quascirev.2004.12.004.

[144] D.C. Barber et al. "Forcing of the cold event of 8,200 years ago by catastrophic drainage of Laurentide lakes". In: *Nature* 400 (1999), pp. 344–348. DOI: 10.1038/22504. URL: https://www.nature.com/articles/22504.

[145] Elise Van Campo and Francoise Gasse. *Pollen- and Diatom-Inferred Climatic and Hydrological Changes in Sumxi Co Basin (Western Tibet) since 13,000 yr B.P.* 1993. DOI: 10.1006/qres.1993.1037.

[146] Chenglin Liu et al. "Holocene yellow silt layers and the paleoclimate event of 8200 a BP in Lop Nur, Xinjiang, NW China". In: *Acta Geologica Sinica-English Edition* 77.4 (2003), pp. 514–518.

[147] Xingqi LIU et al. "A 16000-year pollen record of Qinghai Lake and its paleocli-mate and paleoenvironment". In: *Chinese Science Bulletin* 47.22 (2002), p. 1931. DOI: 10.1360/02tb9421.

[148] Liping Zhu et al. "Ostracod-based environmental reconstruction over the last 8,400 years of Nam Co Lake on the Tibetan plateau". In: *Hydrobiologia* 648.1 (2010), pp. 157–174. ISSN: 00188158. DOI: 10.1007/s10750-010-0149-3.

[149] Annette Kramer et al. "Holocene treeline shifts and monsoon variability in the Hengduan Mountains (southeastern Tibetan Plateau), implications from palynological investigations". In: *Palaeogeography, Palaeoclimatology, Palaeoecology* 286 (2010), pp. 23–41. ISSN: 00310182. DOI: 10.1016/j.palaeo.2009.12.001.

[150] Annette Kramer et al. "Late glacial vegetation and climate oscillations on the southeastern Tibetan Plateau inferred from the Lake Naleng pollen profile". In: *Quaternary Research* 73 (2010), pp. 324–335. ISSN: 00335894. DOI: 10.1016/j.yqres.2009.12.003.

[151] Qingfeng Ma et al. "Pollen-inferred Holocene vegetation and climate histories in Taro Co, southwestern Tibetan Plateau". In: *Chinese Science Bulletin* 59.31 (2014), pp. 4101–4114. DOI: 10.1007/s11434-014-0505-1.

[152] Quan Li et al. "Pollen-inferred climate changes and vertical shifts of alpine vegetation belts on the northern slope of the Nyainqentanglha Mountains (central Tibetan Plateau) since 8.4 kyr BP". In: *The Holocene* 21.6 (Sept. 2011), pp. 939–950. ISSN: 0959-6836. DOI: 10.1177/0959683611400218.

[153] H. Knicker et al. "Modification of biomarkers in pyrogenic organic matter during the initial phase of charcoal biodegradation in soils". In: *Geoderma* 197-198 (2013), pp. 43–50. ISSN: 00167061. DOI: 10.1016/j.geoderma.2012.12.021.

[154] G. Yan et al. "Palynological and stable isotopic study of palaeoenvironmental changes on the northeastern Tibetan plateau in the last 30,000 years". In: *Palaeogeography, Palaeoclimatology, Palaeoecology* 153.1-4 (1999), pp. 147–159. DOI: 10.1016/S0031-0182(99)00064-4.

[155] Shen Ji et al. "Palaeoclimatic changes in the Qinghai Lake area during the last 18,000 years". In: *Quaternary International* 136 (2005), pp. 131–140. DOI: 10.1016/j.quaint.2004.11.014.

[156] Ulrike Herzschuh, Harald Kürschner, and Steffen Mischke. "Temperature variability and vertical vegetation belt shifts during the last 50,000 yr in the Qilian Mountains (NE margin of the Tibetan Plateau, China)". In: *Quaternary Research* 66.1 (2006), pp. 133–146. DOI: 10.1016/j.yqres.2006.03.001.

[157] Knut Kaiser et al. "Charcoal and fossil wood from palaeosols, sediments and artificial structures indicating Late Holocene woodland decline in southern Tibet (China)". In: *Quaternary Science Reviews* 28.15-16 (2009), pp. 1539–1554. DOI: 10.1016/j.quascirev.2009.02.016.

[158] Knut Kaiser et al. "Stratigraphy and palaeoenvironmental implications of Pleistocene and Holocene aeolian sediments in the Lhasa area, southern Tibet (China)". In: *Palaeogeography, Palaeoclimatology, Palaeoecology* 271.3-4 (2009), pp. 329–342. DOI: 10.1016/j.palaeo.2008.11.004.

[159] Heinz Wanner et al. "Mid- to Late Holocene climate change: an overview". In: *Quaternary Science Reviews* 27.19-20 (2008), pp. 1791–1828. ISSN: 02773791. DOI: 10.1016/j.quascirev.2008.06.013.

[160] Cheng-bang An, Zhao-dong Feng, and Lucas Barton. "Dry or humid ? Mid-Holocene humidity changes in arid and semi-arid China". In: *Quaternary Science Reviews* 25 (2006), pp. 351–361. DOI: 10.1016/j.quascirev.2005.03.013.

[161] Chengjun Zhang et al. "Holocene environmental variations recorded by organic-related and carbonate-related proxies of the lacustrine sediments from Bosten". In: *The Holocene* 20.3 (2010), pp. 363–373. DOI: 10.1177/0959683609353428.

[162] Cheng-bang An et al. "A high-resolution record of Holocene environmental and climatic changes from Lake Balikun (Xinjiang , China): Implications for central Asia". In: *The Holocene* 22.1 (2011), pp. 43–52. DOI: 10.1177/0959683611405244.

[163] Xingqi Liu et al. "Holocene environmental and climatic changes inferred from Wulungu Lake in northern Xinjiang, China". In: *Quaternary Research* 70.3 (2008), pp. 412–425. DOI: 10.1016/j.yqres.2008.06.005.

[164] Cheng Zhao et al. "Holocene millennial-scale climate variations documented by multiple lake-level proxies in sediment cores from Hurleg Lake, Northwest China". In: *Journal of Paleolimnology* 44 (2010), pp. 995–1008. DOI: 10.1007/s10933-010-9469-6.

[165] Youbin Sun et al. "East Asian monsoon variability over the last seven glacial cycles recorded by a loess sequence from the northwestern Chinese Loess Plateau". In: *Geochemistry, Geophysics, Geosystems* 7.12 (2006), pp. 1–16. DOI: 10.1029/2006GC001287.

[166] X. Y. Yang et al. "TL and IRSL dating of Jiahu relics and sediments: Clue of 7th millennium BC civilization in central China". In: *Journal of Archaeological Science* 32.7 (2005), pp. 1045–1051. DOI: 10.1016/j.jas.2005.02.003.

[167] F H Chen et al. "Agriculture facilitated permanent human occupation of the Tibetan Plateau after 3600 B.P". In: *Science* 347.6219 (2015), pp. 248–250. DOI: 10.1126/science.1259172.

[168] Torben Kirchgeorg. "Specific molecular markers in lake sediment cores for biomass burning reconstruction during the Holocene". In: (2015), pp. 1–90.

[169] Matthew P Fraser and Kalyan Lakshmanan. "Using Levoglucosan as a Molecular Marker for the Long-Range Transport of Biomass Combustion Aerosols". In: *Environmental Science & Technology* 34.21 (2000), pp. 4560–4564. DOI: 10.1021/es9912291.

[170] Gangjian Wei et al. "Sea surface temperature records in the northern South China Sea from mid-Holocene coral Sr/Ca ratios". In: *Paleoceanography* 22.3 (2007), pp. 1–13. DOI: 10.1029/2006PA001270.

[171] Chao You et al. "Levoglucosan evidence for biomass burning records over Tibetan glaciers". In: *Environmental Pollution* 216.May (2016), pp. 173–181. ISSN: 02697491. DOI: 10.1016/j.envpol.2016.05.074. URL: http://linkinghub.elsevier.com/retrieve/pii/S0269749116304626.

[172] Daniele Colombaroli et al. "Determinants of savanna-fire dynamics in the eastern Lake Victoria catchment (western Kenya) during the last 1200 years". In: *Quaternary International* (2016), pp. 1–14. ISSN: 10406182. DOI: 10.1016/j.quaint.2016.06.028. URL: http://www.sciencedirect.com/science/article/pii/S1040618216300246.

[173] Yongjin Wang et al. "The Holocene Asian Monsoon: Links to Solar Changes and North Atlantic Climate". In: *Science* 308.5723 (2005), pp. 854–857. ISSN: 0036-8075. DOI: 10.1126/science.1106296. arXiv: NIHMS150003. URL: http://www.sciencemag.org/cgi/doi/10.1126/science.1106296.

[174] Gerard Bond et al. "Persistent Solar Influence on North Atlantic Climate During the Holocene". In: *Science* 294.5549 (2001), pp. 2130–2136. DOI: 10.1126/science.1065680. URL: http://science.sciencemag.org/content/294/5549/2130.

[175] Heinz Wanner et al. "Structure and origin of Holocene cold events". In: *Quaternary Science Reviews* 30.21-22 (2011), pp. 3109–3123. ISSN: 02773791. DOI: 10.1016/j.quascirev.2011.07.010. URL: http://dx.doi.org/10.1016/j.quascirev.2011.07.010.

[176] S. Mischke et al. "Holocene climate and landscape change in the northeastern Tibetan Plateau foreland inferred from the Zhuyeze Lake record". In: *The Holocene* 26.4 (2016), pp. 643–654. ISSN: 0959-6836. DOI: 10.1177/0959683615612570.

[177] Anja Eichler et al. “An ice-core based history of Siberian forest fires since AD 1250”. In: *Quaternary Science Reviews* 30.9-10 (2011), pp. 1027–1034. ISSN: 02773791. DOI: 10.1016/j.quascirev.2011.02.007. URL: http://dx.doi.org/10.1016/j.quascirev.2011.02.007.

[178] Bo Cheng, Fahu Chen, and Jiawu Zhang. “Palaeovegetational and palaeoenvironmental changes since the last deglacial in Gonghe Basin , northeast Tibetan Plateau”. In: *Journal of Geographical Sciences* 23.1 (2013), pp. 136–146. DOI: 10.1007/s11442-013-0999-5.

[179] Huabiao Zhao et al. “Records of sulfate and nitrate in an ice core from Mount Muztagata, central Asia”. In: *Journal of Geophysical Research Atmospheres* 116.13 (2011). ISSN: 01480227. DOI: 10.1029/2011JD015735.

[180] A. Berger and M.F. Loutre. “Insolation values for the climate of the last 10 million years”. In: *Quaternary Science Reviews* 10.4 (Jan. 1991), pp. 297–317. DOI: 10.1016/0277-3791(91)90033-Q.

[181] Yan Zhao et al. “Vegetation response to Holocene climate change in monsoon-influenced region of China”. In: *Earth-Science Reviews* 97 (2009), pp. 242–256. ISSN: 00128252. DOI: 10.1016/j.earscirev.2009.10.007.

[182] A. Dallmeyer et al. “Holocene vegetation and biomass changes on the Tibetan Plateau - A model-pollen data comparison”. In: *Climate of the Past* 7.3 (2011), pp. 881–901. ISSN: 18149324. DOI: 10.5194/cp-7-881-2011.

[183] Houyuan Lu et al. “Modern pollen distributions in Qinghai-Tibetan Plateau and the development of transfer functions for reconstructing Holocene environmental changes”. In: *Quaternary Science Reviews* 30.7-8 (2011), pp. 947–966. ISSN: 02773791. DOI: 10.1016/j.quascirev.2011.01.008.

[184] L. G. Thompson et al. “Holocene-Late Pleistocene Climatic Ice Core Records from Qinghai-Tibetan Plateau”. In: *Science* 246.4929 (1989), pp. 474–477. URL: http://www.jstor.org/stable/1704580.

[185] MingRui Qiang et al. “Holocene record of eolian activity fromGenggahai Lake, northeasternQinghai-Tibetan Plateau, China”. In: *Geophysical Research Letters* 41 (2014), pp. 589–595. DOI: 10.1002/2013GL058806.

Estratto per riassunto della tesi di dottorato

L'estratto (max. 1000 battute) deve essere redatto sia in lingua italiana che in lingua inglese e nella lingua straniera eventualmente indicata dal Collegio dei docenti.

L'estratto va firmato e rilegato come ultimo foglio della tesi.

Studente: ALICE CALLEGARO _____ matricola: 823218 _____

Dottorato: SCIENZE AMBIENTALI _____

Ciclo: XXX _____

Titolo della tesi[1] : BIOMASS BURNING RECONSTRUCTION ANALYSING LACUSTRINE SEDIMENT CORES FROM THE TIBETAN PLATEAU

Italian Abstract

La presente ricerca di dottorato fornisce informazioni sugli eventi incendiari dell'Olocene e sui cambiamenti della vegetazione avvenuti nell'altopiano tibetano, studiati nei sedimenti dei laghi Paru Co e Hala Hu, rispettivamente nell'altopiano sud e nord-orientale. Sono state indagate diverse molecole organiche tramite la cromatografia in fase mobile accoppiata alla spettrometria di massa. Gli zuccheri anidri, marcatori specifici di incendi vegetazionali, gli idrocarburi policiclici aromatici, come proxy di combustione, i normal-alcani, indicatori di vegetazione e gli steroli fecali, indicatori dell'antica presenza di umani e animali da pascolo, sono stati confrontati con altri record. I risultati ottenuti indicano intensità elevata di incendi durante il Primo Olocene (8000-11000 anni fa) a Paru co e nel Medio Olocene (4500-7000 anni fa) a Hala Hu. Tali eventi e le relative variazioni vegetazionali sono stati interpretati e correlati a cause climatiche piuttosto che ad attività umana.

English Abstract

This PhD research provides information about Holocene fire events and changes in vegetation on the Tibetan plateau, studied in the sediments from the lakes Paru Co and Hala Hu, respectively in the south and north-eastern plateau. Several organic molecules were investigated by mobile phase chromatography coupled with mass spectrometry. Anhydrousugars, as specific of biomass burning, polycyclic aromatic hydrocarbons, as combustion proxies, n-alkanes, as vegetation indicators and faecal sterols, indicators of the presence of humans and grazing animals were compared with other records. The obtained results show high intensity of fire during the Early Holocene (8000-11000 years ago) at Paru co and in the Middle Holocene (4500-7000 years ago) at Hala Hu. These events and the related vegetational variations have been interpreted and correlated with climatic causes rather than past human activity.

Firma dello studente

[1] Il titolo deve essere quello definitivo, uguale a quello che risulta stampato sulla copertina dell'elaborato consegnato.